Identification of civil engineering structures

Francisco Garcés

UNIVERSITÉ PARIS-EST
ÉCOLE DOCTORALE MODES

Thèse de doctorat
Discipline: Génie Civil

Francisco GARCÉS

IDENTIFICATION OF CIVIL ENGENIEERING STRUCTURES

Thèse dirigée par M. Ahmed MEBARKI

Soutenue le 22 février de 2008

Jury

M. Abdekhalek EL HAMI	Rapporteur
M. Hamid AFRA	Rapporteur
M. Michel LORRAIN	Examinateur
M. Carlos GENATIOS	Examinateur
M. Christian CREMONA	Examinateur

To

My wife Liany and my parents Florinda and Alfonso

Acknowledgements

I would like to express my gratitude to my teacher and friend, Carlos Genatios. I would like to thank them for their guidance and support in the last years.

My special thanks to my friend Pedro García and Marianela Lafuente for their assistance in this thesis.

Thanks to FONACIT, CDCH of the UCV, FUNDAYACUCHO and the French Government, for Bursary provided towards supporting my study.

Thanks to Ahmed Mebarki and Laboratoire de mecanique for giving me the opportunity to work my thesis in the University Paris-Est.

To my Work colleagues and friends in the IMME-UCV, Williams Ascanio, Alcibíades Molina, and work colleagues in France Sandra Jerez, Leila Abdou, Natalia Valencia, Sulpicio Sanchez thank you for your friendship, care and support.

Lastly, I am very grateful to my wife, parents and my family for their support and encouragements.

RÉSUMÉ

Cette thèse présente trois méthodes pour l'identification des rigidités des structures d'usage commun dans l'ingénierie civile, à partir de données dynamiques expérimentales.

La première méthode est développée pour des structures composées pour portiques. La deuxième méthode proposée est appliquée à des structures constituées pour des poutres isostatiques**.** La troisième est une méthodologie d'estimation des rigidités en flexion (EI) et au cisaillement (GA/γ) pour une structure constituée de murs dont les énergies de déformation en flexion et cisaillement peuvent être soit du même ordre de grandeur, soit l'une prépondérante par rapport à l'autre.

Pour chaque méthode, des simulations numériques sont effectuées pour identifier les dommages structuraux ou les variations des rigidités, en termes de localisation et de magnitude de ces dommages. L'incidence et l'impact des erreurs et bruits sur les valeurs estimées des rigidités structurales sont analysés.

Les méthodologies sont également appliquées pour localiser des dommages mécaniques ou des réductions de section sur modèles de laboratoire.

A partir des concepts dynamiques de base et considérant une typologie donnée de structure, la thèse développe les concepts et formulations permettant d'identifier les rigidités résiduelles des structures considérées. Les méthodes peuvent être aisément mises en œuvre pour déterminer les éventuels dommages (localisation et intensité) qui peuvent affecter une structure, par exemple après un séisme. Peu de mesures sont requises à cet effet : des essais de vibration libre et du matériel peu onéreux de mesures sont amplement suffisants dans le cas particulier des structures étudiées.

MOTS CLÉS : Analyse dynamique, Dommage structural, Poutre isostatiques, Murs de contreventement, consoles, portiques, Maintenance et inspection, Bruits et signal.

IDENTIFICATION OF CIVIL ENGENIEERING STRUCTURES

ABSTRACT

This thesis presents three methods to estimate and locate damage in framed buildings, simply-supported beams and cantilever structures, based on experimental measurements of their fundamental vibration modes. Numerical simulations and experimental essays were performed to study the effectiveness of each method.

A numerical simulation of a multi-storey framed building, a real bridge and a real chimney were carried out to study the effectiveness of the methodologies in identifying damage. The influence of measurement errors and noise in the modal data was studied in all cases.

To validate the experimental effectiveness of the damage estimation methods, static and dynamics tests were performed on a framed model, a simply supported beam, and a cantilever beam in order to determine the linear behavior changes due to the increase of the level of damage.

The structural identification algorithms during this thesis were based on the knowledge type of the stiffness matrix or flexibility matrix to reduce the number of modal shapes and required coordinates for the structural assessment. The methods are intended to develop tools to produce a fast response and support for future decision procedures regarding to structures widely used, by excluding experimental information, thereby allowing a cost reduction of extensive and specific testing.

KEYWORDS: Dynamic analysis, structural damaged, simple supported beam, Shear wall building, cantilevers, Framed Buildings, monitoring of structures, noise and signals.

Laboratoire de Modélisation et Simulation Multi-échelle, Université Paris-Est
5, Boulevard Descartes, 77454 Marne la Vallée Cedex 2

TABLE OF CONTENTS

1

2

3

4

5

6

7

8

LIST OF FIGURES

LIST OF TABLES

1. INTRODUCTION

1.1 JUSTIFICATION

The performance of a structure is subjected to possible changes during its lifetime. Circumstances leading to changes in the initial configuration of any structure or reinforcement of the same leads to modification of the initial behavior of the structure, as well as, damages produced by permanent or eventual actions.

Caracas, 1967	2,300 buildings were damaged or destroyed
Guatemala, 1976	222,000 buildings (30% of the total) and 1,215 schools were damaged
Armenia, 1988	The earthquake destroyed some 5,100 buildings in the larger town of Spitak, which included 100% of the houses. In the total region, an estimated number of 100,000 households were destroyed
Loma Prieta, 1989	Numerous roads and bridges were damaged. 22,000 homes were damaged and 1,500 homes were destroyed or rendered uninhabitable.
Oregon, 1993	Over 30,000 buildings destroyed and 1,300 bridges damaged
Northridge, 1994	41,600 buildings and 300 bridges were damaged.
Bam, Iran, 2003	85% of buildings damaged or destroyed and infrastructure damaged in the Bam area
Peru, 2007	35,500 buildings destroyed and 4,200 damaged

Table 1.1 Summary of structures damaged by historical earthquakes

In big cities such as Caracas, San Francisco, Tokyo, among others, there are bridges, buildings, hospitals, and schools that need to be maintained under proper conditions in order to resist any daily action; moreover, such structures must be constructed so that it can resist future earthquake events. For example, the Federal Highway Administration of the U.S. Department of Transportation reported that approximately 15% of the 585,000 bridges in the U.S. are considered structurally deficient. Inadequate load capacity is the

most significant factor contributing to structural deficiency. The U.S. has been replacing deficient bridges at a rate of 5,600 each year [1].

After an extreme event, such as an earthquake, the resistance capacity of a structure shall be kept under supervision in order to assess whether the condition of the structure can sustain future use. Table 1.1 shows a summary of structures damaged after important seismic events.

Among evaluation tasks with regard to structural safety, first, an evaluation of not only the structures whose damages can be visualized shall be carried out in order to establish whether the structure can provide habitability, but also the structures slightly affected or even those structures whose damages cannot be visualized shall be assessed.

A year later, hidden damages were discovered in many steel-frame buildings, which appeared to withstand the Northridge quake. Important cracks in the beam-column connections were hidden beneath fire-proofing and wall cladding [2].

Structural engineering must have the tools that allow it to solve problems of maintenance, analysis and correction of structural models, and also determination of structural damage. The structural engineer must be able to assess possible damage of a structure using visual inspection and the aid of nondestructive testing. These are some of the existing nondestructive tests: Acoustic Emission (AE), X-Ray Radiography, Infrared Thermography (IRT), Ultrasonic Thickness Testing (UT), Magnetic Thickness Gauging, and Strain Gage Application. However, hidden damages in the structural elements (those pertaining to the resistance system) are not always easily discovered due to the fact that these are not visible or are difficult to access; such is the case of beams of bridges, beams of roofs, etc. In addition, the nondestructive techniques require that the area of study be accessible, and they also provide a local result of the condition of the structure. The nondestructive techniques may be classified as global or local. One of the advantages of a global method is that measurements at one location are sufficient to assess the

condition of the whole structure. Vibration-based methods are usually global methods of structural analysis; and in many cases, they are easy to use and can be applied at low cost. Over the past three decades, different methods that use structural dynamics as a nondestructive method of global assessment, from which information regarding mechanical properties of the structure and its possible loss of stiffness are gathered, have been developed.

Vibration-based methods can be applied for monitoring of structures, calculation of damage after an extreme event such as an earthquake, or as a tool to assess the vulnerability of the structure. The application of vibration-based methods requires that a dynamic response of the structure be obtained in a steady, intermittent, or occasional manner.

In the continuous measurement, a shift from a preventive time-based to a predictive condition-based maintenance strategy is achieved. This shift reduces both the risk of a serious failure of the structure and the overall maintenance costs by excluding unnecessary inspection activities.

Engineers and researchers in areas of structural, mechanical, or aerospace engineering have developed several methods to assess the damage based on the modal analysis. Chapter 2 presents a summary of more than 100 works that have been classified as follows:

- Natural frequency changes
- Mode-shape-based methods
- Mode shape curvatures
- Modal strain energy
- Dynamic flexibility
- Residual force vector method
- Model-updating-based methods
- Damping

- Neural network methods
- Genetic algorithm methods
- Nonlinear methods

The various methods presented herein have advantages and disadvantages depending on the objectives to be achieved, the availability of instruments, and the type of structure to be analyzed. In general, these methods are classified into two groups:

a) Methods that require a limited use of a few sensors and testing of easy execution. These methods provide information on the global condition of the structure, determining whether the structure is damaged or not.
b) Methods that require a large number of sensors and measurement of many degrees of freedom. These methods allow for the location and quantification of the damage in the structures.

Taking into consideration the differences between methods a) and b), this study has developed methods of detection of stiffness of structures that allow for the location and quantification of the damage in structures using a limited number of sensors and testings of easy execution.

The algorithms of structural identification developed during this study are based on knowledge of the form of the matrix of stiffness or flexibility to reduce the number of modal shapes and necessary coordinates for the structural assessment. This work is mainly intended to suggest and demonstrate the efficiency of methods that allow for the estimation of the stiffness of framed buildings, cantilever, or simply supported beams**,** just using one or two modal shapes and their corresponding frequencies.
It is a great advantage that just little experimental information is required because it does not require measurements of rotational coordinates that are difficult to obtain; however, it is possible to determine the condition of the damage or stiffness from various sections or stories of the structure. For that reason, these methods act as a first step intended to develop tools that will produce a rapid response and support for future decision

procedures regarding structures widely used, by excluding experimental information, thereby allowing for the reduction of the cost of extensive and specific testings.

1.2 OBJECTIVES

This study is intended to present and experimentally validate methods to assess changes of stiffness of structural systems. The following structural systems are considered: framed buildings, simply supported beams, and systems that can be modeled as a cantilever**.**

The specific objectives can be summed up as follows:

- Develop a method that allows for the assessment of the changes in stiffness in the framed building**,** considering its modal shapes, modal frequencies, mass of the structure, and geometric configuration.
- Establish the influence of the errors of experimental measurement and the severity of the damage in the method of identification of framed buildings.
- Carry out experimental free vibration test in a three-story framed model on a reduced scale, determining its natural frequencies and its corresponding modal shapes.
- Estimate changes in stiffness of a framed model based on the method developed in this work.
- Develop a method that allows for the estimation of the flexure stiffness of simply supported beams, considering its modal shapes, modal frequencies, mass of the structure, and geometric configuration.
- Establish the influence of the errors of experimental measurement and the severity of the damage in the method of identification of structures composed of simply supported beams.
- Carry out experimental free vibration test in a simply supported beam specimen**,** determining its natural frequencies and its corresponding modal shapes.

- Estimate changes in stiffness in an experimental simply supported beam specimen, based upon the method developed in this work.
- Develop a method that allows for the estimation of the flexural stiffness and shear stiffness of cantilever structures or shear wall buildings, considering its modal shapes, modal frequencies, mass of the structure, and geometric configuration.
- Establish the influence of model of masses used in the identification of structures composed of shear walls**.**
- Establish the influence of the errors of experimental measurement and the severity of the damage in the method of identification of simulated structures such as cantilever.
- Application of the method of identification of structures composed of walls to structures of low-height confined masonry.
- Carry out experimental free vibration test in a cantilever model, determining its natural frequencies and its corresponding modal shapes.
- Estimate changes in stiffness in a cantilever model based on the method developed in this work.

1.3 CONTENTS OF THE STUDY

This study introduces three methods of structural identification for the three different types of the abovementioned structures. Each method is described in separate chapters and is validated using numeric and experimental simulations considering dynamic data. One chapter is intended to detail the dynamic testings of the three models constructed.

The contents of the different chapters in the thesis are as follows:

Chapter 2 introduces some aspects related to the damage in structures and a summary of some of the methods used to determine the damage in structural systems considering dynamic data.

Chapter 3 describes some theoretical aspects related to the free vibration test, the determination of the dynamic properties using this testing technique, and some recommendations to perform the testing and the processing of data obtained.

Chapter 4 describes a series of experimental test developed in this study and its results. The results and procedures used in the vibration tests and static load tests are presented therein; in addition, this chapter presents the numeric simulations of the models.

Chapter 5 presents the method of identification of changes in stiffness of the framed buildings**.** This method is validated through its numeric and experimental application.

Chapter 6 presents the identification of the changes in flexural stiffness of the simply supported beams**.** This method is validated through its numeric and experimental application.

Chapter 7 is dedicated to the method of identification of the stiffness in structures that can be simulated using cantilever or those composed of shear walls**.** This method is validated through its application to numeric and experimental simulations.

Finally, Chapter 8 presents the final conclusions and comments on possible future developments.

2. STRUCTURAL DAMAGE: METHODS OF IDENTIFICATION USING EXPERIMENTAL STRUCTURAL DYNAMICS

2.1 INTRODUCTION

Structural damage can be identified using visual inspection or range-location techniques such as acoustic or ultrasonic methods, magnetic field methods, radiographs, eddy-current methods, and thermal field methods. These methods require that the area of study be accessible in order to provide a local outcome of the state of the structure. The need for systems for identifying damage using techniques that may provide details on the overall condition of the structure and on those areas that are difficult to access has led to the development of methods that examine changes in the vibration characteristics of the structure.

An outlook since the study of the basic concepts of structural dynamics shows that changes in stiffness and mass properties cause changes in modal parameters (vibration frequencies, mode shapes, and modal damping); over the last three decades, a significant number of research studies have been carried out in order to provide methods for identifying structural damage using dynamic data for numerous applications involving detection of structural damages and monitoring of structure for civil, mechanical, and aerospace engineering.

This chapter presents several aspects related to structural damage and a summary of some of the methods used to determine damage in structural systems using dynamic data. The methods are classified according to the type of technique used to identify the damage using the evaluated data.

2.2 STUDY OF DAMAGE

During its lifetime, a structure is subjected to various physical, chemical, and biological actions that may cause damage to the structure depending on intensity, duration, and location; these damages produce changes in aesthetics, functionality, or mechanical capability of the building structure.

Damage may occur on different elements of the building structure; these elements are classified into four groups [3]:

- Structural elements: elements that form systems of vertical and lateral load resistance.
- Architectonic elements: elements that do not contribute to resistance of applications but whose main functions are decorative or filling, such as divisive walls, windows, and coating.
- Installations: systems that provide services to building structures, such as water pipes, gas pipes, electricity systems, and systems of sewers.
- Contents: elements present in building structures but are not part of the structure, such as machinery, equipments, and furniture.
-

The last three elements mentioned above are considered nonstructural elements. The dynamic behavior of the system may be influenced by the arrangement and linkage of nonstructural elements of the structural system. In general, these elements affect the stiffness of structural systems or modify the center of vibration of the building structure. Likewise, the mass of elements considered as contents will produce an effect on the vibration of the structure to a high or low degree.

The state of functionability and repair of the structure may be determined by the type of elements that are damaged and the magnitude of the damage. The study of the scope of the damage is based on two conditions:

- The calculation of the damage after an extreme event such as an explosion, fire, or seism. It is of vital importance to consider the state of the structure and of its installations as well as the decisions to be taken in order to repair it or demolish it.
- Structural Health Monitoring (SHM). Structural monitoring allows to check continually the condition of the structure. This task is mandatory for structures of social or economic value, such as bridges, hospitals, schools, and oil platforms

2.2.1 DAMAGE ESTIMATION AFTER AN EXTREME EVENT

If a structure is subjected to an extreme event, it is necessary to immediately evaluate the condition of the structure. In the event of a seism, damage suffered by the structure is classified according to the magnitude of the damage, functionability, necessary repairs, or a combination of all of them.

2.2.1.1 Classification according to damage observed

Park et al. [4] suggested that the following five states of damage be considered for a structure of concrete that has suffered a seism:

- No damage: it shows a maximum of just a few fissures in the concrete.
- Slight damage: it shows fissures in various structural elements.
- Moderate damage: it shows severe cracking along with falling concrete.
- Severe damage: it shows crushed concrete and loss of coating of steel bars.
- Collapse.
-

2.2.1.2 Classification according to functionability

Anagnostopoulos et al. [5] suggested three levels of functionability in a structure according to the damage:

- Usable: The level of damage is low, hence the structure can be put to use immediately after the seism.
- Temporarily usable: The level of damage is between moderate and severe. The structure requires repairs, hence it can not be used temporally.
- Total loss or completely non-usuable: The level of damage is such that the structure may suffer a total or partial collapse. The structure cannot be put to use after the seism.

2.2.1.3 Classification according to level of repair required

Bracci et al. [6] suggested four levels of damage according to the repair required in the structure:

- No damage or some damage.
- Reparable
- Irreparable
- Collapse

2.2.1.4 Combined Classification

The EERI [7] established five levels of damage. This classification is based on level of damage, time required for repair, and risk to dwellers in the building:

- No damage
- Minor damage: Minor damage in non-structural elements. The structure will be usable in less than a week.
- Moderate damage: Considerable damage in non-structural elements. The structure may not be usable up to a period of three months. The risk of loss of human life is minimum.
- Severe damage: Severe structural damage. The structure may not be usable for a long period of time. As the final option, the structure may be demolished. The risk of loss of human life is high.
- Total collapse or very severe damage: Damage to the structure is irreparable. The risk of loss of human life is very high.
-

The abovementioned classifications are just a few of the many existing classifications, which vary according to the level of complexity and the method used. This study only attempts to show the importance of an evaluation of a structure after an extreme event has occurred, especially in the case of a seism.

2.2.2 STRUCTURAL HEALTH MONITORING (SHM)

Structural Health Monitoring (SHM) is the practice of monitoring a structure over its lifetime to detect changes in its structural properties that may indicate a reduction in performance. It may be used to monitor aeronautical, mechanical, civil, electrical, and other systems.

SHM is mandatory for a building structure, which due to its social value, economic value, or due to the fact that it houses productive activities or service activities, may be classified as a structure of vital importance, such as hospitals, schools, bridges, historical monuments, or buildings, electrical installations, oil installations, nuclear installations, governmental, or financial building structures.

Depending on the type of structure, a continuous or periodic monitoring may be established in order to assure a good structural performance and proper functioning of the system. This task is a vital tool for the decision of actions to be taken regarding maintenance, repair, or restoration of a building structure.

Knowing the integrity of in-service structures on a continuous real-time basis is very important with regard to security and structural maintenance. In effect, SHM:

- Indicates possible structural damage present.
- Evaluates effectiveness of tasks of structural maintenance.
- Allows optional use of the structure, minimizes downtime, and prevents catastrophic failures.
- Evaluates the structural capacity to withstand the effects of extreme events.
- Moreover, monitoring programs may be used to compare and calibrate theoretical structural models.

2.3 DAMAGE IDENTIFICATION METHODS USING MODAL DATA

The idea of using vibration measurements to detect damage was proposed by Cawley and Adams [8]. It is based on the fact that damage will reduce the local stiffness of the structure, which in turn reduces the natural frequencies of the whole structure. Most studies use vibration measurements to detect damage examine changes in modal properties.

A system of classification of damage identification methods, as presented by Rytter [9], defines four levels of damage identification, as follows:

- Level 1: Detection of the existence of damage in the structure
- Level 2: Determination of the geometric location of the damage
- Level 3: Quantification of the severity of the damage
- Level 4: Prediction of the remaining service life of the structure

The next section presents a review of some methodologies for damage estimation in structures using modal data. The methods in this review can be classified mostly as Level 1, Level 2, or Level 3 because these levels are most often related directly to structural dynamics testing and modeling issues. Level 4 is generally categorized under the fields of fracture mechanics, fatigue-life analysis, or structural design assessment and, as such, is not addressed in the structural vibration or modal analysis studies.

2.3.1 SURVEY OF PREVIOUS LITERATURE

A detailed survey of the technical literature and interviews of selected experts to determine the state-of-art of the damage-detection field (using modal analysis procedures) as of 1979 was presented by Richardson [10]. The survey focused on monitoring of structural integrity for nuclear power plants, large structures, rotating machinery, and offshore platforms, with by far the largest number of literature surveys associatedwith rotating machinery. The author stated that while monitoring of overall vibration levels of rotating machinery had become commonplace, attempts to relate

structural damage to measured modal changes were still at their primitive stages. Several doctoral dissertations that address damage detection and related issues have recently been published. Each dissertation contains a survey of literature and a development of the theory relevant to its scope. These dissertations included Rytter [9], Hemez [11], Kaouk [12], and Doebling [13]. Mottershead and Friswell [14] presented a survey of the literature related to dynamic finite element model (FEM) updating, which has been used extensively for detection of structural damage. Their review included a long list of references on the topic of model updating. Bishop [15] reviewed the literature in the field of neural networks. Neural-network-based damage identification methods are reviewed in Section 2.3.9

2.3.2 CHANGES IN NATURAL FREQUENCY

Any structural system that experiences changes in stiffness and mass will experience changes in natural frequency of the vibration in the structure. As a result, the presence of damage or deterioration in a structure causes changes in the resonant frequencies of the structure. The above reasoning and the possibility of measuring frequencies of vibrations favored the development of methods to detect structural damage. A bibliographical assessment shows a list of case studies of applications involving detection of structural damage. A brief overview of the advantages and disadvantages of the most important case studies are given below.

The somewhat low sensitivity of natural frequency to damage requires high levels of damage and measurements made with high accuracy in order to obtain reliable results. However, some studies have shown that resonant frequencies have much less statistical variation from random error sources than other modal parameters [16].

Cawley and Adams [8] established that the ratio of the frequency changes in the two modes is only a function of damage location. To locate the damage, theoretical frequency shifts, due to damage at selected positions on the structure, are calculated and compared with measured values. The pair giving the lowest error indicates the location of the

damage. The formulation does not account for possible multiple-damage locations. The results are based on FE models of aluminum and CFRP plates.

Stubbs and Osegueda [17, 18] developed damage detection methods based on modal changes. The method relates frequency shifts to changes in member stiffness using the sensitivity of modal frequency changes. Stiffness reductions were located by solving an inverse problem, since damage is defined as a reduction in the stiffness of one of the elements forming the structure. The authors point out that this frequency-change sensitivity method relies on sensitivity matrices that are computed using a FEM. This requirement increases the computational burden of these methods and also increases the dependence on an accurate available numerical model.

Sanders et al. [19] used the frequency sensitivity method of Stubbs and Osegueda [17] combined with an internal-state-variable theory to detect damage in composite beams. The damage theory includes parameters, which indicate two possible types of damage: matrix micro-cracking (identified by changes in the extensional stiffness) and transverse cracks in the 90-degree plies (identified by changes in the flexural stiffness). The technique is applicable in general to any internal variable theory that can predict changes in stiffness resulting from changes in the measured parameters.

Hearn and Testa [20] developed a damage detection method that examines the ratio of changes in natural frequency for various modes. In this case, the mass is invariable and second-order terms in the formulation are neglected. The authors then summarize a two-step procedure, both qualitative and quantitative, for correlating changes in the measured frequency ratios with the damage location.

Chen et al. [21]questioned the effectiveness of using the changes in natural frequencies to indicate damage in a structure. The first four frequencies of a steel channel exhibited no shifts greater than 5%, due to a single notch that is severe enough to cause the channel to fail at its design load. Given that it is acknowledged that frequency variation due to incidental/ambient vibration and environmental effects can be as high as 5–10%, they argued that lower frequency shifts would not necessarily be useful damage indicators.

Messina and Williams [22] proposed a correlation coefficient that compares changes in a structure's resonant frequencies with predictions based on a frequency-sensitivity model derived from a finite element model. This approach is termed Multiple Damage Location Assurance Criterion (MDLAC). Tests have shown that 10–15 modes are required to give sufficient discrimination for reliable damage localization. Applications in the analytical and experimental cases showed the capacity of prediction of the proposed methods. The authors note that, in practice, errors in frequency measurements can alter the patterns of change in apparent frequency and affect the ability of the MDLAC approach to give a correct prediction.

De Roeck et al. [23] monitored the Z24 Bridge in Switzerland over the course of a year. Environmental effects of air temperature, humidity, rain, wind speed, and wind direction were monitored along with readings recorded from 16 accelerometers on an hourly basis. Following a progressive damage testing program, it was demonstrated that once the effects of environmental influences were filtered out, stiffness degradations could be detected if the corresponding frequency shifts were more than just 1%.

Boltezar et al. [24] devised a method for locating transverse cracks in flexural vibrations of free-free beams by following an inverse problem. The method is based on the assumption that the crack stiffness does not depend on the frequency of vibration (i.e., the values of the crack stiffness, which is modeled as a linear torsional spring, must be the same at the crack position for all of the measured natural frequencies). As a result, by plotting the relative stiffness along the length of the beam for at least two distinct natural frequencies, the crack location can be identified by the intersection of these curves.
Sampaio et al. [25] proposed the detection and relative damage quantification indicator (DRQ), based on the use of the frequency domain assurance criterion (FDAC), as an effective damage indicator, capable of distinguishing a positive occurrence from a false alarm.

Zang et al. [26] presented two criteria to correlate measured frequency responses from multiple sensors and proposed indicators for structural damage detection using them. The first criterion is the global shape correlation (GSC) function, which is sensitive to differences in mode shape but not to relative scales. The second criterion, based on actual response amplitudes, is the global amplitude correlation (GAC). An experimental test on a bookshelf structure was conducted, but it was concluded that further studies would be needed to develop approaches that could accurately assess structural states and damage.

The vast information available regarding the use of the frequency changes of vibrations to estimate the damage in structures has contradictory points of views regarding the efficiency or nonefficiency of the use of this parameter. Some studies have established that the relatively low sensitivity of natural frequency to damage requires high levels of damage and measurements made with high accuracy in order to achieve reliable results. Moreover, the capacity to locate damage is somewhat limited, as natural frequencies are global parameters and modes can only be associated with local responses at high frequencies. Successful identification algorithms have generally been limited to identification of a single or a few damage locations. Equally, the most successful applications have been with respect to small laboratory structures. Only frequency shifts have been used in identifying damage in full-scale structures.

2.3.3 METHODS BASED ON MODE SHAPES

One of the parameters that characterize the dynamic response of a structure is its mode shape. The natural feature of vibration from a system can be obtained by a sampled dynamic array of sensors. This section describes two of the most common methods used in damage estimation. The first is based on the analysis of the changes in the mode shapes, whereas the second is based on the analysis of the changes in the curves of those mode shapes.

2.3.3.1 Comparison of modes shapes

Several methods are used to compare two sets of mode shapes. Brief overviews of some of them are presented here.

Yuen [27] examined changes in the mode shape and mode-shape-slope parameters. The changes in these parameters were simulated for a reduction in stiffness in each structural element, and then the predicted changes were compared with the measured changes to determine the damage location. The author identified the need for some orthonormalization process in order to account for higher mode shapes.

The MAC (Modal Assurance Criterion), which is probably the most common means of establishing a correlation between experimental and analytical models, is defined by Allemang and Brown [28]. The MAC value can be considered as a measure of the similarity of two mode shapes. An MAC value of 1 is a perfect match and a value of 0 means they are completely dissimilar. Thus, a decrease in MAC value may be an indication of damage.

The COMAC (Coordinate Modal Assurance Criterion) is used to calculate a correlation factor between the undamaged and damaged experimental coordinates in all mode shapes for a specific degree of freedom [29]. The COMAC is a pointwise measure of the difference between two sets of mode shapes and takes a value between 1 and 0. A low COMAC value would indicate discordance at a point and thus is also a possible indicator of damage location.

The MSF (Modal Scale Factor) represents the slope of the best straight line through the points for a pair of mode shapes, which in this case is the undamaged and damaged mode shapes [30]. This criterion gives no indication as to the quality of the fit of the points to the straight line, simply its slope.

The RD (relative Difference) used is the Relative difference between the shapes of the scaled modes [31]. This criterion uses the graphical comparison of the mode shapes in order to indicate the position of damage.

Mayes [32] presented a method for model error localization based on changes in mode shape known as structural translational and rotational error checking (STRECH). By taking ratios of relative modal displacements, STRECH assesses the accuracy of the structural stiffness between two different structural degrees of freedom (DOF). STRECH can be applied to compare the results of a test with an original FEM or to compare the results of two tests.

2.3.3.2 Mode shape curvatures

The Euler–Bernoulli equation evidently shows that the bending curvature of the beam is inversely proportional to its stiffness. Damage at any section results in an increase incurvature at that section, which is local in nature. Hence, curvature-based methods can be used to identify damage.

Mode shape curvature (MSC) method was first presented by Pandey et al. [33]. The location of the damage is assessed by the largest absolute difference between the mode shape curvatures of the damaged and undamaged structure

Salawu and Williams [34] used a mode shape curvature measure computed using a central difference approximation. They compared the performance of this relative difference method with that of a mode shape relative difference method. They demonstrated that the change in curvature does not typically give a good indication of the damage using experimental data. They pointed out that the most important factor is the selection of the modes that are used in the analysis.

Wahab and De Roeck [35] applied a curvature-based method to the Z24 Bridge in Switzerland successfully. They introduced a damage indicator named the curvature

damage factor, CDF, the difference in curvature before and after damage averaged over a number of modes.

Ho and Ewins [36] attempted to evaluate using both simulated and experimental data that whether the presumption that damage is located at the point where the change in mode shape is the greatest is valid, since the differentiation process enhances the experimental variations inherent to mode shapes. They addressed five methods based on mode shapes and their derivatives: flexibility index (FI), mode shape curvature (MSC), mode shape curvature square (MSCS), mode shape slope (MSS), and mode shape amplitude comparison (MSAC).

The review shows some contradictions from the some authors over the use of mode shapes alone in damage detection. Ren and De Roeck [37] cast doubts on the use of mode shapes in large structures, whereas Wahab and De Roeck [35] presented promising results when applied to a bridge.

2.3.4 MODAL STRAIN ENERGY

The distribution of strain energy along a structure can be measured between any two points. Experimental results show that the damage at any point of the structure causes an increase in the curvature, thereby leading to higher values of strain energy at the region of damage location. The difference between the strain energy distributions of undamaged and damaged structures can be used to indicate the severity of damage.

Kim and Stubbs [38] proposed a damage identification method based on the decrease in modal strain energy between two structural DOF, as defined by the curvature of the measured mode shapes. Kim and Stubbs [39] derived a new damage index, which improved the accuracy of damage localization in a simulated two-span beam, compared with Kim and Stubbs . By assuming that damage has only highly localized effects on mode shape curvature, Stubbs and Kim [40] used only post-damage data to localize and estimate severity of damage of an experimental two-span beam.

Farrar and Doebling [41] were successful in using Kim and Stubbs [38] damage index in localizing controlled damage to a bridge. They found that this method outperformed the method involving the direct comparison of mode shape curvature before and after the damage.

Law et al. [42] proposed the use of the elemental energy quotient (EEQ), defined as the ratio of the modal strain energy of an element to its kinetic energy. The difference in the EEQ before and after damage is normalized and averaged over several modes and used as an indicator of the region of damage location.

Choi and Stubbs [42] developed a method to locate and determine the size of damage in a structure by measuring time-domain responses in a set of measurement points. The mean strain energy for a specified time interval is obtained for each element of the structure and is used in turn to build a damage index that represents the ratio of the stiffness parameters of the pre-damaged and post-damaged structures:

Patil and Maiti [43] proposed damage index behavior as an indicator of the amount of strain energy stored in the crack (or torsional spring). The method is based on the concept that the strain energy U of a beam containing a crack is reduced because the beam can deform more easily to the same extent than an uncracked beam. This work provided an experimental verification of an energetic method for prediction of the location and size of multiple cracks based on the measurement of natural frequencies for slender cantilevered beams with two or three normal edge cracks.

2.3.5 DYNAMIC FLEXIBILITY

The flexibility matrix is defined as the inverse of the static stiffness matrix. Each column of the flexibility matrix represents the displacement pattern of the structure associated with a unit force applied at the corresponding DOF. The measured flexibility matrix can be estimated from the mass-normalized measured mode shapes and frequencies. Due to the inverse relation to the square of the modal frequencies, the dynamic flexibility matrix

is very sensitive to changes in the lower order modes, whereas the stiffness matrix is more sensitive to higher order modes. Damage is then identified by comparison of the flexibility matrices of the structure in the undamaged (obtained using a FE model in general) and damaged states.

Pandey and Biswas [44] identify damage in beam-type tructures using changes in the flexibility matrix of the structure. Using numerical and experimental examples of the different types of beams, Pandey and Biswas [44, 45] demonstrated the uses of changes in the flexibility matrix for locating damage in beam- type structures.

Doebling and Paterson [46] presented a method for synthesizing a statically complete flexibility matrix, which reproduces specific partitions of the dynamically measured flexibility matrix. A statically complete flexibility matrix based on the assumed elemental connectivity of the structure is scaled such that it reproduced (approximately) the statically complete partitions of the dynamically measured flexibility matrix.

Lim [47] proposed the unity check method for locating modeling errors and used the location of the entry with maximum magnitude in each column to determine the error location. He applied the method to FEM examples and also investigated the sensitivity of the method to non-orthogonality in the measured modes. Lim [48] extended the unity check method to the problem of damage detection. He defined a least-squares problem for changes in the elemental stiffness—that are consistent with the unity check error—in potentially damaged members.

Ho and Ewins [36] presented the stiffness error matrix as an indicator of errors between measured parameters and analytical stiffness and mass matrices. For damage identification, the stiffness matrix generally provides more information than the mass matrix, so it is more widely used in the error matrix method.
Park, et al. [49] presented a weighted error matrix, where the entries are divided by the variance in natural frequency resulting from damage in each member. The authors applied their formulation to both beam models and plate models.

Yan and Golinval [50] presented a damage localization technique based on a combined consideration of measured flexibility and stiffness. The covariance-driven subspace identification technique is applied to identify parameters of structural modes and then used to assemble the flexibility matrix. The stiffness matrix is obtained by a pseudo-inversion of the flexibility matrix. Damage localization is achieved by a combined assessment of changes in the two measured matrices in moving from the reference state to the damaged state.

By knowing the stiffness or flexibility matrix topology, it is possible to reduce the number of modal forms and the number of coordinates necessary for structural estimation. In general, this reduces the number of measurement points on the structures, which drastically reduces the costs and the number of tests needed. The damage is estimated from the mass-normalized measured mode shapes and frequencies. On the basis of this approach, methods are developed for estimation of damage in framed structures [51, 52], shear wall buildings and cantilevers [53], and simply-supported-beams [54]. These methods are verified through laboratory models and numerical simulations.

2.3.6 RESIDUAL FORCE VECTOR METHOD (RFV)

The residual force method is used for quantification and localization of the damage in structures. This method is based on identifying the difference in modal properties between the undamaged and damaged structures.

Sheinman [55] proposed numerical examples of a closed-form algorithm for damage identification using RVF. In a study, Kosmatka and Ricles [56] identified single damage events (stiffness loss, connection loosening, lump mass addition) in a laboratory test. In this work, measurements were made at each DOF to obtain complete mode shapes. A weighted sensitivity algorithm estimated the magnitude of stiffness/mass change. As

expected, it was found that increased correlation between the analytical model and the baseline modal properties improved the estimates of damage severity.

Farhat and Hemez [57] minimized the norm of the RFV by updating both stiffness and mass elemental parameters in a sensitivity-based algorithm. Incomplete mode shapes were expanded by minimising the RFV. This methodology was verified on a simulated cantilever and a simulated plane truss. It was important that identification includes modes that stored sufficient strain energy in the damaged elements. Brown et al. [58] applied the method to lightly damped structures. The mass and stiffness matrices are first updated and then the remaining RFV is absorbed by the damping matrix. The method worked well in numerical studies with damping less than 3%.

Castello et al. [59] presented the use of a continuum damage model where a scalar parameter represented the local cohesion state of the material. The method was established on a simulated cantilever and a planar truss with up to two damage locations.

Ge and Lui [60] proposed the method that uses finite element modeling and locates damage by the use of a pseudo structure residual force. Matrix condensation is then applied to extract the degrees of freedom associated with the damaged elements. Damage is evaluated using a proportional damage model that makes use of the measured frequencies of the damaged structures. Numerical examples are considered and the validity of the method is demonstrated by applying the procedure to detect damage in the structures.

2.3.7 MODEL UPDATING BASED METHODS

Model updating can be defined as the process of correcting the numerical values of individual parameters in a mathematical model using data obtained from an associated experimental model such that the updated model describes the dynamic properties of the subject structures more correctly. A typical way to establish a numerical model for a civil structure or mechanical system is via the use of the finite-element method. Closely related to model updating is the model-based method for damage determination, which

serves as an indicator of damage and can be used to quantify the location and extent of damage.

Baruch [61] proposed a method by which a given stiffness and flexibility matrix can be corrected optimally by using corrected mode shapes and natural frequencies obtained from vibration test. The procedure assumes that the mass matrix is correct. Berman [62] introduced a formulation that modifies the mass matrix and assumes that the measured modes are exact. Consequently, Berman and Nagy [63] combined the mass-matrix adjustment procedure of Berman with the stiffness matrix adjustment procedure of Baruch [61] to create the so-called analytical model improved (AMI) procedure.

Kabe [64] proposed the matrix adjustment procedure (KMA) using constrained minimization theory. This work presented error function that is independent of the system's mass properties and magnitudes of stiffness coefficient. The minimization of the error function minimizes the percentage change to each stiffness coefficient. The optimally adjusted stiffness matrix is obtained by minimizing this error function subject to symmetry constraints, connectivity constraints, and constraints derived from a system of force Equilibrium equations.

Chen and Garba [65] proposed a method for minimizing the norm of the perturbations of model property with a zero modal force error constraint. They also enforced a connectivity constraint to impose a known set of load paths onto the allowable perturbations. The updates are thus obtained at the element parameter level, rather than at the matrix level. This method is demonstrated on a truss FEM.

Kim and Bartkowicz [66] investigated damage detection capabilities with respect to various matrix updating methods, model reduction methods, mode shape expansion methods, number of damaged elements, number of sensors, number of modes, and levels of noise. The authors developed a hybrid model reduction/eigenvector expansion approach to match the order of the undamaged analytical model and the damaged test

mode shapes in the matrix updating method. They also introduced a more realistic noise level into frequencies and mode shapes for numerical simulation.

Zimmerman and Kaouk [67] presented the basic minimum rank perturbation theory (MRPT) algorithm. A nonzero entry in the damage vector is interpreted as an indication of the location of damage. The resulting perturbation has the same rank as the number of modes used to compute the modal force error.

Kaouk and Zimmerman [68] presented a technique that can be used to implement the MRPT algorithm with no original FEM. The technique involves using a baseline data set to correlate an assumed mass and stiffness matrix, so that the resulting updates can be used as the undamaged property matrices. Zimmerman et al. [69] extended the theory to determine matrix perturbations directly from measured FRFs. This method is implemented by solving for the perturbation in the dynamic impedance matrix from the generalized off-resonance, dynamic-force residual equation.

Zimmerman and Kaouk [70] implemented such an eigenstructure assignment technique for damage detection. They included algorithms to improve the assignability of the mode shapes and to preserve sparsity in the updated model. They applied their technique to the identification of the elastic modulus of a cantilevered beam.

Li and Smith [71, 72] presented a hybrid model updating technique for damage identification that uses a combination of the sensitivity and optimal-update approaches. This method constraints the stiffness matrix perturbation to preserve the connectivity of the FEM, and the solution minimizes the magnitude of the vector of perturbations to the elemental stiffness parameters.

Sheinman [55] proposed an algorithm for updating the stiffness and mass matrices and for damage detection and location. It is found that only one mode is needed for exact locating the damage and very few modes for determining the extent of the damage. The

method preserves the initial connectivities and assumes that both the stiffness and mass matrices can be defectives.

Cobb and Liebst [73] presented a method that uses a mathematical optimization strategy to minimize deviations between measured and analytical model frequencies and partial mode shapes.

Teughels et al. [74] presented a sensitivity-based finite element updating method that used the experimental modal data. The damage identification procedure is performed in two updating steps. In the first step, the initial FE model is tuned to a reference state of the structure, using the measured vibration data of the undamaged structure. In the second step, the reference FE model is updated to obtain a model which can reproduce the measured vibration data of the damaged state. The damage is identified by comparing both the reference and the damaged FE model.

Jaishi and Ren [75] presented a methodology for sensitivity-based finite element model updating. In this work, the objective function consisting of the model flexibility residual is formulated and its gradient is derived. The proposed method is applied in the laboratory to the tested reinforced concrete beam, which is damaged.

The damage scheme proposed by Titurus et al. [76, 77] consists of model updating of the baseline finite element model, followed by the use of the sensitivity matrix along with the vector of changes of the chosen dynamic properties for locating the damage.

2.3.8 DAMPING

Similar to the frequency changes, the damping changes are used to estimate structural damage. However, crack detection in a structure based on damping is advantageous over detection schemes based on frequencies and mode shapes in that damping changes can be used to detect the nonlinear, dissipative effects that cracks produce. Modena, Sonda, and Zonta [78] showed that visually undetectable cracks cause very little change in resonant

frequencies and larger changes in damping and that the detection of such cracks requires higher mode shapes.

During vibration tests of prestressed reinforced concrete hollow panels, Zonta, Modena, and Bursi [79] observed that cracking in reinforced concrete specimens results in a frequency splitting in the frequency domain and the beat phenomenon of the free decay signals in the time domain. The authors claimed that crack formation in prestressed reinforced concrete triggers a nonviscous dissipative mechanism, making damping more sensitive to damage, and they proposed to use this dispersive phenomenon as a feature for detecting damage.

Keye et al. [80] developed a method which is capable of relating modal damping deviations caused by structural damage to the damage location on the structure.

2.3.9 NEURAL NETWORK METHODS

Neural networks are computing systems with the ability to learn from trainings and are developed to imitate the way humans manage and process information. On the basis of trained neural networks, the behavior of complex system may be modeled and predicted, even without a priori information about the structural or mathematical model. In the fields of dynamic system identification, prediction and control, application of neural networks has increased considerably in recent years.

Neural networks have been applied successfully in many diverse applications including vibration-based damage identification [81-84]. In general, neural networks are particularly applicable to problems where a significant database of information is available but where it is difficult to specify an explicit algorithm.
Both Ramu and Johnson [85] and Pandey and Barai [86] applied back propagation neural networks to identify damage. In both cases, the network was found to be effective, except that the topology of the network was found to be critically important for performance.

Marwala [87] demonstrated the use of the committee approach on a damaged experimental cylinder. Three networks were trained and their outputs combined to give better predictions than those by the three networks separately.

2.3.10 GENETIC ALGORITHM METHODS

Some damage identification structures based on optimizing processes employ genetic algorithms (GA). Genetic algorithms are methods for optimization of functions based on the random variation and selection of a population of solutions. They are part of what may be described as evolutionary algorithms, which have been developed since the 1950s [88].

Many authors, for example Chiang and Lai [89] and Moslem and Nafaspour [90], described a two-stage process where the RFV is used to locate damage initially and then in a second stage a GA is successfully used to quantify the damage in the identified elements. The method was demonstrated on a simulated truss structure of 13 elements, with up to 3 elements being damaged.

Ostachowicz et al. [91] identified the location and magnitude of an added concentrated mass on a simulated rectangular plate by using the shifts in the first four natural frequencies. A genetic algorithm was employed to overcome the problem of multiple peaks in the objective function.

2.3.11 NON-LINEAR METHODS

It is clear from the literature that non-linear damage assessment methods are very less investigated than linear assessment methods. To incorporate the non-linear behavior of a cracked beam, a bilinear spring is often used to model the crack.

Van Den Abeele and De Visscher [92] considered the amplitude dependency of the dynamic behavior of a gradually damaged RC beam. The non-linearity is quantified as a function of the damage and compared with linear damage assessment techniques. A time stepping model is described by Neild [93] to understand the non-linearities in the vibration characteristics. The model is capable of including damage in the form of a moment–rotation relationship over the cracked region. The beam test showed that there is a change of nonlinear behavior with damage. The change is the greatest at low damage levels.

Vanlanduit et al. [94] employed vibration characteristics to detect cracks during a fatigue test on a steel bar. To perform this test, an experimental setup is developed to simultaneously estimate static and dynamic response, as well as linear and non-linear vibration features. In this setup, it turned out that the non-linear dynamic response is far more sensitive to damage than the static non-linear and the linear elastic responses. Also, a double crack could be detected using a non-linear identification technique near the region of fatigue failure.

2.4 CONCLUSION

Various methods that use modal data to determine structural damage and to provide damage assessments of the structures have been described in the literature. These methods can be used for estimation of damage after an extreme event or for structural monitoring

According to the literature review, it is clear that an ideal methodology for the damage estimation cannot be established. Each method presents advantages and disadvantages depending on the desired applications. Many methods are not available for damage quantification, and there are only limited methods to establish the presence and location of damage.

One of the limitations that is frequently encountered is the capacity to detect small damages. The methodologies require high levels of damage and measurements made with high accuracy in order to obtain reliable results.

Several studies continue to focus on laboratory tests and numerical simulations. These tests and simulations, while beneficial in terms of testing proposed detection algorithms, cannot replicate the environmental effects to which real structures are subjected to.

Depending on the chosen algorithm less or more number of sensors are needed. The algorithms which use few sensors are limited to Level 1 identification.

Some methods require complete data on the mode shapes so that all coordinates of the finite-element prototype are included in the model. However, measurement of all the fundamental frequencies and mode shapes, including rotational modes, is impractical in some cases.

It is clear that although some promising work has been reported on damage detection using linear methods, there are still major problems to be overcome, particularly those of sensitivity and effect of environmental conditions, experimental error, and incompleteness.

3. INTRODUCTION TO EXPERIMENTAL STRUCTURAL DYNAMICS

3.1 INTRODUCTION

The process of prognosis of structural damage involves a preceeding stage of recognition of modal parameters. There are various techniques of dynamic test of structures such as free vibration, forced vibration, and environmental vibration; each one involves a test procedure, data processing, and dynamic properties (frequencies, buffers, and mode shapes). The extraction of dynamic features of the structural models studied herein was included in the test of free vibration; for that reason, this chapter is intended to present theoretical aspects regarding dynamic tests of free vibration, detection of dynamic properties based on this test technique, some recommendations to carry out the test, and the processing of data obtained.

3.2 FREE VIBRATION TEST

In the free vibration test, the structure is subjected to an initial condition of velocity or movement displacement**,** allowing it to vibrate freely and thereby enabling the recording of its resulting movement.

In the event of an initial condition of velocity applied to the structure, a compulsive force must be applied to the structure so that the time frame is shorter than that of the period of the system. In order to do so, several techniques are applied: strike the structure with heavy weights, produce small explosions, launch rockets from the structure, among others [95].

For the application of an initial deformation to the structure, a steel cable containing a steel fuse designed to break at certain force is tightened to it. Then, using heavy duty machinery or other system, the steel cable is tightened until the fuse breaks. Figure 3.1 shows a graph of this test. In most cases, it is convenient to apply force in a horizontal way (θ=0), so the modes of vertical vibrations are not excited**.**

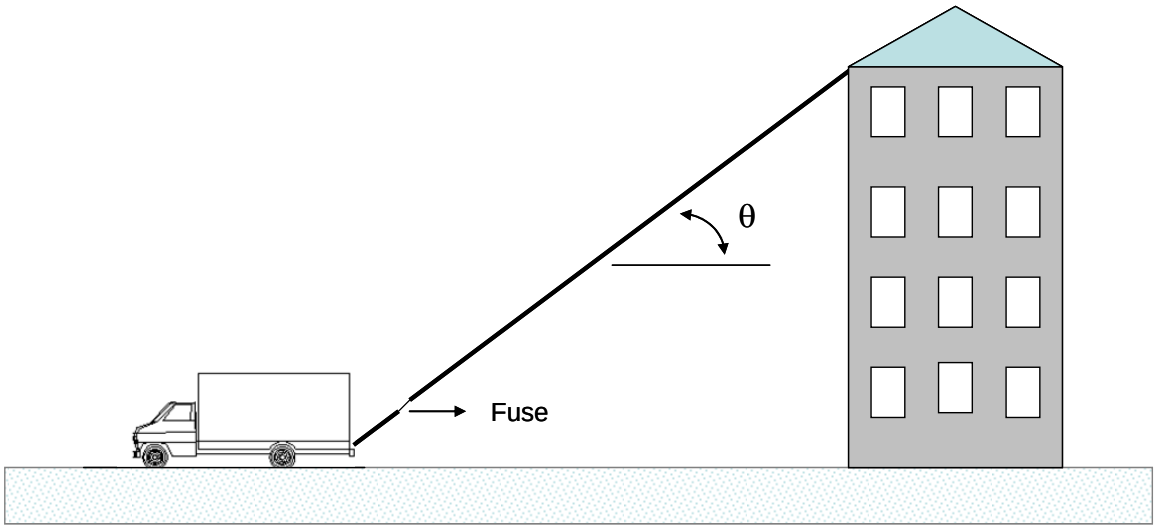

Figure 3.1 Free vibrations test

3.2.1 THEORY OF TEST SCREENING

The equation of movement for a structural system of N degrees of freedom that is subjected to a free vibration can be written as:

$$M\ddot{u}(t) + C\dot{u}(t) + Ku(t) = 0 \qquad (3.1)$$

where:

M = Mass matrix

C = Damping matrix

K = Stiffness matrix

$\ddot{u}(t), \dot{u}(t), u(t)$ = acceleration, velocity, and displacement vector

For most structures K and M are symmetric and positive definite matrices.

Through the following transformation of coordinates,

$$u(t) = \sum_{i=1}^{N} \phi_i \eta_i(t) \qquad (3.2)$$

where ϕ_i = mode shape "i"

Considering that the C matrix complies with the conditions of orthogonality [96], equation 3.1 is modified as follows

$$\ddot{\eta}_i(t) + 2\zeta_i\omega_i\dot{\eta}_i(t) + \omega_i^2\eta_i(t) = 0 \tag{3.3}$$

Since,

$\eta_i(t)$ = principal coordinates

ω_i = circular natural frequency "i"

ζ_i = modal damping factor "i"

The solution to equation (3.3) is (clough):

$$\eta_i(t) = e^{-\zeta_i\omega_i t\left(\eta_i(0)Cos(\omega_{d_i}t)+\left(\frac{\dot{\eta}_i(0)+\zeta_i\omega_i\eta_i(0)}{\omega_{d_i}}Sin(\omega_{d_i}t)\right)\right)} \tag{3.4}$$

where:

$$\omega_{d_i} = \omega_i\sqrt{1-\zeta_i^2} \tag{3.5}$$

In case of systems of low damping $(\zeta << 1)$, $\omega_{d_i} = \omega_i$.

The values of $\eta_i(0)$ and $\dot{\eta}_i(0)$ are determined by the initial conditions of the system and can be demonstrated by the following equation:

$$\eta_i(0) = \frac{\phi_i^t M u_0}{M_r}$$

$$\dot{\eta}_i(0) = \frac{\phi_i^t M \dot{u}_0}{M_r} \tag{3.6}$$

Since, $M_r = \phi_i^t M \phi_i$

In case of $\dot{u}(0) = 0$, considering that $\dot{\eta}_i(0) = 0$ and equation (3.4), it can be written as:

$$\eta_i(t) = e^{-\zeta_i \omega_i t\left(\eta_i(0)Cos(\omega_{d_i} t)+\left(\zeta_i \eta_i(0)Sin(\omega_{d_i} t)\right)\right)} \tag{3.7}$$

If the system has an initial deformation $u(0)$ contained only in mode shape "i": (3.8)

With A = constant (3.8)

Substituting (3.8) in (3.6), by condition of orthogonality:

$$\eta_j(0) = \begin{cases} A & si \ \ \text{j} = \text{i} \\ 0 & \text{si j} \neq \text{i} \end{cases} \tag{3.9}$$

Considering the above equations, equation (3.2) is written as:

$$u(t) = \phi_i R_i e^{(-\zeta_i \omega_i t)(Cos(\omega_{d_i} t - \psi_i))} \tag{3.10}$$

Where:

$$R_i = A\sqrt{1+\left(\frac{\zeta_i \omega_i}{\omega_{d_i}}\right)^2}$$

$$\psi_i = \tan^{-1}\left(\frac{\zeta_i \omega_i}{\omega_{d_i}}\right)$$

The above equations show that with a given deformation in equation 3.8, the structure vibrates solely in mode "i", oscillating as a system of 1DOF. For that reason, the

frequency of such mode can be obtained directly from the time recorded. The value of the damping factor can be obtained from the equation of logarithmic decrease for systems of 1DOF [97].

Considering the neper logarithm of the quotient of two maximum peaks (separated "n" periods) of equation 3.10, the following is obtained: (3.11)

$$\xi_i = \left(\frac{1}{2\pi n}\right)\ln\left(\frac{u_{\max_i}(t_1)}{u_{\max i}(t_1 + nT_i)}\right) \tag{3.11}$$

Since,

$u_{maxi}(t_1)$= peak positive at time t_1

$$T_i = \frac{2\pi}{\omega_d}$$

In practice, the initial deformation u_0 does not have the form of the first mode, even though it is common that the initial deformation is predominant. For structures with separate frequencies, the superior modes damps faster than the first, with the structure vibrating in its fundamental frequency, immediately after the recording is initiated. For that reason, using the records in the time domain, solely in just a few cases, the frequency of the second mode can be obtained.

Previous observations are also valid for the records of velocity or acceleration, with the observation of superior modes being more feasible in these cases, due to the fact that equation (3.10) would be multiplied by ω_i in the case of velocity and ω_i^2 in the case of acceleration, in the case of a low damping.

3.2.2 FREQUENCY DOMAIN ANALYSIS

Due to the limitations in the time-domain analysis for the study of the superior modes, this method is based on work performed in the frequency domain. In this way, the

frequencies, damping factors and modal shapes corresponding to the last modes can be obtained**.**

Fourier's techniques are used in this study, and the following is a brief overview of those techniques:

3.2.2.1 Frequency domain equations

The following section presents the equations to obtain the frequency (ω) and the damping factor (ζ) of a system through its transformation to the frequency.

3.2.2.2 Single degree-of-freedom systems (SDOF)

The displacement of a SDOF subject to free vibration is:

$$u(t) = \rho e^{-\zeta\omega_0 t} Cos(\omega_d t - \psi) \tag{3.12}$$

where ρ depends on the initial conditions. Let us introduce the equality of Euler

$$e^{\hat{j}x} = \cos x + \hat{j}\sin x$$

Substituting equation (3.12) in Euler's equation gives equation (3.13)

$$u(t) = \rho e^{-\zeta\omega t}\left(e^{\hat{j}(\omega_d t-\alpha)} + e^{-\hat{j}(\omega_d t-\alpha)}\right) \tag{3.13}$$

In order to account for the frequency domain in the above equation, the transformed equation of Fourier [98] can be applied, defined by:

$$h(p) = \int_{-\infty}^{\infty} h(t) e^{\hat{j}pt}\, dt \tag{3.14}$$

Applying the transformed equation of Fourier to the displacement result yields equation (3.15)

$$u(p) = \frac{\rho}{2}\left[\frac{e^{-\hat{j}\alpha}}{\hat{j}(p-\omega_d)+\zeta\omega} + \frac{e^{\hat{j}\alpha}}{\hat{j}(p+\omega_d)+\zeta\omega}\right] \tag{3.15}$$

3.2.2.2.1 Initial condition of displacement

Considering an initial displacement with a variable of velocity rule and low damping (ζ<<1), the following equation is obtained:

$$u(p) = \frac{u_o}{\omega}\frac{\zeta + \hat{j}(p/\omega)}{\sqrt{\left(1-(p/\omega)^2\right)^2 + \left(2\zeta(p/\omega)\right)^2}} e^{\hat{j}\sigma} \tag{3.16}$$

$$tg\sigma = \frac{2\zeta(p/\omega)}{1-(p/\omega)^2} \tag{3.17}$$

If $z = (p/\omega)$, we will obtain:

$$u(z) = \frac{u_o}{\omega}\frac{\zeta + \hat{j}z}{\sqrt{\left(1-z^2\right)^2 + \left(2\zeta z\right)^2}} e^{\hat{j}\sigma} \tag{3.18}$$

$$tg\sigma = \frac{2\zeta z}{1-z^2} \tag{3.19}$$

Simplifying equation (3.18):

$$u(z) = \frac{u_o}{\omega}\frac{\zeta(1+z^2) + \hat{j}z(1-2\zeta^2-z^2)}{\left(1-z^2\right)^2 + \left(2\zeta z\right)^2} \tag{3.20}$$

Generally, the module of the transformed equation is used to characterize the result, assuming again that (ζ<<1), which results in equation (3.21)

$$\|u(z)\| = \frac{u_o}{\omega} \frac{z}{\sqrt{\left(1-z^2\right)^2 + \left(2\zeta z\right)^2}} \tag{3.21}$$

3.2.2.2.2 Determination of the ω

Equation (3.21) is used to determine as to when the maximum of $\|u(z)\|$ occurs. The optimum result is described by Genatios [96]:

$$\|u(z)\|_{\max} = \|u(z=1)\| = \frac{u_0}{\omega} \frac{1}{2\zeta} \tag{3.22}$$

In a graph of z vs. ω, the point where the module is maximum corresponds to the frequency. Figure 3.2 shows the procedure.

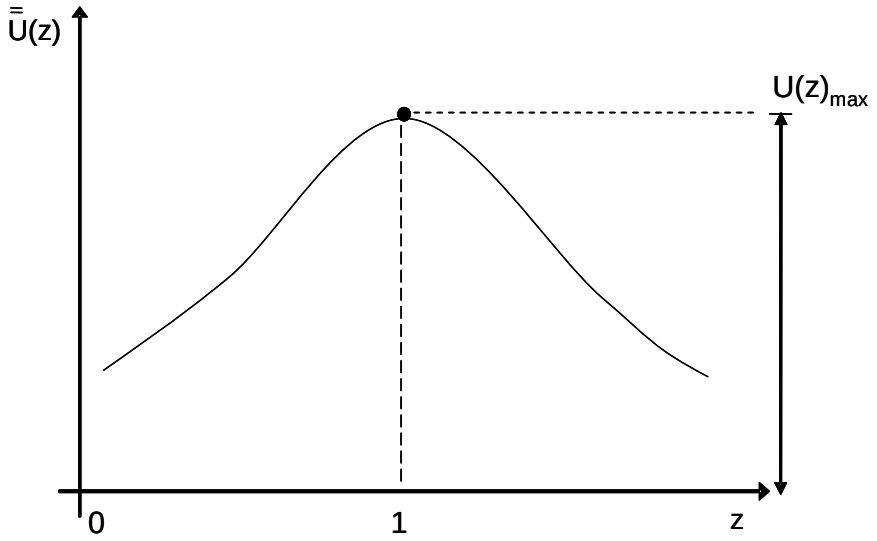

Figure 3.2 Determination of the ω

3.2.2.2.3 Determination of the ζ

There are various methods to calculate the damping factor; in this case, let us determine the damping factor according to the method of band width [97]. Let us examine the value

of $\|u(z)\| = \|u(z)\|_{\max} / \sqrt{2}$ .In the curve of answer in the frequency, there are two points that have that value

$\|u(z_1)\| = \|u(z_2)\| = \|u(z)\|_{\max} / \sqrt{2}$, This value is:

$$\frac{\|u(z)\|_{\max}}{\sqrt{2}} = \frac{u_0}{\omega\zeta}\frac{1}{2\sqrt{2}} = \frac{u_o}{\omega}\frac{z}{\sqrt{\left(1-z^2\right)^2 + (2\zeta z)^2}} \tag{3.23}$$

Where $z_i = z_1$ or z_2, Equation 3.23 may be rewritten as

$$z^4 - 2(1-2\zeta^2)z^2 + (1-8\zeta^2) = 0 \tag{3.24}$$

Whose roots are given by

$$z_1 = \sqrt{1-2\zeta+2\zeta^2}\ ,\ \ z_2 = \sqrt{1+2\zeta+2\zeta^2} \tag{3.25}$$

Assuming (ζ<<1) and neglecting high-order terms in ζ, we arrive at the result

$$z_1 = 1-2\zeta \ \text{ and } \ z_1 = 1+2\zeta \tag{3.26}$$

Using the binomial expansion, we get

$$z_1 = (1-2\zeta^2)^{1/2} = 1 - \frac{1}{2}2\zeta + \cdots \tag{3.27}$$

$$z_2 = (1+2\zeta^2)^{1/2} = 1 + \frac{1}{2}2\zeta + \cdots$$

Or, since (ζ<<1),

$$z_2 - z_1 = 2\zeta \tag{3.28}$$

Thus,

$$\zeta = \frac{1}{2}\frac{p_2 - p_1}{\omega} \tag{3.29}$$

Figure 3.3 shows the band-width method

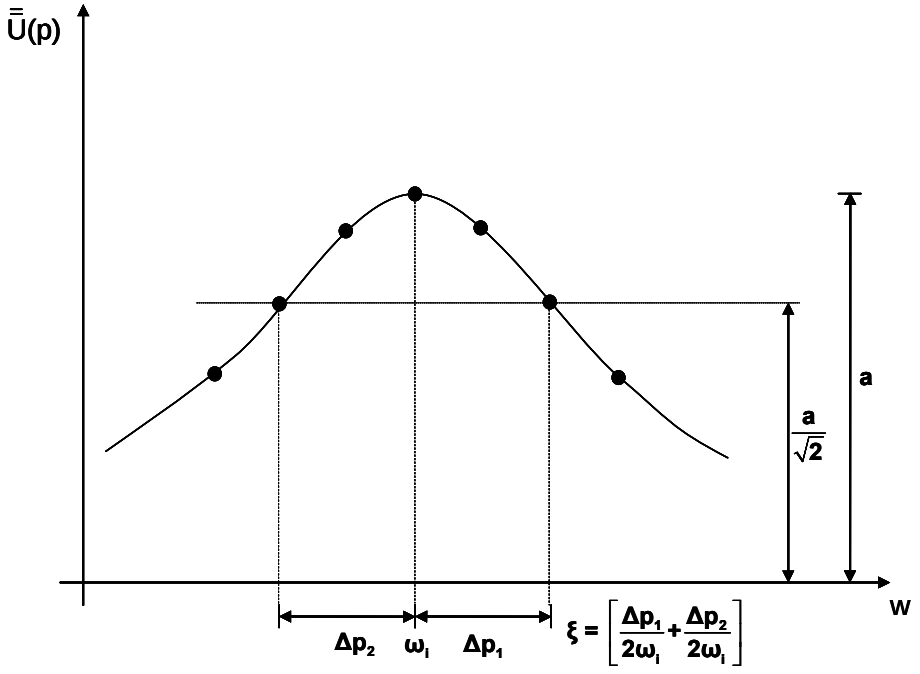

Figure 3.3 Response curve showing band-width method

3.2.2.3 Multiple degree-of-freedom systems (MDOF)

In the case of systems of MDOF, the displacement can be expressed as the sum of the modal contributions (eq. 3.2):

$$u(t) = \sum_{i=1}^{N} \phi_i \eta_i(t) \tag{3.2}$$

Let us consider the transformed equation of Fourier of equation (3.4), and the result is:

$$u(t) = \sum_{i=1}^{N} \frac{\phi_i \phi_i^t M u(0)}{\phi_i^t M \phi_i} \frac{(2\zeta_i + z_i(1 - z_i^2 - (2\zeta_i)^2)}{\omega_i (1 - z_i^2)^2 + (2\zeta_i z_i)^2} \hat{i} \tag{3.30}$$

The above expression can be written for DOF "j" as:

$$U_j(\omega) = \sum_{i=1}^{N} U_{ji}$$

where:

$$U_{ji} = \sum_{k=1}^{N} \frac{\phi_k \phi_k^t M u(0)}{\phi_k^t M \phi_k} \frac{(2\zeta_i + z_i(1 - z_i^2 - (2\zeta_i)^2)}{\omega_i (1 - z_i^2)^2 + (2\zeta_i z_i)^2} \hat{i} \tag{3.31}$$

Therefore, under common suppositions (low damping and well-separated frequencies), modal interference can be neglected in the area of the resonance and the same techniques can be applied to determine the frequency of resonance and damping factor ω_i and ζ_i. The modal forms can be constructed by evaluating the magnitude of the displacement (eq. 3.31) and the corresponding phase for the frequency of interest.

3.3 DATA PROCESSING

3.3.1 FOURIER ANALYSIS OF SIGNALS

Time-domain data is very difficult to interpret, which makes it necessary to work in the frequency domain. The process of converting the analogue time-domain signal into a digital frequency-domain signal is carried out inside a spectrum analyzer, where the energy of a signal is separated into various frequency bands through a set of filters, and the method used is called Fourier transform.

Fourier transform is a method of analysis that is used on linear systems to recast a problem in a format that can be solved more readily than is possible in the original format. For the application of transient response prediction of structures, the Fourier transform is widely used. More specifically, a version known as the discrete Fourier transform (DFT) is often used, as this can very readily be implemented by using an efficient set of algorithms on computers, known as the 'fast Fourier transform' (FFT).

3.3.2 FOURIER RESPONSE INTEGRAL

For any signal *x(t)*, which is periodic, an interval T can be decomposed into a constant part and infinite series of harmonic contributions. When superimposed, these result in the original total time-signal function. This harmonic decomposition results in a Fourier series for the signal [99]:

$$x(t) = \sum_{-\infty}^{\infty} X_n e^{\hat{i}\omega_n t} \tag{3.32}$$

$$X_n = \frac{1}{T}\int_0^T x(t) e^{-\hat{i}\omega_n t}\, dt \tag{3.33}$$

ω_n is the fixed repetition frequency of the excitation corresponding to the period T. The frequencies of the harmonic components are multiples of the frequency ω_n. By letting $T \to \infty$, equation (3.33) becomes an integral, so that for a continuous function we get the Fourier transform pair [99]:

$$x(t) = \int_{-\infty}^{\infty} X(\omega) e^{\hat{i}\omega t}\, d\omega \tag{3.34}$$

$$X(\omega) = \frac{1}{2\pi}\int_{-\infty}^{\infty} x(t) e^{-\hat{i}\omega t}\, dt \tag{3.35}$$

which are known as the direct and inverse Fourier transforms, respectively.

3.3.3 DISCRETE FOURIER TRANSFORM (DFT)

The Discrete Fourier Transform (DFT) is an approximate formula for calculating the coefficients of the Fourier series. In most practical applications, a signal is discretized taking a section and dividing it into J discrete points (at $t=t_k$, k=1..J). The Fourier representation of the section is then [99]:

$$x(t_k) = x_k = \sum_{n=0}^{J-1} X_n e^{\hat{i}k(2\pi/J)n} \qquad (3.36)$$

where

$$X_n = \frac{1}{J}\sum_{k=1}^{J} x_k e^{-\hat{i}k(2\pi/J)n} \qquad \text{for n = 1…, J} \qquad (3.37)$$

Equation (3.36) is known as the discrete Fourier series of signal and equation (3.37) is known as its discrete Fourier transform (DFT).

3.3.4 FAST FOURIER TRANSFORM (FFT)

The Fast Fourier Transform, which allows very efficient and accurate evaluations of the discrete Fourier transforms, is based on an algorithm developed by Cooley and Tukey [100]. The complete calculation requires fewer operations than evaluation of the transform directly, and this means that are fewer rounding errors in the computation. Overall, this results in quicker and more accurate procedure, which is widely used in practice.

3.3.5 RELATED TOPICS IN SIGNAL ANALYSIS

In the Fourier transformation of any signal, there is a basic relationship between the sampling duration, T; the number of discrete values, J; the sampling rate, $f_{s;}$ and the frequency resolution, $\Delta f = 1/T$. The range of spectrum is 0-f_{nyq}, where f_{nyq} is the Nyquist frequency given by $f_{nyq} = 1/2T$ as the size of transform N is generally fixed for a given analyzer at a power of 2 (256, 512, 1024, etc.). f_{nyq} and Δf are determined by sample time length T. This fact introduces constraints and descretisation approximations, which may lead to errors. Hence, there is a need to limit the length of the time history. Some important features to reduce these errors are:

3.3.5.1Aliasing

Two sinusoidal signals of different frequencies can produce identical signals. Figure 3.4 shows an example of this phenomenon, where the crosses represent the sampled data points. The problem is caused by a sampling rate that is very low, as a result of which high frequencies appear as low frequencies. The problem can be avoided by maintaining the sampling rate below the Nyquist frequency, which is twice the highest frequency of interest.

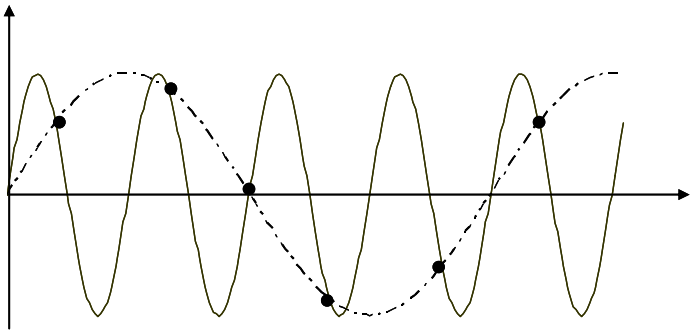

Figure 3.4 Aliasing phenomena

3.3.5.2 Leakage

One problem with the analysis of vibration data is that the signal is assumed to be periodic over the sampling interval chosen. In general, this will not be true and leads to a

problem known “Leakage”. Figure 3.5 illustrates the problem, showing a sinusoidal signal with one sampling interval equal to an integer multiple of the signal period and a second different sampling interval. As the signal is sinusoidal, the Fourier transform should only be non-zero at one frequency. In the second case, leakage has caused some of the power contained in the frequency of the sinusoidal to “leak” into adjacent frequencies. Leakage can be corrected by the use of window functions.

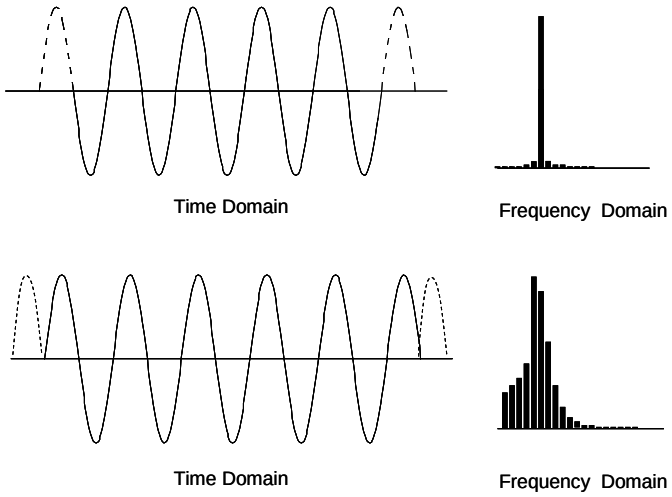

Figure 3.5 Sample length and leakage of spectrum

3.3.5.3 Windowing

The windowing involves multiplying the original signal by a prescribed time function before performing the Fourier transform. The result of this mathematical operation is to provide a sampled time waveform that appears to be continuous and periodic. Discontinuities are “filled in” by forcing the sampled signal to be equal to zero at the beginning and end of the sampling period (window).

However, in using a window, there is a trade-off between the ability to resolve frequencies and the resolution of amplitudes. If the window function (Rectangular Window) is not applied, the frequency and amplitude resolution is excellent, provided the signal is periodic and fits the time sample exactly. For example, with a sine wave that

starts at zero at the beginning of the sample, it would also need to finish at zero to give good resolution. If it does not, the waveform has the characteristics of a sine wave and a square wave -- that gives rise to “leakage” into the bins on either side of the main frequency on our FFT. Most windows, for this reason, ensure that the signal starts and finishes in our time sample at the same level, thus avoiding the need for a synchronous signal.

There are many available windowing functions. Rectangular (actually no window), Flat-Top, Hamming, Kaiser–Bessel, and Hanning are some of the windowing functions available. Perhaps, the most commonly used window is Hanning (raised cosine). It is good to analyze sine waves, as it provides a good compromise on both frequency and amplitude resolution.

3.3.5.4 Averaging

When an FFT is produced, the instrument uses a digitized time waveform and performs the mathematical operation to produce the FFT. However, observation of only one section of time waveform may exclude some peak caused by the influence of a random vibration. To minimize this, it is common to consider several sections of the time waveform, calculate several FFTs, and display an average result. Four averages are commonly taken.

Averaging is available in most FFT analyzers to assist in interpreting data. Averaging provides more repeatable results in data collection and is an early indication of machine deterioration. Averaging also helps in the interpretation of complex, noisy signals.

3.4 PRACTICAL CONSIDERATIONS IN THE FREE VIBRATIONS TEST

The following text presents some recommendations to carry out dynamic tests of free vibration. These recommendations are acquired from experience acquired during the

performance of dynamic tests at the Institute of Materials and Structural Models (IMME) of the *Universidad Central de Venezuela.* This summary is taken from Genatios [96], Genatios [95], Genatios et al. [101], Lopez et al. [102], and Garcia [103].

Before the execution of a dynamic test, it is required and mandatory to perform a simulation of the structure to be tested and the techniques to be applied. This will allow to determine the band of frequency that is to be studied, thereby, defining the type of test to be used and the resources for measurement and excitation of the structure. Also, through the simulation of a modal analysis, possible problems of processing of the signal can be avoided and the most suitable strategy for the test and the most suitable processing technique can be established [103].

Genatios [96] suggests that before a dynamic test of free vibration is performed, it is recommended to ask yourself four questions, the answers of which will determine the strategy of a test to be applied:

a) Where to apply the initial displacement? At what level of the structure?
b) Where to measure? At what level?
c) What kinds of record to use?
d) What is the influence of the structural typology on the answer?

The answers to these questions will allow deciding on the test strategies to be implemented, in particular, if we want to study the first mode above the superior ones.

a) Site of application of the load. The form of the initial condition (displacement or velocity) given to the structure will define the initial component which will determine the amplitude of each vibration mode. If a deformation containing strong components of the superior modes is introduced, these (the components) will strongly appear in the Fourier transform of the answer. In the case of a regular building, if a load is applied on a lower floor, we will have a major contribution of the superior modes in the answer. Whereas if a load is applied on the last floor, the initial deformation is similar to the first mode of vibration, and it

is convenient for the study of the fundamental mode, in which case the contribution of the superior modes will be reduced.

b) Site of measurement of the answer. In case of maximization of the answer of the superior modes and following recommendations given above, data will be collected from the site where major contributions of the superior modes will be produced. It is suggested that measurement instruments be placed at inferior levels, where superior modes have greater participation.

In the case of study of the fundamental mode of a regular building, the last floor will have priority for the placement of instruments, if the first mode is required to be registered. If there is a need to precisely record a certain mode or frequency, it has to be observed that the instruments should not to placed in an area where a possible "node" (point where a modal coordinate is null or close to zero) might be present for that vibration mode, since a good recording of the desired frequency will not be obtained. Whereas if we want to eliminate the influence of an undesired mode, it is advised that measurements be taken where its coordinate is minimum [102].

Let us review the answer of displacement and acceleration for a NGDL system

$$u(t) = \sum_{i=1}^{N} \phi_i \eta_i(t) \tag{3.2}$$

$$\ddot{u}(t) = \sum_{i=1}^{N} -(\omega_i^2)\phi_i \eta_i(t) \tag{3.38}$$

c) From the above equations, it is observed that in the case of the result of accelerations, the result to each mode is multiplied by ω_i^2. The values of ω_i will increase as the mode increases. For that reason, it is recommended to use the records of acceleration for the study of the superior modes and the records of displacement to determine the properties of the first mode. The case of the records of velocities is an intermediate case, since they are multiplied by ω [102].

d) The structural typology has a strong influence on the possible separation of the natural frequencies of the vibration of a building. As frequencies are quite close to

each other, there is a less possibility of modal interference as it is easier to carry out the modal analysis.

3.5 PRACTICAL CONSIDERATIONS FOR THE TEST AND APPLICATION OF FOURIER TRANSFORM

As already stated, there is a need to work in the frequency domain, in order to obtain the greatest possible information of the last mode shapes. The FFT, which is the most common technique applied for the modal analysis, is applied in this study. The following recommendations are provided in order to make proper use of the Fourier transform [96]:

- Define a value as $\Delta\omega,<\zeta\omega$
- Define a value ω_{max} as to be a minimum of four times greater than the maximum frequency of vibration expected to be measured.
- If $\Delta\omega$ and ω_{max} are established**,** then the number of points to be analyzed will be determined by $n = 2\omega_{max} / \Delta\omega$, n being the result of elevate 2 to a integral base of M, such that $n > 2\omega_{max} / \Delta\omega$

  The following values are defined: $\Delta t = \pi / \omega_{max}$

  $T_{max} = 2\pi / \Delta\omega$

The resultant discrete time record is determined by these variables.

3.6 CONCLUSIONS

In the bibliographic summary of the Chapter 2, a review of some methods was made to determine damage in structures using modal analysis. This review shows the link between the type of dynamic test and the method of damage detection. So, the type of method for damage identification to be applied is determined by the specificity of the

requirement or the damage to be measured. The objectives pursued in the dynamic test have to be established a priori in order to correspond to the method of identification chosen. The type of test, the form, and the site of excitation of the structure, and the instruments and location of the transducers are established according to the variables to be measured.

It is recommended that the performance of a previous numeric simulation of the structure be considered, in order to obtain an approximation of possible values of frequency and modal forms. It is also recommended that a simulation of the modal analysis be performed, in order to control the variables that determine the processing of the signal.

The test of free vibration allows to perform a single dynamic test which depends on the initial condition input into the system. The processing of data obtained from a test of free vibration can be performed following the method commonly used for the analysis of the frequency domain.

4. TEST PROGRAMME OF EXPERIMENTAL MODELS

4.1 INTRODUCTION

This chapter describes a series of experimental test developed in this work and its results. The aim of the test performed on three models was to assess the change in linear behavior with increase in the extent of damage. In addition to the vibration tests, static load tests and numerical simulation were also performed. For each model, the principal objectives of its test programme can be summarized as follows:

- Geometric and mechanical characterization of model.
- Determination of modal parameters from numerical simulation.
- Obtaining the flexibility matrix from static test.
- Determination of modal parameters from free vibration test.

4.2 FRAMED BUILDING EXPERIMENTAL MODEL

The structural model (figure 4.1) is a simplified frame building of three levels and one span. The model has 4 steel columns of 4 mm width, with rigid acrylic plastic slabs. Simplified hypothesis are applied to represent the structural model in terms of lateral floor displacements, depending only on the flexural behavior of the columns. A single lateral stiffness coefficient can then be determined for each level. Table 4.1 presents the geometric and mechanical properties of the model.

Total height		32.09 cm
Bay length		0.20 m
Cross-section of the columns (w x t)	Floor 1	0.1777 m x 3.86 x 10^{-3}m
	Floor 2	0.1798 m x 3.86 x 10^{-3}m
	Floor 3	0.1772 m x 3.86 x 10^{-3}m
Total mass (model and accelerometers)		2.716 kg
Modulus of elasticity		213.6 GPa

Table 4.1 Geometric and mechanical properties of the model

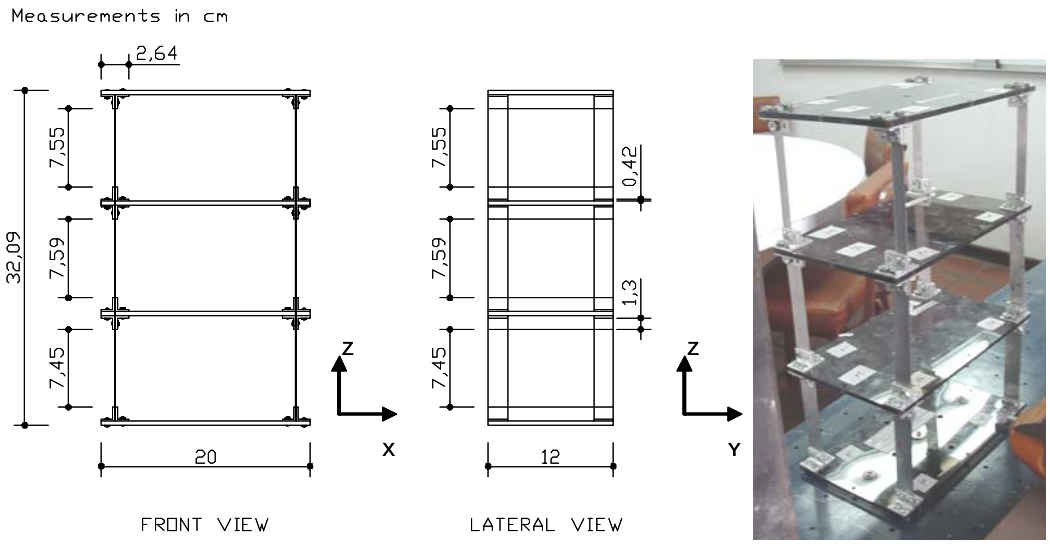

Figure 4.1 Tested model

4.2.1 MATERIALS

Strain tests were conducted on steel specimens in order to determine elastic modulus. Three tensile specimens were tested and the results summarized in Table 4.2. Representative strain–stress curves for #1, #2, and # 3 deformed specimens are shown in Figure 4.2

Specimen	Maximun Stress (Mpa)	Modulus (Gpa)
1	545.69	218.91
2	534.15	216.94
3	501.39	204.94

Table 4.2 Steel Properties

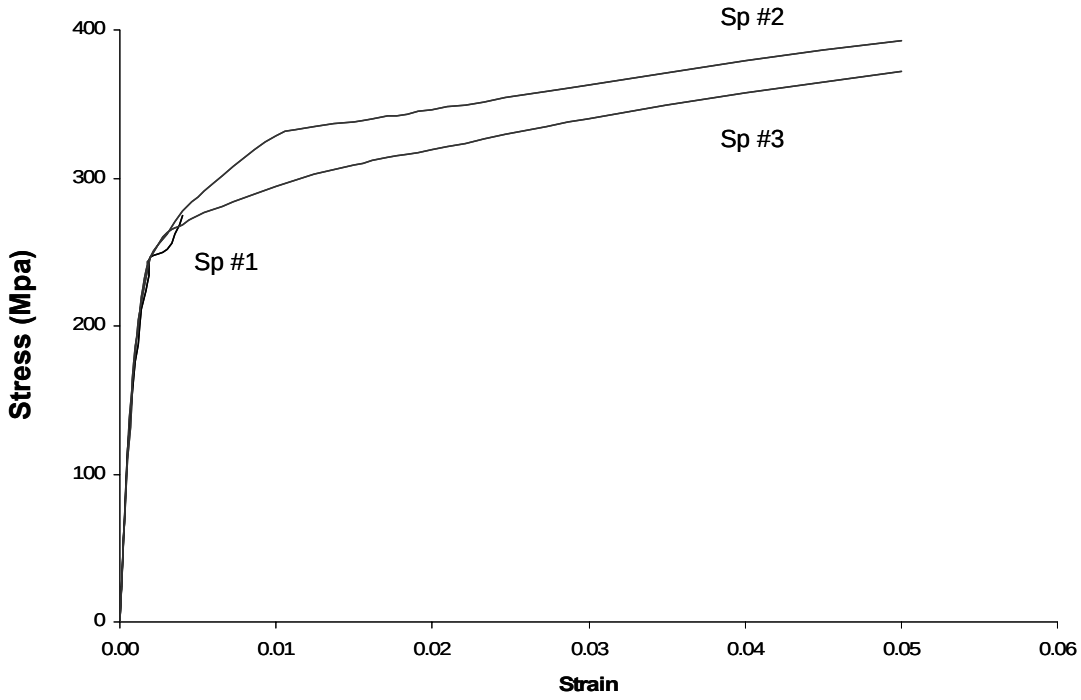

Figure 4.2 Strain–Stress Curves of Steel

4.2.2 ANALYTICAL MODEL

The Framed model was modelled analytically with undeformable slab with lumped mass values and columns with infinite axial stiffness. K is a banded matrix and M is a diagonal matrix:

$$\text{MASS MATRIX} \qquad M = \begin{bmatrix} 0.9331 & 0 & 0 \\ 0 & 0.9324 & 0 \\ 0 & 0 & 0.9034 \end{bmatrix} \text{kg} \tag{4.1}$$

$$\text{STIFFNESS MATRIX} \qquad K = \begin{bmatrix} 4.100 & -2.015 & 0 \\ -2.015 & 4.065 & -2.049 \\ 0 & -2.049 & 2.049 \end{bmatrix} * (kN/m) \tag{4.2}$$

FLEXIBILITY MATRIX $$F = \begin{bmatrix} 0.480 & 0.480 & 0.480 \\ 0.480 & 0.976 & 0.976 \\ 0.480 & 0.976 & 1.464 \end{bmatrix} (m/kN) \quad (4.3)$$

Using matrices (4.1) and (4.2), the natural frequencies and mode shapes were obtained:

ω_1 (rad/s)	ω_2 (rad/s)	ω_3 (rad/s)
20.09	56.15	80.39

Table 4.3 Natural frequencies from analytical model

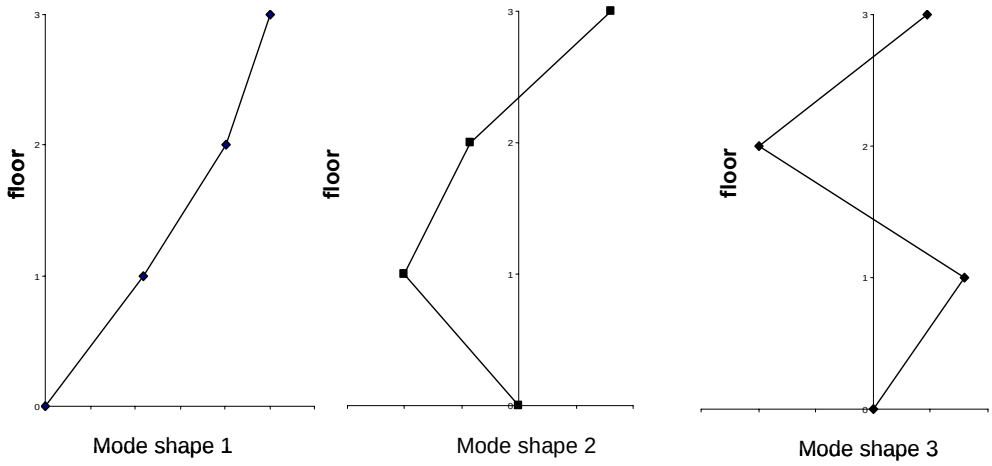

Figure 4.3 Mode Shapes from analytical model

4.2.3 FLEXIBILITY TEST

The flexibility characteristics of the model structure for the lateral displacement degrees of freedom at each floor level were obtained. From the mass matrix and the flexibility experimental matrix, the frequencies and the mode shapes are calculated and then compared with the analytical and experimental results from the free vibration test.

The structure was loaded at each floor slab level, as illustrated in Figure 4.4. During the tests, displacement transducers (LDVT`S) were used to measure the lateral displacements at each floor level.

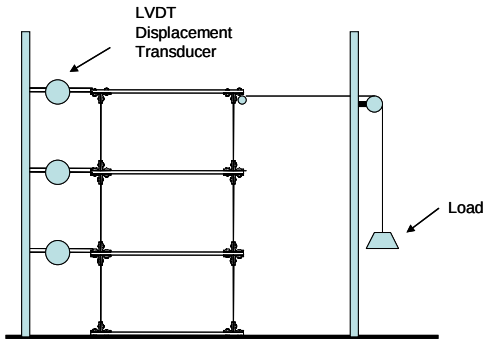

Figure 4.4 Test for determining the lateral Flexibility of the framed model

The results of the tests are shown in equation (4.4) in the form of the flexibility matrix of structure; each column "j" of the matrix (4.4) is generated during the loading of the floor at level "j". The terms $f_{1,j}$ to $f_{3,j}$ of column "j" represent the lateral displacements at the successive floor levels (1-3) of the structure as shown in Figure 4.5, when loaded with a load applied at level 3.

FLEXIBILITY MATRIX
$$F = \begin{bmatrix} 0.534 & 0.533 & 0.532 \\ 0.533 & 1.089 & 1.088 \\ 0.532 & 1.088 & 1.646 \end{bmatrix} (m/kN) \qquad (4.4)$$

STIFFNESS MATRIX
$$K = \begin{bmatrix} 3.655 & -1.787 & 0 \\ -1.787 & 3.577 & -1.787 \\ 0 & -1.787 & 1.789 \end{bmatrix} * (kN/m) \qquad (4.5)$$

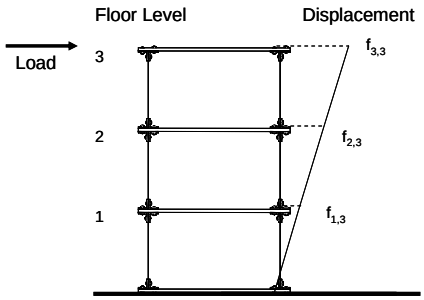

Figure 4.5 Correspondence of the flexibility coefficients, 3rd column of the flexibility matrix.

The natural frequencies and mode shapes derived from the matrices (4.5) and (4.1) are:

ω_1 (rad/s)	ω_2 (rad/s)	ω_3 (rad/s)
19.94	55.23	79.22

Table 4.4 Natural frequencies from flexibility test

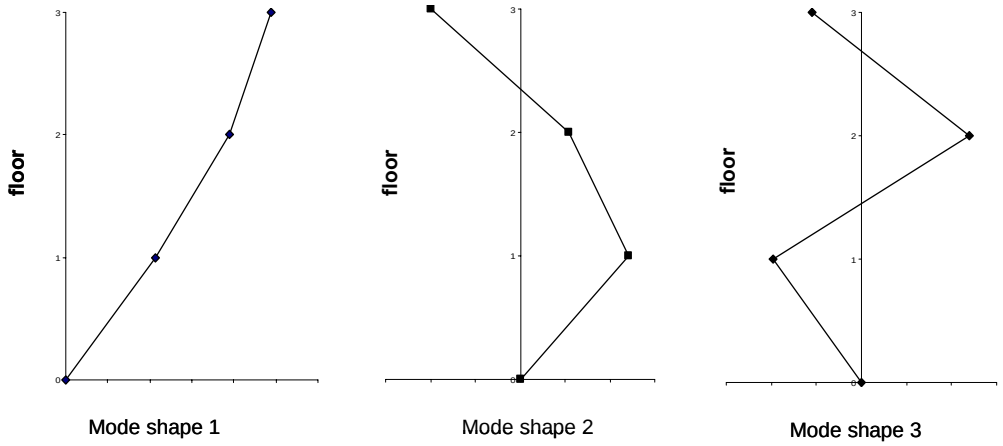

Figure 4.6 Mode Shapes from flexibility test

4.2.4 FREE VIBRATION TEST

To verify the experimental effectiveness of the damage estimation method presented in chapter 5, we tested the dynamic mode shapes of one model structure. The physical parameter of the model is identified by using the dynamic data from the assays.

The model was subjected to a free vibration test, applying an initial displacement or velocity in the slab. As a result, a total of 3 responses in the lateral direction (along the X-axis) were recorded in one series. Six series for each case of study (section 5.4) was recorded. Each series contained the accelerations of slabs due to initial displacement or velocity in one of the three slabs.

4.2.4.1 System identification

The model was clamped to an experiment bench, and submitted to free vibration tests by applying specified initial displacements or velocities to each slab (along the x-axis). The acceleration was measured by three accelerometers (Kinemetrics FBA-11 single-axis force balance) placed in each slab. Each accelerometer was connected to one channel of Altus K2 Digital Recorder. Altus K2 is a signal conditioner unit that is used to improve the quality of the signals by removing undesired frequency contents (filtering) and amplifying the signals. More details on Altus K2 can be accessed at www.kinemetric.com [104].

For each channel, the analog signal passed through a signal-conditioning amplifier and then through a simple, RC-analog, anti-alias filters. The DSP (digital signal processor) filters and decimates the 2000 sps data from the ADCs (analog-to-digital) using multi-rate FIR (finite impulse response) filters. After decimation, the number of samples in each record was 8192 with a sampling interval of 4 ms, corresponding to a sampling frequency of 250 Hz and a Nyquist frequency of 125 Hz. The signals converted to a digital form are stored on the hard disk of a data-acquisition computer. Figure 4.7 shows the instrumentation system used in the framed model test.

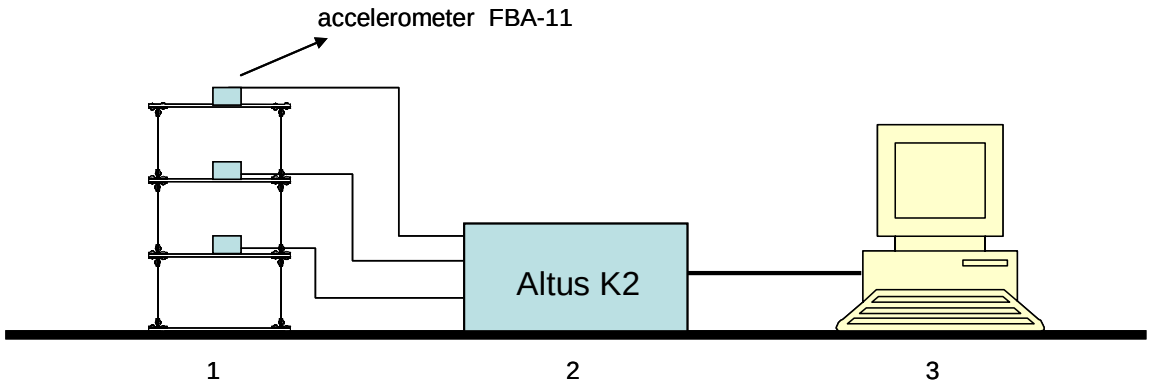

Figure 4.7 Instrumentation system

4.2.4.2 Modal parameters

Figure 4.8 presents a schematic representation of output-only modal identification. The time response (figure 4.9) was converted to a frequency domain by applying FFT to 8192 points (Figure 4.10). The experimental modal identification was carried out using the peak picking technique [105], and this method yielded satisfactory result because the damping was low and the mode shapes were well separated.

The dynamic properties were assessed using a software system developed to process structural dynamic signals in experimental tests (SADEX) (Figure 4.11) [106]. For this test, the damping was estimated using the half power method and logarithmic decrement [107]. Once the natural frequency was estimated, its corresponding mode shape was constructed by inspection of the amplitude and phase angle of spectral density.

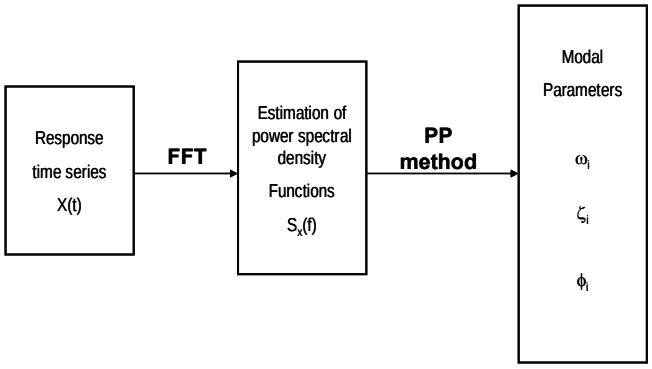

Figure 4.8 Schematic representation of output-only modal identification

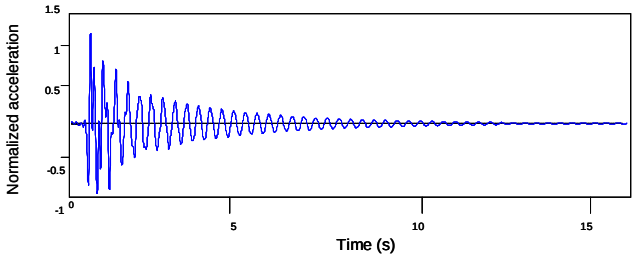

Figure 4.9 Acceleration time response Framed model (3rd Floor)

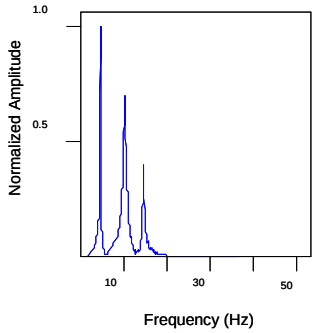

Figure 4.10 Power spectral densities (3rd Floor)

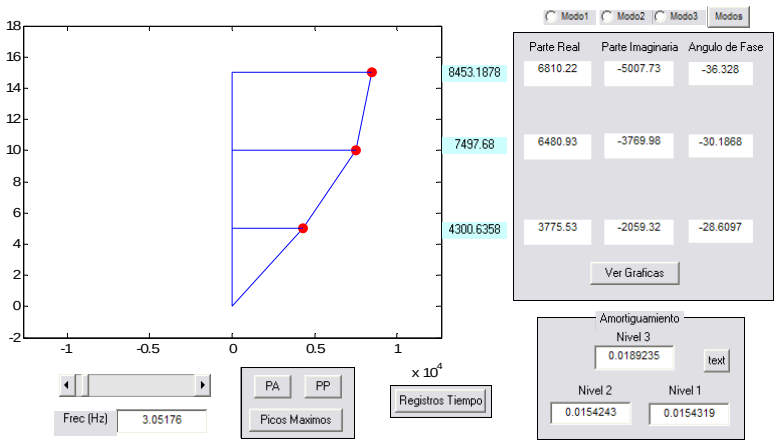

Figure 4.11 SADEX structural software identification

The three identified frequencies of the test framed model for undamaged and each damaged state are summarized in Table 4.5. Figures 4.12–4.14 show the mode shapes and Table 4.6 presents the damping ratios.

	ω_1 (rad/s)	ω_2 (rad/s)	ω_3 (rad/s)
Undamaged	19.16	52.72	78.56
Case b	17.09	49.83	---
Case c	14.95	47.19	76.82
Case d	16.46	43.54	62.77

Table 4.5 Natural frequency from the free vibration test

	ζ_1	ζ_2	ζ_3
Undamaged	0.0183	0.0205	0.0115
Case b	0.0217	0.0109	---
Case c	0.0273	0.0112	0.0142
Case d	0.0140	0.0188	---

Table 4.6 Damping ratio from the free vibration test

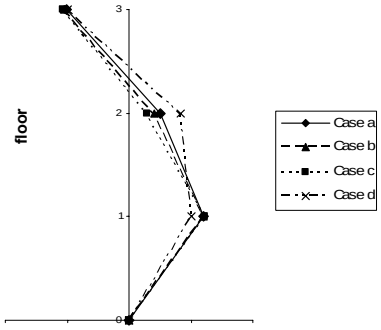

Figure 4.12 First mode shape from free vibration test

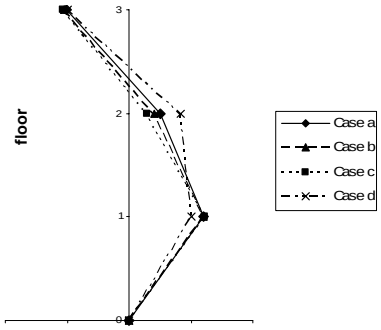

Figure 4.13 Second mode shape from free vibration test

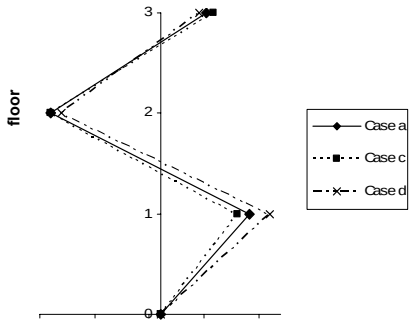

Figure 4.14 Third mode shape from free vibration test

4.3 SIMPLE SUPPORTED BEAM EXPERIMENTAL MODEL

We have tested the method on a wide-flanged steel I-beam (IPN 80), with an 80 mm deep web and a 42 mm wide flange. The beam is 4100 mm long, with 4 meters suspended between the two outermost supports. This part of the beam is divided into 5 sections of 800 mm. The outer supports are elastomeric bearings (Figure 4.15).

In order to obtain lower values of the beam's modal frequencies and facilitate the process of obtaining a variety of modal shapes, the beam was supported by flanges. Table 4.7 presents the geometric and mechanical properties of the model.

Total Length	4.05 m
Section Length	0.80 m
$\mathbf{I_{xx}}$=5.69 cm^4, $\mathbf{I_{yy}}$=74.9 cm^4, **A**= 7.66 cm^2	
Total weight (model and accelerometers)	22.84 kg
Elastic Modulus	209.5 GPa

Table 4.7 Geometric and mechanical properties of the simply supported beam

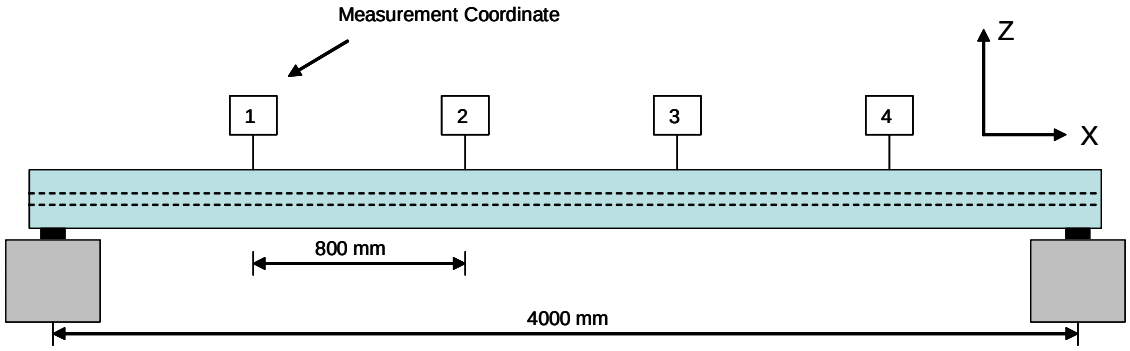

Figure 4.15 Tested model

4.3.1 MATERIALS

The simple supported beam was loaded in the middle of the span (figure 4.16) in order to determine EI coefficient. The average EI is obtained from the Force Vs displacement graphic (figure 4.17). Finally the elastic modulus is obtained from the equation (4.7).

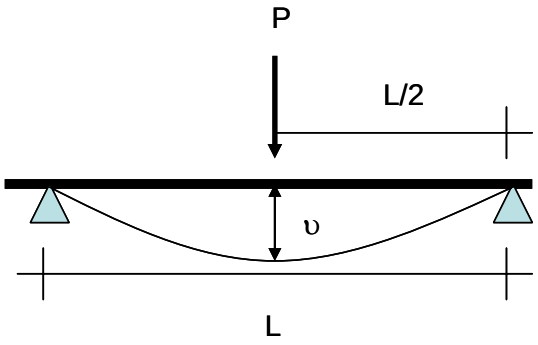

Figure 4.16 Test to obtain the coefficient EI

$$EI = -\frac{PL^3}{48\upsilon} \tag{4.6}$$

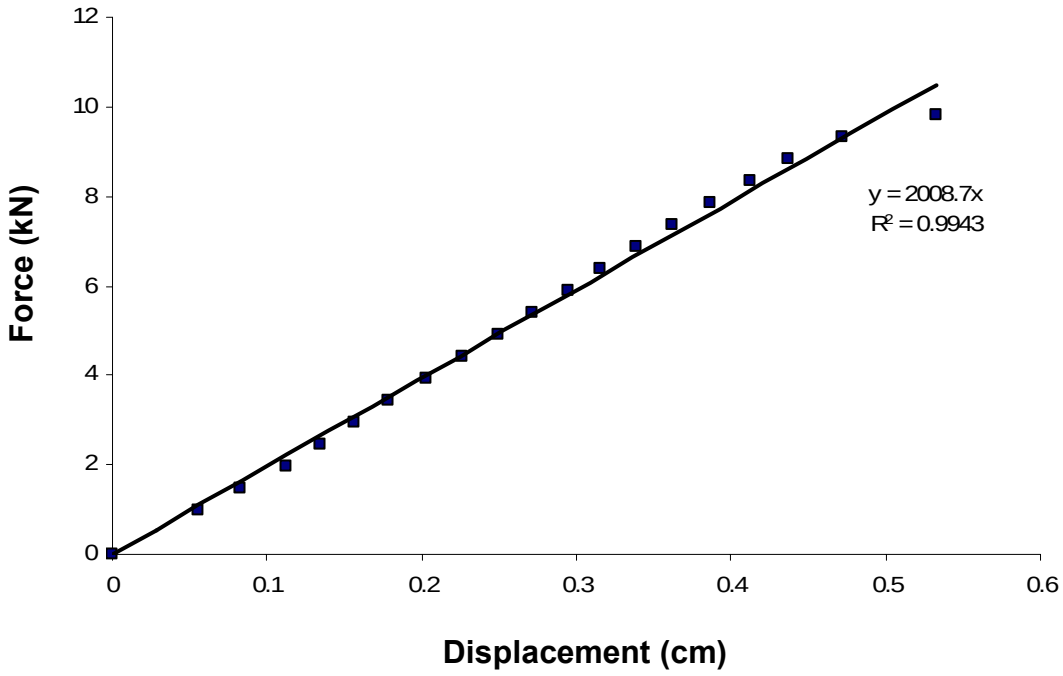

Figure 4.17 Beam force Vs Displacement

Average EI	12.607 kN
Modulus Elasticity (E)	215.01 GPa
Inertia Section	5.83 cm^4

Table 4.8 Steel Properties

4.3.2 ANALYTICAL MODEL

The simple supported beam was modeled analytically considering only flexure deformation and lumped mass values.

MASS MATRIX
$$M = \begin{bmatrix} 5.961 & 0 & 0 & 0 \\ 0 & 5.675 & 0 & 0 \\ 0 & 0 & 5.678 & 0 \\ 0 & 0 & & 5.967 \end{bmatrix} \text{kg} \quad (4.7)$$

STIFFNESS MATRIX
$$K = \begin{bmatrix} 2.3854 & -2.2953 & 0.9985 & -0.2496 \\ -2.2953 & 3.3840 & -2.5449 & 0.9985 \\ 0.9985 & -2.5449 & 3.3840 & -2.2953 \\ -0.2496 & 0.9985 & -2.2953 & 2.3854 \end{bmatrix} * 10^{5} \ (kN/m) \quad (4.8)$$

FLEXIBILITY MATRIX
$$F = \begin{bmatrix} 0.4416 & 0.6210 & 0.5520 & 0.3174 \\ 0.6210 & 0.9936 & 0.9384 & 0.5520 \\ 0.5520 & 0.9384 & 0.9936 & 0.6210 \\ 0.3174 & 0.5520 & 0.6210 & 0.4416 \end{bmatrix} * 10^{-4} \ (m/kN) \quad (4.9)$$

Using of matrices (4.7) and (4.8) the natural frequencies and mode shapes were obtained:

ω_1 (rad/s)	**ω_2 (rad/s)**	**ω_3 (rad/s)**	**ω_4 (rad/s)**
25.57	100.92	223.47	372.08

Table 4.9 Natural frequencies from analytical model

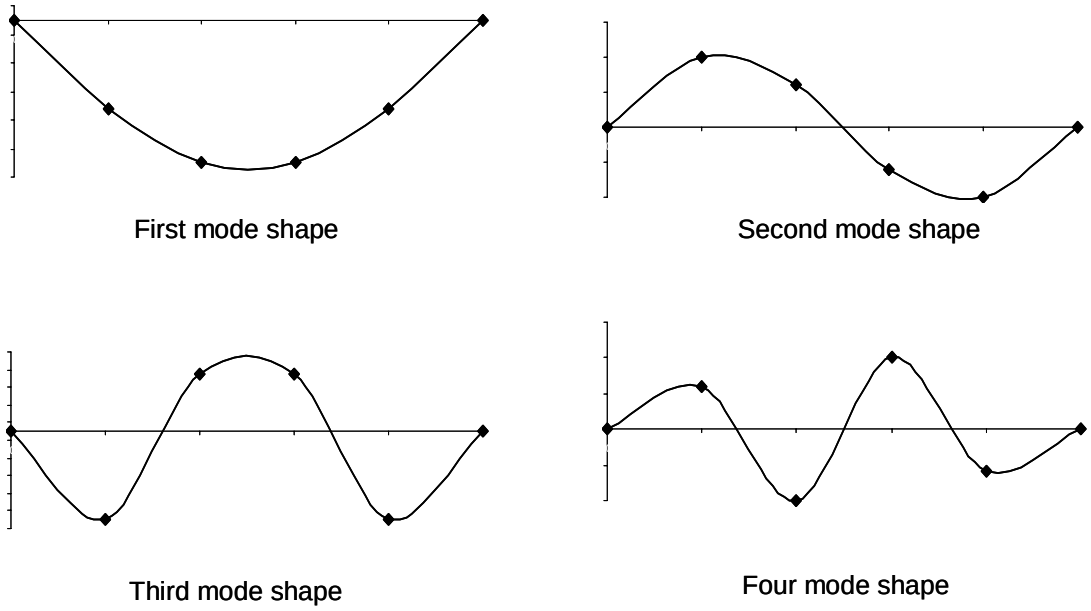

Figure 4.18 Mode Shapes from analytical model

4.3.3 FLEXIBILITY TEST

The flexibility characteristics of the beam for the lateral displacement degrees of freedom at each point were obtained. From the mass matrix and the flexibility experimental matrix, the frequencies and the mode shapes are calculated and then compared with the analytical and experimental results from the free vibration test.

The beam was loaded at each floor slab level, as illustrated in Figure 4.19. During the tests, displacement transducers (LDVT`S) were used to measure the lateral displacements at each point.

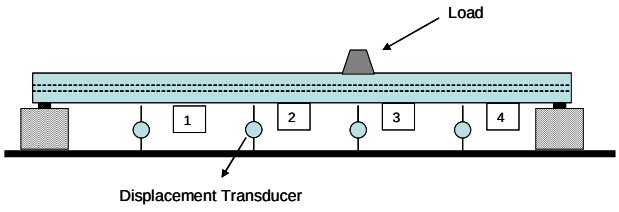

Figure 4.19 Test for determining the lateral Flexibility of the simply supported beam

The results of the tests are shown in equation (4.10) in the form of the flexibility matrix of structure; each column "j" of the matrix (4.10) is generated during the loading of the coordinate at point "j". The terms $f_{1,j}$ to $f_{4,j}$ of column "j" represent the vertical displacements at the successive points (1-4) of the structure as shown in Figure 4.20, when loaded with a load applied at point 3.

$$\text{FLEXIBILITY MATRIX} \quad F = \begin{bmatrix} 0.4415 & 0.6285 & 0.5523 & 0.3164 \\ 0.6285 & 0.9975 & 0.9357 & 0.5474 \\ 0.5523 & 0.9357 & 0.9639 & 0.6055 \\ 0.3164 & 0.5474 & 0.6055 & 0.4438 \end{bmatrix} * 10^{-4} \ (m/N) \quad (4.10)$$

$$\text{STIFFNESS MATRIX} \quad K = \begin{bmatrix} 3.7630 & -4.3198 & 2.6250 & -0.9359 \\ -4.3198 & 6.5329 & -5.1695 & 2.0746 \\ 2.6250 & -5.1695 & 5.5102 & -3.0126 \\ -0.9359 & 2.0746 & -3.0126 & 2.4436 \end{bmatrix} * 10^{5} \ (kN/m) \quad (4.11)$$

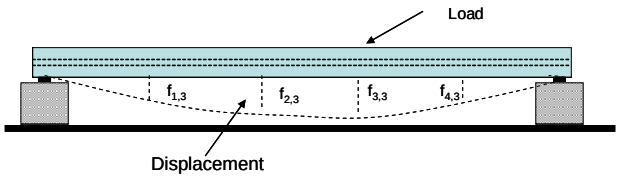

Figure 4.20 Correspondence of the flexibility coefficients, 3rd column of the flexibility matrix.

The natural frequencies and mode shapes derived from the matrices (4.11) and (4.8) are:

ω_1 (rad/s)	**ω_2 (rad/s)**	**ω_3 (rad/s)**	**ω_4 (rad/s)**
25.65	101.58	220.08	506.79

Table 4.10 Natural frequencies from flexibility test

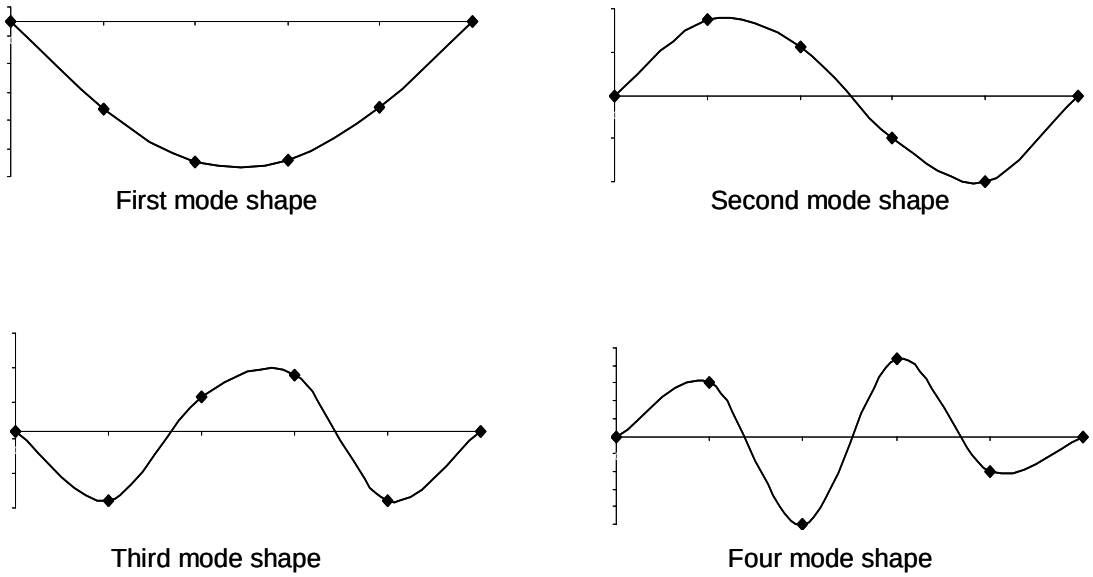

Figure 4.21 Mode Shapes from flexibility test

4.3.4 FREE VIBRATION TEST

To verify the experimental effectiveness of the damage estimation method presented in chapter 6, we tested the dynamic mode shapes of one model structure. The physical parameter of the model is identified by using the dynamic data from the assays.

4.3.4.1 System identification

Free vibrations were induced by applying the appropriate initial displacements or velocities to each measurement coordinate. The resulting motion was measured using 4 accelerometers (Kinemetrics FBA-11, single-axis force balance) placed at equal intervals along the beam. Each accelerometer was connected to one channel of an Altus K2 Digital Recorder. This unit is also a signal conditioner, and removes unphysical frequency components (filtering) from the data before amplifying the signal. More details on Altus K2 can be accessed at www.kinemetrics.com [104].

Each channel also passes through a simple, RC-analog, anti-alias filter. The DSP (digital signal processor, also part of the Altus 2K system) filters and decimates the 2000 sps data from the ADC (analog-to-digital converter) using multi-rate FIR (finite impulse response) filters. After decimation, each record consisted of 8192 data points with a sampling interval of 4 ms. This period corresponds to a sampling frequency of 250 Hz and a Nyquist frequency of 125 Hz. The digital signals are stored on the hard disk of the data acquisition computer. Figure 4.22 shows the instrumentation system used in the simply supported beam test.

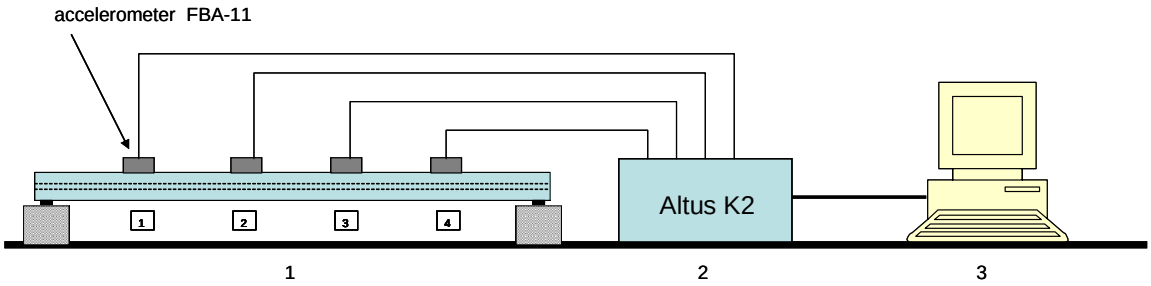

Figure 4.22 Instrumentation system

4.3.4.2 Modal parameters

Figure 4.23 presents a schematic representation of output-only modal identification. The time response (figure 4.24) was converted to a frequency domain by applying FFT to 8192 points (Figure 4.25). The experimental modal identification was carried out using the peak picking technique [105], and this method yielded satisfactory result because the damping was low and the modes were well separated.

The dynamic properties were assessed using a software system developed to process structural dynamic signals in experimental tests (SADEX) (Figure 4.26) [106]. For this test, the damping was estimated using the half power method and logarithmic decrement [107]. Once the natural frequency was estimated, its corresponding mode shape was constructed by inspection of the amplitude and phase angle of spectral density.

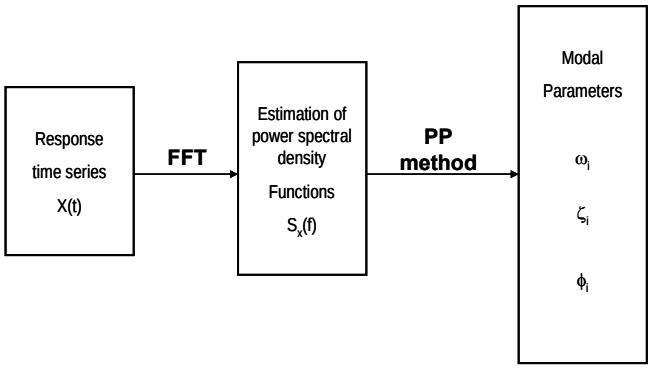

Figure 4.23 Schematic representation of output-only modal identification

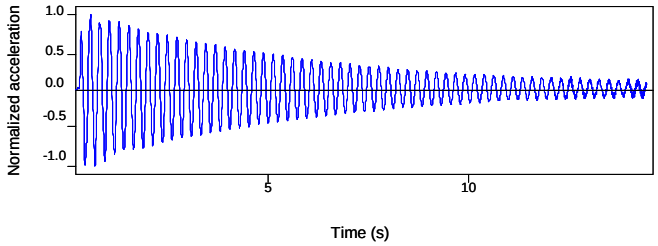

Figure 4.24 Acceleration time response Framed model (4th point)

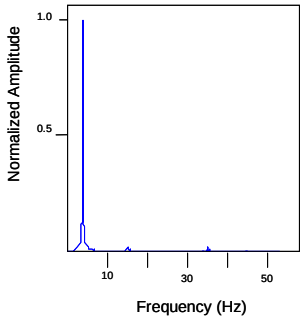

Figure 4.25 Power spectral densities (3th point)

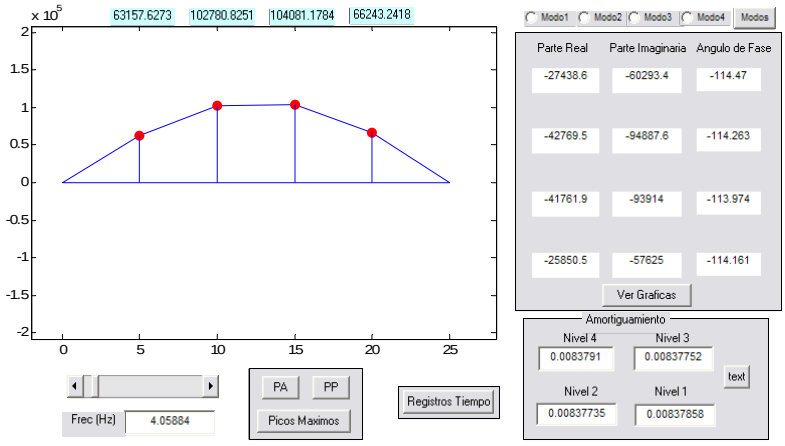

Figure 4.26 SADEX structural software identification

The three identified frequencies of the test beam for undamaged and each damaged state are summarized in Table 4.11. Figures 4.27–4.29 show the mode shapes and Table 4.12 presents the damping ratios.

	ω1 (rad/s)	ω2 (rad/s)	ω3 (rad/s)
Undamaged	25.50	97.60	---
Case b	25.12	95.87	---
Case c	24.93	95.68	219.55
Case d	23.01	87.63	196.93

Table 4.11 Natural frequency from the free vibration test

	ζ_1	ζ_2	ζ_3
Undamaged	0.0094	0.0144	0.0115
Case b	0.0089	0.0142	---
Case c	0.0095	0.0200	0.0189
Case d	0.0098	0.0188	0.0300

Table 4.12 Damping ratio from the free vibration test

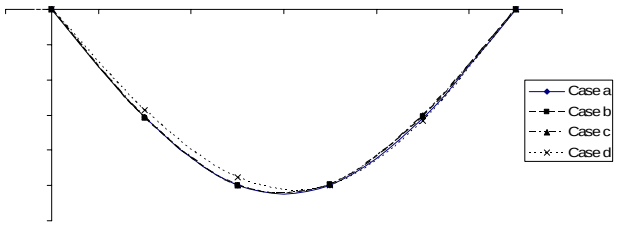

Figure 4.27 First mode shape from free vibration test

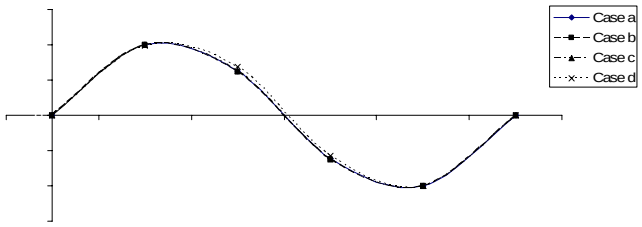

Figure 4.28 Second mode shape from free vibration test

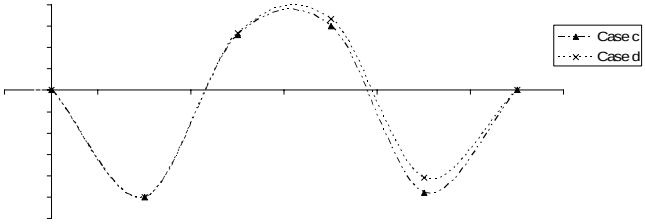

Figure 4.29 Third mode shape from free vibration test

4.4 CANTILEVER BEAM

The model test item is a wide-flanged steel I-beam (IPN 80), consisting of a 80 mm deep web and a 42 mm wide flange. The Beam is 3.03 meters in length, divided in 5 sections. The model was fixed at the reinforced concrete beam (figure 4.30).

In order to obtain lower values of the modal frequencies and to obtain more mode shapes with the equipment available, the beam was excited in axis X direction (figure 4.30). Previous numerical simulations established a predominant flexural behavior for the beam. For this reason, the experimental study is limited only for estimate coefficients EI for each section.

Total Length	3.03 m
$\mathbf{I_{xx}}$=5.83 cm^4, $\mathbf{I_{yy}}$=74.9 cm^4, **A**= 7.66 cm^2	
Total weight (model and accelerometers)	24.76 kg
Elastic Modulus	215.01 GPa

Table 4.13 Geometric and mechanical properties of the simply supported beam

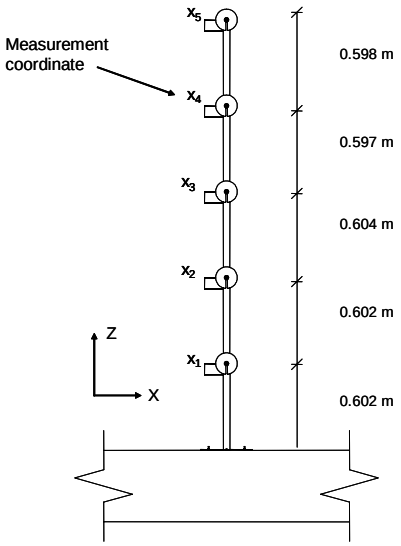

Figure 4.30 Tested model

4.4.1 MATERIALS

The steel beam utilized for the cantilever construction was the same utilized in the simple supported beam. For this reason the mechanical characteristic are same of section 4.3.1

Average EI	12.607 kN
Modulus Elasticity (E)	215.01 GPa
Inertia Section	5.83 cm^4

Table 4.14 Steel Properties

4.4.2 ANALYTICAL MODEL

The cantilever beam was modeled analytically considering only flexure deformation and lumped mass values.

MASS MATRIX
$$M = \begin{bmatrix} 5.249 & 0 & 0 & 0 & 0 \\ 0 & 5.438 & 0 & 0 & 0 \\ 0 & 0 & 5.416 & 0 & 0 \\ 0 & 0 & 0 & 5.374 & 0 \\ 0 & 0 & 0 & 0 & 3.579 \end{bmatrix} \text{kg} \qquad (4.12)$$

STIFFNESS MATRIX
$$K = \begin{bmatrix} 1.0877 & -0.6867 & 0.2758 & -0.0698 & 0.0116 \\ -0.6867 & 0.8440 & -0.6186 & 0.2434 & -0.0405 \\ 0.2758 & -0.6186 & 0.8184 & -0.5588 & 0.1521 \\ -0.0698 & 0.2434 & -0.5588 & 0.5828 & -0.2151 \\ 0.0116 & -0.0405 & 0.1521 & -0.2151 & 0.0948 \end{bmatrix} * 10^3 (kN/m) \qquad (4.13)$$

FLEXIBILITY MATRIX
$$F = \begin{bmatrix} 0.0058 & 0.0144 & 0.0231 & 0.0317 & 0.0403 \\ 0.0144 & 0.0461 & 0.0809 & 0.1152 & 0.1496 \\ 0.0231 & 0.0809 & 0.1563 & 0.2337 & 0.3112 \\ 0.0317 & 0.1152 & 0.2337 & 0.3678 & 0.5050 \\ 0.0403 & 0.1496 & 0.3112 & 0.5050 & 0.7160 \end{bmatrix} * (m/kN) \qquad (4.14)$$

Using of matrices (4.12) and (4.14) the natural frequencies and mode shapes were obtained:

ω_1 (rad/s)	ω_2 (rad/s)	ω_3 (rad/s)	ω_4 (rad/s)	ω_5 (rad/s)
13.49	82.41	226.97	432.80	634.57

Table 4.15 Natural frequencies from analytical model

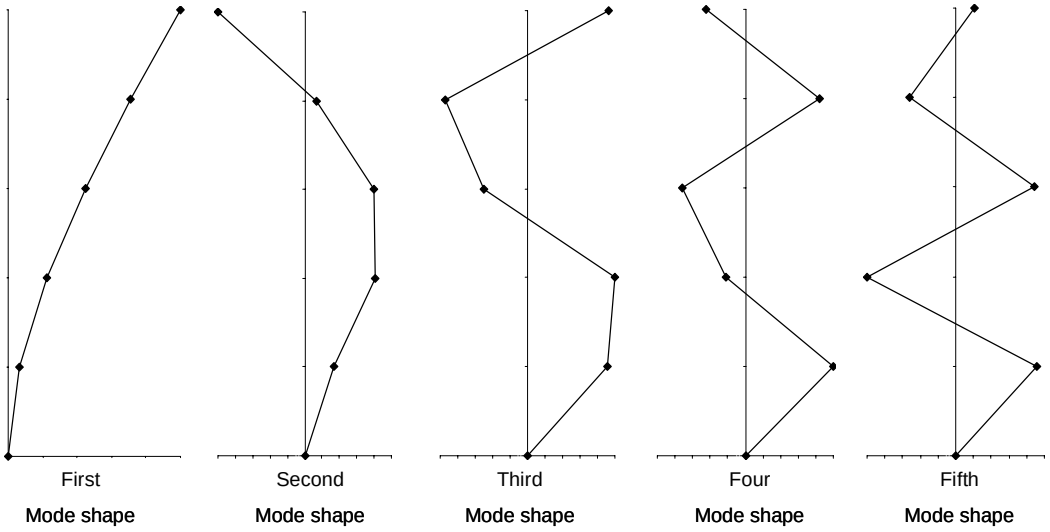

Figure 4.31 Mode Shapes from analytical model

4.4.3 FLEXIBILITY TEST

The flexibility characteristics of the cantilever beam for the lateral displacement degrees of freedom at each level were obtained. From the mass matrix and the flexibility experimental matrix, the frequencies and the mode shapes are calculated and then compared with the analytical and experimental results from the free vibration test.

The beam was loaded at each level, as illustrated in Figure 4.32. During the tests, displacement transducers (LDVT`S) were used to measure the lateral displacements at each level.

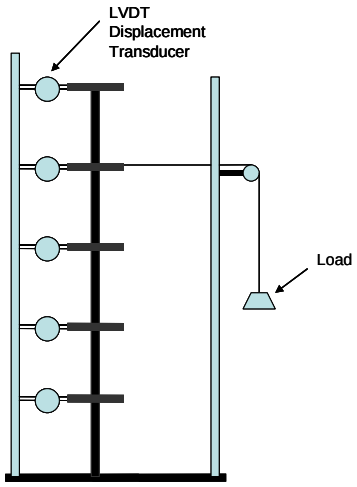

Figure 4.32 Test for determining the lateral Flexibility of the simply supported beam

The results of the tests are shown in equation (4.15) in the form of the flexibility matrix of structure; each column "j" of the matrix (4.15) is generated during the loading of the coordinate "j". The terms $f_{1,j}$ to $f_{5,j}$ of column "j" represent the lateral displacements at the successive points (1-5) of the beam as shown in the Figure 4.33, when loaded with a load applied at coordinate 4.

FLEXIBILITY MATRIX $$F = \begin{bmatrix} 0.0058 & 0.0145 & 0.0232 & 0.0325 & 0.0411 \\ 0.0145 & 0.0462 & 0.0808 & 0.1179 & 0.1523 \\ 0.0232 & 0.0808 & 0.1558 & 0.2393 & 0.3167 \\ 0.0325 & 0.1179 & 0.2393 & 0.3895 & 0.5320 \\ 0.0411 & 0.1523 & 0.3167 & 0.5320 & 0.7498 \end{bmatrix} * (m/kN)$$ (4.15)

STIFFNESS MATRIX $$K = \begin{bmatrix} 1.0861 & -0.6861 & 0.2690 & -0.0640 & 0.0116 \\ -0.6861 & 0.8397 & -0.5944 & 0.2238 & -0.0407 \\ 0.2690 & -0.5944 & 0.7426 & -0.4905 & 0.1404 \\ -0.0640 & 0.2238 & -0.4905 & 0.5148 & -0.2001 \\ 0.0116 & -0.0407 & 0.1404 & -0.2001 & 0.0916 \end{bmatrix} * 10^3 (kN/m)$$ (4.16)

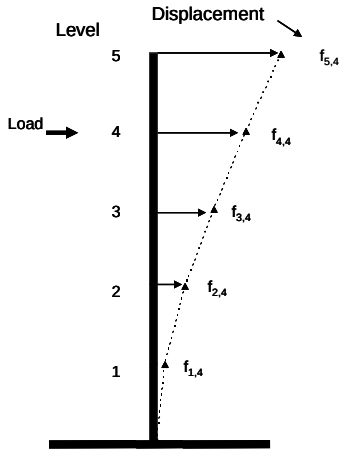

Figure 4.33 Correspondence of the flexibility coefficients, 4th column of the flexibility matrix.

The natural frequencies and mode shapes derived from the matrices (4.12) and (4.16) are:

ω_1 (rad/s)	ω_2 (rad/s)	ω_3 (rad/s)	ω_4 (rad/s)	ω_5 (rad/s)
13.22	80.42	223.79	417.81	623.33

Table 4.16 Natural frequencies from flexibility test

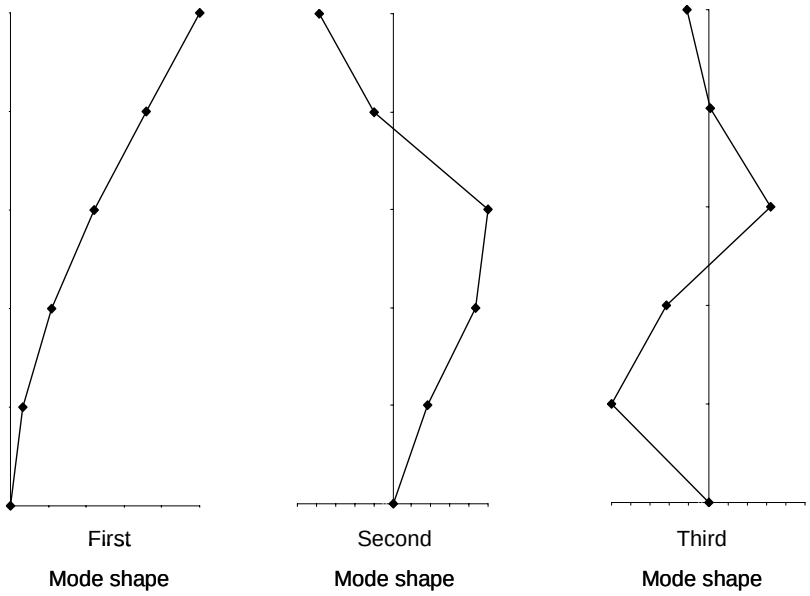

Figure 4.34 Mode Shapes from flexibility test

4.4.4 FREE VIBRATION TEST

To verify the experimental effectiveness of the damage estimation method presented in chapter 7, we tested the dynamic mode shapes of one model structure. The physical parameter of the model is identified by using the dynamic data from the assays. Free vibrations were induced by applying the appropriate initial displacements or velocities to each measurement coordinate, as a result, a total of 5 responses in the lateral direction (along the X-axis) were recorded in one series (figure 4.30). 10 series for each case of study was recorded. Each series contain the accelerations of coordinates due to initial displacement or velocity in one of the five coordinates.

4.4.4.1 System identification

The cantilever model was campled at the big concreted beam. The resulting motion was measured using 4 accelerometers (Kinemetrics FBA-11, single-axis force balance) placed in each measured coordinate. Each accelerometer was connected to one channel of an Altus K2 Digital Recorder. This unit is also a signal conditioner, and removes unphysical frequency components (filtering) from the data before amplifying the signal. More details on Altus K2 can be accessed at www.kinemetrics.com [104].

Each channel also passes through a simple, RC-analog, anti-alias filter. The DSP (digital signal processor, also part of the Altus 2K system) filters and decimates the 2000 sps data from the ADC (analog-to-digital converter) using multi-rate FIR (finite impulse response) filters. After decimation, each record consisted of 8192 data points with a sampling interval of 4 ms. This period corresponds to a sampling frequency of 250 Hz and a Nyquist frequency of 125 Hz. The digital signals are stored on the hard disk of the data acquisition computer. Figure 4.35 shows the instrumentation system used in the simply supported beam test.

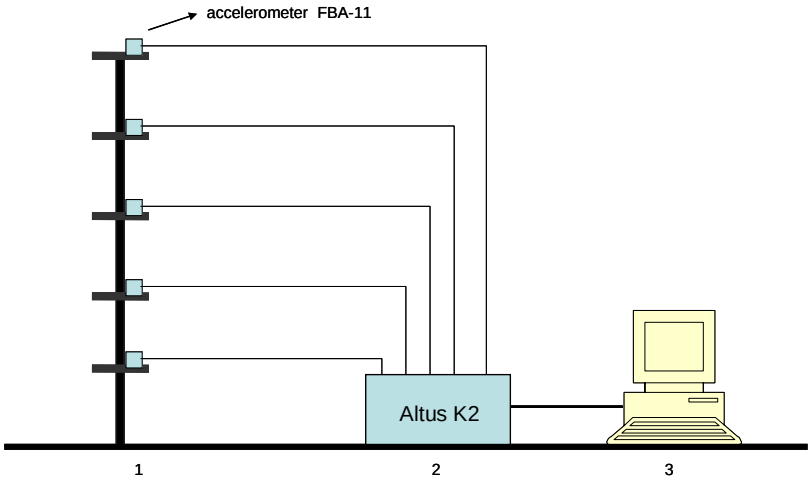

Figure 4.35 Instrumentation system

4.4.4.2 Modal parameters

Figure 4.36 presents a schematic representation of output-only modal identification. The time response (figure 4.37) was converted to a frequency domain by applying FFT to 8192 points (Figure 4.38). The experimental modal identification was carried out using the peak picking technique [105], and this method yielded satisfactory result because the damping was low and the modes were well separated.

The dynamic properties were assessed using a software system developed to process structural dynamic signals in experimental tests (SADEX) (Figure 4.39) [106]. For this test, the damping was estimated using the half power method and logarithmic decrement [107]. Once the natural frequency was estimated, its corresponding mode shape was constructed by inspection of the amplitude and phase angle of spectral density.

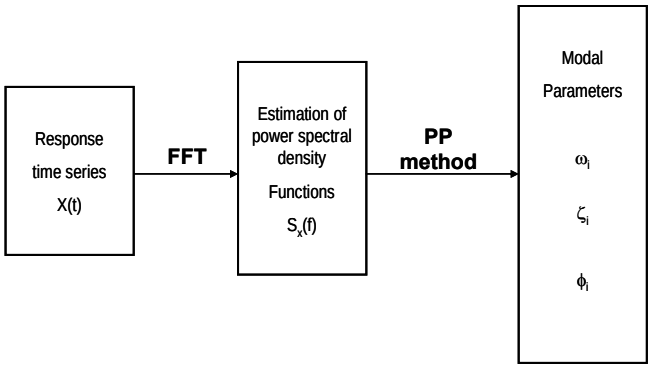

Figure 4.36 Schematic representation of output-only modal identification

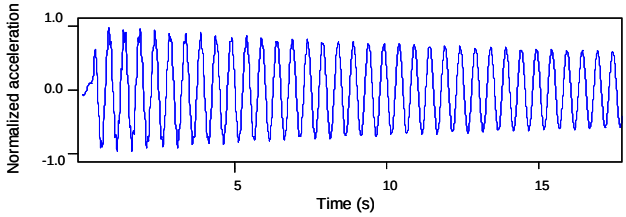

Figure 4.37 Acceleration time response Framed model (2nd Level)

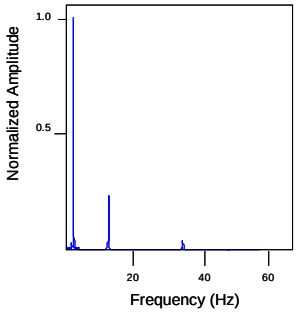

Figure 4.38 Power spectral densities (3rd Level)

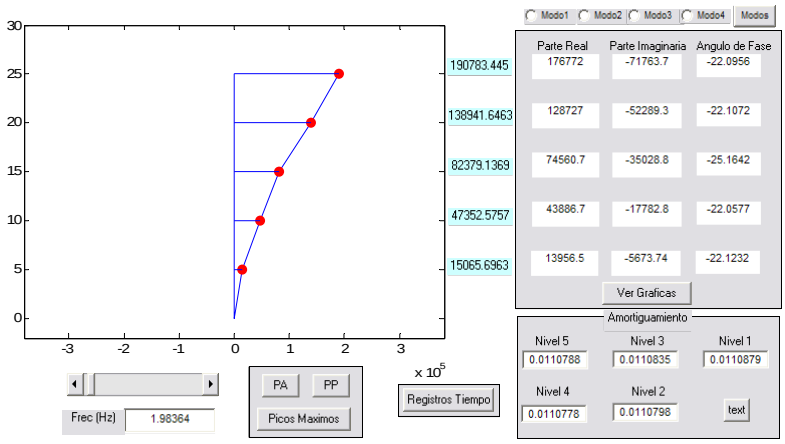

Figure 4.39 SADEX structural software identification

The identified frequencies of the test beam for undamaged and each damaged state are summarized in Table 4.17. Figures 4.40–4.42 show the mode shapes and Table 4.18 presents the damping ratios.

	ω_1 (rad/s)	ω_2 (rad/s)	ω_3 (rad/s)
Undamaged	12.46	78.96	218.78
Case b	11.89	78.39	207.47
Case c	11.87	77.24	202.49

Table 4.17 Natural frequency from the free vibration test

	ζ_1	ζ_2	ζ_3
Undamaged	0.0120	0.0029	0.0024
Case b	0.0137	0.0030	0.0039
Case c	0.0143	0.0041	----

Table 4.18 Damping ratio from the free vibration test

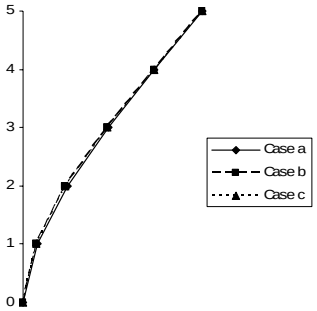

Figure 4.40 First mode shape from free vibration test

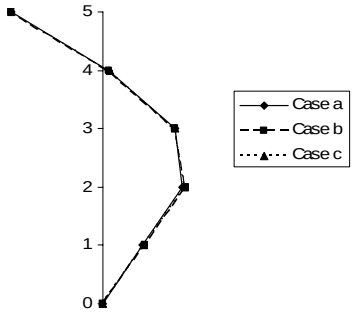

Figure 4.41 Second mode shape from free vibration test

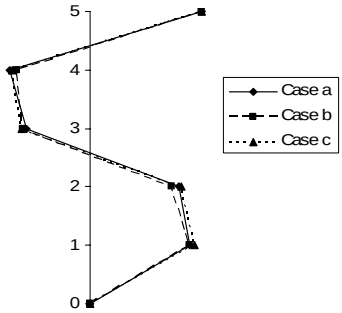

Figure 4.42 Third mode shape from free vibration test

4.5 CONCLUSIONS

The dynamics and static tests were performed on framed model, simply supported beam, and cantilever beam to determine the changes in linear behavior with increase in the level of damage. The assays were performed at increasing levels damage. For each model, dynamic parameters were determined from the analytical study, flexibility test, and free

vibration test. The free vibration responses were measured. This allowed the time–frequency relationship to be estimated from the spectral density using the FFT. The dynamic parameters derived from the free vibration test will be used in the damage estimation described in chapters 4, 5, and 6.

5. STIFFNESS IDENTIFICATION OF FRAMED MODELS

5.1 INTRODUCTION

An original identification method is proposed in this chapter to estimate damage location and severity in framed buildings based on experimental dynamic data. In the first part of this chapter stiffness identification procedures are developed, and two methodologies are presented: when the mass matrix is known and when it is unknown. The identification procedure requires an experimental test as well as an analytical model, in order to establish an initial undamaged condition of the structure. To study the effectiveness and accuracy of the identification damage methodology under noise conditions, a numerical simulation of a multi-storey framed building is carried out. The frame building scale model and the performed experimental test, leading to the dynamic identification of the structure, are described. Different controlled damage conditions of the structure are considered, and their dynamic properties are evaluated by experimental procedures.

5.2 FRAMED BUILDING STIFFNESS ASSESSMENT

Two identification methodologies are summarized for the assessment of stiffness changes on framed structures with shear behavior. The first methodology requires the knowledge of the mass matrix. The second methodology admits the mass matrix as an unknown variable that needs to be identified before the stiffness matrix is evaluated.

5.2.1 STIFFNESS VARIATIONS ESTIMATION

K and *M* are the stiffness and mass matrices, and N is the number of degrees of freedom. An experimental test must be carried out before the damage conditions appear on the structure, in order to know the exact initial dynamic parameters: modal frequencies and shapes of at least one eigenpair (one frequency and its corresponding modal shape).

The structural system is considered as non damped and is subjected to free vibration tests. The system complies:

$$K\Phi = M\Phi\Delta \tag{5.1}$$

Δ is the matrix that includes the eigenvalues ($\lambda_i = \omega_i^2$), with ω_i as the ith modal frequency and Φ is the matrix containing the eigenvectors (modal shapes).

Framed buildings with shear behavior can be modeled with undeformable slab with lumped mass values and columns with infinite axial stiffness. K is then a banded matrix and M is a diagonal matrix:

$$K = \begin{bmatrix} k_1 + k_2 & -k_2 & \cdots & \cdots & 0 \\ -k_2 & k_2 + k_3 & -k_3 & & \vdots \\ \vdots & & \ddots & & -k_N \\ 0 & \cdots & \cdots & -k_N & k_N \end{bmatrix} \tag{5.2}$$

$$M = \begin{bmatrix} m_1 & \cdots & & 0 \\ & m_2 & & \\ \vdots & \ddots & & \vdots \\ & & m_{N-1} & \\ 0 & \cdots & & m_N \end{bmatrix} \tag{5.3}$$

m_i is the lumped mass value for the ith floor and k_i is the stiffness value of ith floor.

To represent stiffness variations at the i level, the initial k_i is multiplied by α, a reduction factor, so K becomes:

$$K = \begin{bmatrix} \alpha_1 k_1 + \alpha_2 k_2 & -\alpha_2 k_2 & \cdots & \cdots & 0 \\ -\alpha_2 k_2 & \alpha_2 k_2 + \alpha_3 k_3 & -\alpha_3 k_3 & & \vdots \\ \vdots & & \ddots & & -\alpha_N k_N \\ 0 & \cdots & \cdots & -\alpha_N k_N & \alpha_N k_N \end{bmatrix} \tag{5.4}$$

K and *M* from eq. (5.3) and (5.4) can be introduced to eq. (5.1) for a particular *a* mode:

$$\left(\begin{bmatrix} \alpha_1 k_1 + \alpha_2 k_2 & -\alpha_2 k_2 & \cdots & & 0 \\ -\alpha_2 k_2 & \alpha_2 k_2 + \alpha_2 k_3 & & & \\ \vdots & & \ddots & & \vdots \\ & & & \alpha_{N-1} k_{N-1} + \alpha_N k_N & -\alpha_N k_N \\ & & \cdots & -\alpha_N k_N & \alpha_N k_N \end{bmatrix} - \lambda_a \begin{bmatrix} m_1 & & \cdots & & 0 \\ & m_2 & & & \\ \vdots & & \ddots & & \\ & & & m_{N-1} & \\ 0 & & \cdots & & m_N \end{bmatrix}\right) \begin{Bmatrix} \phi_a^1 \\ \phi_a^2 \\ \vdots \\ \phi_a^{N-1} \\ \phi_a^N \end{Bmatrix} = \begin{pmatrix} 0 \\ 0 \\ \vdots \\ 0 \\ 0 \end{pmatrix} \quad (5.5)$$

Each equation from this (5.5) system becomes:

$$\begin{gathered} (\alpha_1 k_1 + \alpha_2 k_2)\phi_a^1 - \alpha_2 k_2 \phi_a^2 - \lambda_a m_1 \phi_a^1 = 0 \\ -\alpha_2 k_2 \phi_a^1 + (\alpha_2 k_2 + \alpha_3 k_3)\phi_a^2 - \alpha_3 k_3 \phi_a^3 - \lambda_a m_2 \phi_a^2 = 0 \\ \vdots \\ -\alpha_{N-1} k_{N-1} \phi_a^{N-2} + (\alpha_{N-1} k_{N-1} + \alpha_N k_N)\phi_a^{N-1} - \alpha_N k_N \phi_a^N - \lambda_a m_{N-1} \phi_a^{N-1} = 0 \\ -\alpha_N k_N \phi_a^{N-1} + \alpha_N k_N \phi_a^N - \lambda_a m_N \phi_a^N = 0 \end{gathered} \quad (5.6)$$

As α_i values are unknown eq. (5.7) can be rewritten as follows:

$$\begin{bmatrix} k_1\phi_a^1 & k_2(\phi_a^1 - \phi_a^2) & \cdots & & 0 \\ & k_2(\phi_a^2 - \phi_a^1) & k_3(\phi_a^2 - \phi_a^3) & & \\ \vdots & & \ddots & & \\ & & & k_{N-1}(\phi_a^{N-1} - \phi_a^{N-2}) & k_N(\phi_a^{N-1} - \phi_a^N) \\ 0 & & \cdots & & k_N(\phi_a^N - \phi_a^{N-1}) \end{bmatrix} \begin{bmatrix} \alpha_1 \\ \alpha_2 \\ \vdots \\ \alpha_{N-1} \\ \alpha_N \end{bmatrix} = \begin{bmatrix} \lambda_a m_1 \phi_a^1 \\ \lambda_a m_2 \phi_a^2 \\ \vdots \\ \lambda_a m_{N-1} \phi_a^{N-1} \\ \lambda_a m_N \phi_a^N \end{bmatrix} \quad (5.7)$$

leading to: *[A] (x) = (c)* (5.8)

with *x* as the vector of unknowns α_i. The solution of eq (5.8) will determine the stiffness changes of the structure.

5.2.2 STIFFNESS CHANGES EVALUATION AND MASS VALUES ESTIMATION

The second methodology applies when mass characteristics are unknown. It allows the evaluation of the mass values (m_i) and stiffness changes coefficients for each floor (α_i) of a framed building. This methodology requires a previous knowledge of at least two experimental frequencies and their corresponding modal shapes. Initial stiffness values are also required; they can be obtained by experimental means or estimated by analytical F/E models. The mass characteristics of each level are considered as constant even if the structure is affected by stiffness damage.

The initial equations are identical to (5.1) to (5.5):

$$\left(\begin{bmatrix} \alpha_1 k_1 + \alpha_2 k_2 & -\alpha_2 k_2 & \cdots & 0 \\ -\alpha_2 k_2 & \alpha_2 k_2 + \alpha_2 k_3 & & \\ \vdots & & \ddots & \vdots \\ & & \alpha_{N-1} k_{N-1} + \alpha_N k_N & -\alpha_N k_N \\ & & \cdots & -\alpha_N k_N \quad \alpha_N k_N \end{bmatrix} - \lambda_a \begin{bmatrix} m_1 & \cdots & 0 \\ & m_2 & \\ \vdots & \ddots & \\ & & m_{N-1} \\ 0 & \cdots & m_N \end{bmatrix}\right) \begin{Bmatrix} \phi_a^1 \\ \phi_a^2 \\ \vdots \\ \phi_a^{N-1} \\ \phi_a^N \end{Bmatrix} = \begin{pmatrix} 0 \\ 0 \\ \vdots \\ 0 \\ 0 \end{pmatrix} \quad (5.9)$$

Equation (5.9) can be expanded for modes (eigenvalues) *a* and *b*, so it incluyes ω_a, ω_b modal frequencies and the corresponding modal shapes ϕ_a, ϕ_b.

$$\begin{aligned}
(\alpha_1 k_1 + \alpha_2 k_2)\phi_a^1 - \alpha_2 k_2 \phi_a^2 - \lambda_a m_1 \phi_a^1 &= 0 \\
(\alpha_1 k_1 + \alpha_2 k_2)\phi_b^1 - \alpha_2 k_2 \phi_b^2 - \lambda_b m_1 \phi_b^1 &= 0 \\
-\alpha_2 k_2 \phi_a^1 + (\alpha_2 k_2 + \alpha_3 k_3)\phi_a^2 - \alpha_3 k_3 \phi_a^3 - \lambda_a m_2 \phi_a^2 &= 0 \\
-\alpha_2 k_2 \phi_b^1 + (\alpha_2 k_2 + \alpha_3 k_3)\phi_b^2 - \alpha_3 k_3 \phi_b^3 - \lambda_b m_2 \phi_b^2 &= 0 \\
&\vdots \\
-\alpha_{N-1} k_{N-1} \phi_a^{N-2} + (\alpha_{N-1} k_{N-1} + \alpha_N k_N)\phi_a^{N-1} - \alpha_N k_N \phi_a^N - \lambda_a m_{N-1} \phi_a^{N-1} &= 0 \\
-\alpha_{N-1} k_{N-1} \phi_b^{N-2} + (\alpha_{N-1} k_{N-1} + \alpha_N k_N)\phi_b^{N-1} - \alpha_N k_N \phi_b^N - \lambda_b m_{N-1} \phi_b^{N-1} &= 0 \\
-\alpha_N k_N \phi_a^{N-1} + \alpha_N k_N \phi_a^N - \lambda_a m_N \phi_a^N &= 0 \\
-\alpha_N k_N \phi_b^{N-1} + \alpha_N k_N \phi_b^N - \lambda_b m_N \phi_b^N &= 0
\end{aligned} \quad (5.10)$$

α_i and m_i are unknowns. The equation can be rearranged as:

$$\begin{bmatrix} k_1\phi_a^1 & -\lambda_a\phi_a^1 & k_2(\phi_a^1-\phi_a^2) & & & & & \\ k_1\phi_b^1 & -\lambda_b\phi_b^1 & k_2(\phi_b^1-\phi_b^2) & & & & & \\ 0 & 0 & k_2(\phi_a^2-\phi_a^1) & -\lambda_a\phi_a^2 & k_3(\phi_a^2-\phi_a^3) & 0 & & \\ 0 & 0 & k_2(\phi_b^2-\phi_b^1) & -\lambda_b\phi_b^2 & k_3(\phi_b^2-\phi_b^3) & 0 & & \\ & & & & \ddots & & & \\ & & & & & \ddots & & \\ & & & & 0 & 0 & k_N(\phi_a^{N-1}-\phi_a^N) & \lambda_a\phi_a^N \\ & & & & 0 & 0 & k_N(\phi_b^{N-1}-\phi_b^N) & \lambda_b\phi_b^N \end{bmatrix} \begin{bmatrix} \alpha_1 \\ m_1 \\ \alpha_2 \\ m_2 \\ \vdots \\ \vdots \\ \alpha_N \\ m_N \end{bmatrix} = \begin{bmatrix} 0 \\ 0 \\ 0 \\ 0 \\ \vdots \\ \vdots \\ 0 \\ 0 \end{bmatrix} \tag{5.11}$$

This system of equations *[A] (b) = (0)* is singular, so the solution requires an additional value. A convenient solution can be obtained if a particular mass value m_N of a given floor level such as N, is imposed as a known or normalization value, leading to the following equation:

$$\begin{bmatrix} k_1\phi_a^1 & -\lambda_a\phi_a^1 & k_2(\phi_a^1-\phi_a^2) & 0 & 0 & \cdots & \cdots & 0 \\ k_1\phi_b^1 & -\lambda_b\phi_b^1 & k_2(\phi_b^1-\phi_b^2) & 0 & 0 & \cdots & \cdots & 0 \\ 0 & 0 & k_2(\phi_a^2-\phi_a^1) & -\lambda_a\phi_a^2 & k_3(\phi_a^2-\phi_a^3) & 0 & \cdots & 0 \\ 0 & 0 & k_2(\phi_b^2-\phi_b^1) & -\lambda_b\phi_b^2 & k_3(\phi_b^2-\phi_b^3) & 0 & \cdots & 0 \\ \vdots & & & & \ddots & \ddots & & \vdots \\ \vdots & & & & & k_N(\phi_a^{N-1}-\phi_a^{N-2}) & -\lambda_a\phi_a^{N-1} & k_N(\phi_a^{N-1}-\phi_a^N) \\ 0 & 0 & & & 0 & k_N(\phi_b^{N-1}-\phi_b^{N-2}) & -\lambda_b\phi_b^{N-1} & k_N(\phi_b^{N-1}-\phi_b^N) \\ 0 & 0 & \cdots & \cdots & 0 & 0 & 0 & k_N(\phi_a^{N-1}-\phi_a^N) \end{bmatrix} \begin{bmatrix} \alpha_1 \\ m_1 \\ \alpha_2 \\ m_2 \\ \vdots \\ \alpha_{N-1} \\ m_{N-1} \\ \alpha_N \end{bmatrix} = \begin{bmatrix} 0 \\ 0 \\ 0 \\ 0 \\ \vdots \\ 0 \\ 0 \\ \lambda_a m_N \phi_a^N \end{bmatrix} \tag{5.12}$$

The solution allows the evaluation of all mass and stiffness values for each level α_i / m_N and m_i / m_N as a function of m_N.

5.3 NUMERICAL STUDY

To demonstrate the effectiveness of the identification procedures developed in the section 5.2, a numerical study using a finite element model of the reinforced concrete multi-storey framed building was conducted. Dynamic parameters are determined in two different conditions: a) undamaged and b) damage in two stories of the building. The influence of simulated noise in the modal data is also presented.

5.3.1 NUMERICAL MODEL

Figure 5.1 shows the geometric characteristics of the structural axis considered for the numerical study. This structural axis has five stories and six bays of 8 m., the cross-section of the columns are 0.80 m of diameter. The system floor is a slab with columns capitals and drop panels. The thickness of the slab is 0.20 m. The modulus of elasticity is $E=25{,}000MN/m^2$.

Natural frequencies and mode shapes for the structural axis was calculated by performing a finite element analysis with SAP2000 [108]. The slab masses are lumped to the nodes belonging to each floor. The building is clamped at the ground level.

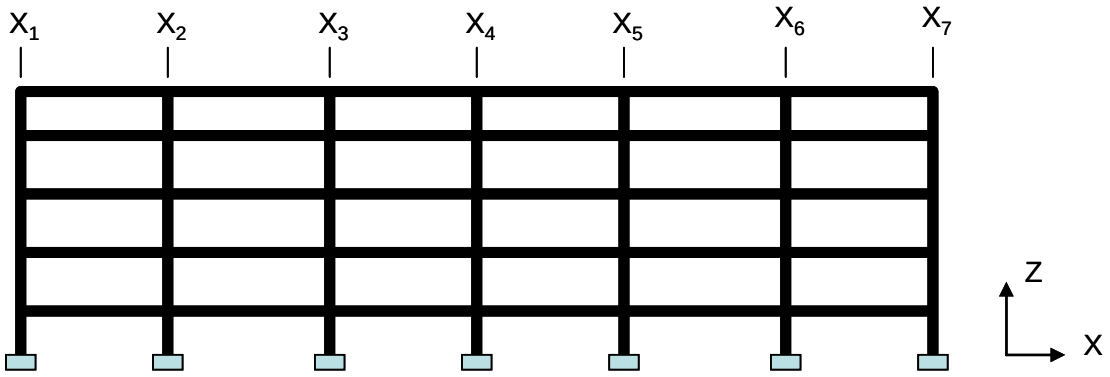

Figure 5.1 Numerical model of the structural axis.

5.3.2 STUDY CASES

Two cases of study were established: a) initial undamaged structure and b) 40% stiffness reduction at the first and 20% at the third level. The damage identification was performed by each mode shape and its frequency.

5.3.3 EFFECTS OF ERRORS IN DYNAMICS MEASUREMENTS

In order to study the effect of noise on the measurement of modal shapes and frequencies on the damage estimation method, the modal shapes and frequencies obtained from the numerical simulation were corrupted using the Sohn and Law algorithm [109]:

$$\phi_c(n) = \phi\left(1 + \frac{p}{100} R\right) \tag{5.13}$$

Where $\phi_c(n)$ is the corrupted modal shape, ϕ is the uncorrupted modal shape obtained from numerical simulations, p is a specified percentage of noise level, and R is a random number between 0 and 1. A set of ten vibration tests was carried out. It was used the normally distributed random number from Matlab [110].

Three study cases were proposed to study the effect of measurement noise on the damage identification:

Case a: frequency is corrupted and modal shape uncorrupted

Case b: frequency is uncorrupted and modal shape corrupted

Case c: frequency is corrupted and modal shape corrupted with same noise level.

Tree values noise level were considered: 2%, 5% and 10%.

5.3.3.1 Results

The damage identification with different level of noise in frequency or mode shapes, and different order modes was performed to verify the efficiency and accuracy of the proposed method. Tables 5.1, 5.2 and 5.3 identified the errors in the damage identification for the defined cases in 5.3.2. The following observations can be made:

1. The quality of the damage identification is very more sensitive to the perturbation of the mode shapes than that of frequencies.
2. The quality of damage identification is independent of the mode shape utilized.
3. The damage identification with level noise in the modal parameters give a reasonable agreement between the damage estimated and damage assumed
4. In all cases the methodology identifies with precision the location of the stiffness changes as well as the variation of stiffness. For the study noise level the relative error of the estimation remain smaller that 10%. Only for the case b and c when the identification is made with the modal shape 5, a larger relative error was obtained (32.6 and 32.8%).

	Noise Level (%)														
	Mode shape 1			Mode shape 2			Mode shape 3			Mode shape 4			Mode shape 5		
Storey	**2**	**5**	**10**	**2**	**5**	**10**	**2**	**5**	**10**	**2**	**5**	**10**	**2**	**5**	**10**
1	0.08	0.15	0.26	0.11	0.17	0.29	0.06	0.13	0.24	0.09	0.16	0.27	0.37	0.45	0.56
2	0.22	0.16	0.04	8.25	8.32	8.45	0.12	0.18	0.30	0.02	0.05	0.17	0.03	0.03	0.15
3	0.00	0.06	0.15	0.10	0.16	0.25	0.11	0.16	0.25	0.03	0.08	0.17	0.09	0.15	0.24
4	0.40	0.34	0.22	0.19	0.12	0.01	0.06	0.13	0.24	0.24	0.30	0.41	0.00	0.07	0.19
5	0.71	0.64	0.53	0.40	0.33	0.22	0.11	0.04	0.08	0.06	0.01	0.12	0.13	0.20	0.31

Table 5.1 Relative errors Case a

	Noise Level (%)														
	Mode shape 1			Mode shape 2			Mode shape 3			Mode shape 4			Mode shape 5		
Storey	**2**	**5**	**10**	**2**	**5**	**10**	**2**	**5**	**10**	**2**	**5**	**10**	**2**	**5**	**10**
1	0.66	1.43	3.31	0.33	0.95	2.10	1.94	4.93	10.1	0.75	1.88	3.99	6.78	16.4	32.6
2	0.52	1.99	4.25	6.02	2.89	1.25	2.14	5.40	11.3	0.22	0.48	0.98	1.34	3.38	7.24
3	2.10	5.11	9.89	1.03	2.57	5.43	0.30	0.65	1.26	1.10	2.86	6.11	0.59	1.43	2.96
4	1.16	4.06	9.06	0.31	0.43	0.65	0.38	0.98	2.03	0.25	0.35	0.52	0.07	0.11	0.20
5	1.11	2.03	2.69	0.44	0.44	0.44	0.18	0.23	0.31	0.14	0.20	0.31	0.04	0.02	0.14

Table 5.2 Relative errors Case b

	Noise Level (%)														
	Mode shape 1			Mode shape 2			Mode shape 3			Mode shape 4			Mode shape 5		
Storey	**2**	**5**	**10**	**2**	**5**	**10**	**2**	**5**	**10**	**2**	**5**	**10**	**2**	**5**	**10**
1	1.12	2.67	5.4	0.23	0.85	2.00	1.84	4.84	10	0.85	1.99	4.09	6.89	16.6	32.8
2	0.27	0.98	2.35	6.12	3.00	1.15	2.24	5.50	11.4	0.12	0.38	0.88	1.24	3.28	7.14
3	2.01	5.01	9.78	1.11	2.65	5.52	0.38	0.73	1.34	1.18	2.95	6.20	0.67	1.51	3.00
4	0.80	2.70	6.44	0.21	0.33	0.55	0.28	0.88	1.93	0.35	0.45	0.62	0.03	0.01	0.09
5	0.28	0.27	1.15	0.34	0.34	0.34	0.08	0.13	0.21	0.04	0.10	0.21	0.14	0.07	0.04

Table 5.3 Relative errors Case c

5.3.4 INFLUENCE OF DAMAGE SEVERITY

To study the effect of damage severity on the stiffness identification, multiple damage scenarios with 2% noise in frequency and modes were performed. The structure is subjected to different simulated damage cases. Table 5.4 shows the damages cases. Damage is simulated by reducing the stiffness of Level. Each damage case is identifying with each modal shape its frequency.

CASE	Damage Location	Damage severity (%)
a	Level 1	80
	Level 2	20
b	Level 1, 2	80
c	Level 1, 2, 3	80
d	Level 1, 2, 3, 4	80

Table 5.4 Simulated damage cases

5.3.4.1 Results

The effects of multiple and severe stiffness reductions on the damage identification have investigated. Tables 5.5, 5.6, 5.7 and 5.8 show the relative error in stiffness estimation defined in Table 5.4. The collected results show that:

1. It is found that the damage identification is affected by damage severity of the structure. In contrast with the study in section 5.3.3 in very levels the relative errors are greater that the noise level.
2. For the large damage in any level, the quality of damage identification dependent of the mode shape utilized. When the first's three modes shapes were utilized, the methodology identifies with acceptable precision the location of the stiffness changes as well as the variation of stiffness. The unacceptable errors were obtained when the damage identification was performed with the modal shape 5.

	Mode Shape				
Level	**1**	**2**	**3**	**4**	**5**
1	0.02	1.10	3.52	-7.00	-33.78
2	-0.24	4.09	-0.31	1.26	2.5
3	4.91	-2.43	-3.56	-4.37	-4.09
4	-0.68	2.27	1.34	-0.58	-0.56
5	5.84	0.01	-2.76	-2.60	-3.25

Table 5.5 Relative Errors Case a

	Mode Shape				
Level	**1**	**2**	**3**	**4**	**5**
1	-0.01	0.76	10.52	-4.10	-77.50
2	-0.28	16.45	-6.22	1.19	6.00
3	-1.01	-3.39	-5.53	-4.90	-7.93
4	-1.02	2.53	2.63	-18.68	0.53
5	7.31	1.62	-1.29	1.58	-3.24

Table 5.6 Relative Errors Case b

	Mode Shape				
Level	**1**	**2**	**3**	**4**	**5**
1	0.01	0.72	-0.80	-30.90	-1031.40
2	0.01	-0.78	0.80	9.01	72.39
3	0.02	-3.21	-3.33	-5.68	-8.02
4	-1.32	3.47	2.80	3.54	0.51
5	10.61	3.34	0.33	-0.61	-3.20

Table 5.7 Relative Errors Case c

	Mode Shape				
Level	**1**	**2**	**3**	**4**	**5**
1	-0.01	0.46	0.87	-3.27	-289.83
2	-0.03	-0.51	-0.28	1.74	-2.20
3	0.05	-3.58	-3.62	-3.94	4.36
4	-0.10	1.04	0.82	0.92	-1.53
5	12.18	2.91	-0.68	-0.78	-1.48

Table 5.8 Relative Errors Case d

5.4 EXPERIMENTAL ASSESSMENT

To verify the experimental effectiveness of the damage estimation method presented, we tested the dynamic modes of one model structure. The physical parameter of the model, experimental test developed and its results are describes in section 4.2.

5.4.1 STUDY CASES AND IDENTIFICATION RESULTS

Initial stiffness characteristics of the model were modified following defined patterns in order to simulate damage conditions and then verify the identification procedures. To simulate the structural damage, the width of the steel columns was decreased, leading to four case studies:

Case a: initial undamaged structure (reference case to establish stiffness modifications).
Case b: 18% columns stiffness reduction at the first level.
Case c: 40% columns stiffness reduction at the first level.
Case d: 19% stiffness reduction at the 2nd level and 40% at the third level.

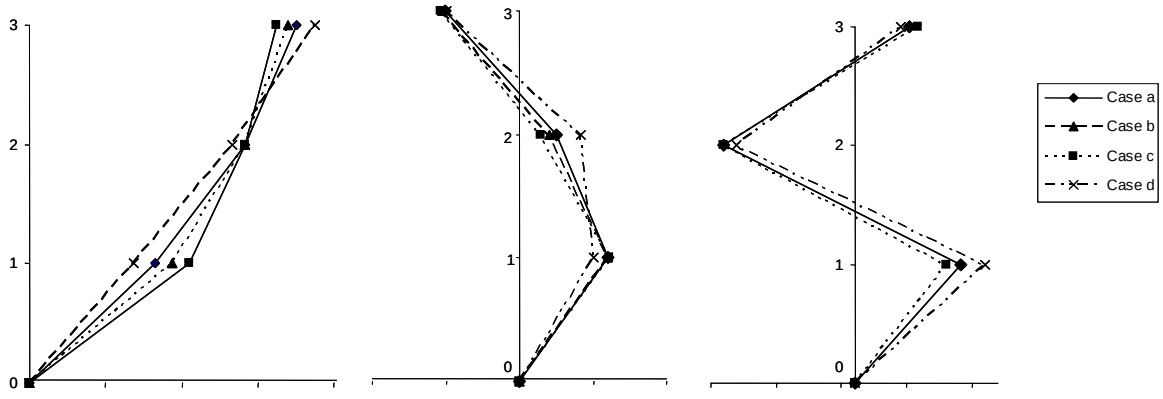

Figure 5.2 Modal Shapes 1, 2 and 3 for each case

	ω_1 (rad/s)	ω_2 (rad/s)	ω_3 (rad/s)
Undamaged	19.16	52.72	78.56
Case b	17.09	49.83	---
Case c	14.95	47.19	76.82
Case d	16.46	43.54	62.77

Table 5.9 Experimental Modal frequency for each case

	Case b				**Case c**				**Case d**			
	Real Value	**Identified**			**Real Value**	**Identified**			**Real Value**	**Identified**		
		Mode 1	**Mode 2**	**Mode 3**		**Mode 1**	**Mode 2**	**Mode 3**		**Mode 1**	**Mode 2**	**Mode 3**
α_1	0.82	0.71	0.75	0.61	0.60	0.49	0.51	--	1	0.98	0.96	0.96
α_2	1	0.99	1.01	0.98	1	1	0.98	--	0.81	0.76	0.71	0.60
α_3	1	0.99	0.98	0.99	1	1.01	0.97	--	0.60	0.56	0.57	0.55

Table 5.10 Stiffness changes for each level with known mass values.

	Case b		**Case c**		**Case d**	
Stiffness variation	**Real value**	**Identified**	**Real value**	**Identified**	**Real value**	**Identified**
α_1	0.82	0.70	0.60	0.48	1.00	0.98
α_2	1.00	0.97	1.00	1.00	0.81	0.62
α_3	1.00	0.98	1.00	0.97	0.60	0.58
m_1/m_3	1.03	1.01	1.03	1.04	1.03	1.04
m_2/m_3	1.03	1.03	1.03	1.06	1.03	1.06

Table 5.11 Stiffness values changes identification and mass adjustment at each level.

The mode shapes and frequencies for each study case are show in figure 5.2 and table 5.9. The damage identification was performed for the methods presented in section 5.2. The first case (a), corresponding to the undamaged condition, was employed as a reference to determine the efficiency of the identification procedures and to evaluate the damage coefficients $\alpha_{i.}$

Table 5.10 shows obtained damage coefficients for cases b, c and d. from the identification methodology with mass is known (section 5.2.1). “Identified values” are the results of the proposed identification algorithm. The results show adequate approximations of damage values for each floor, and also show the location of the damage. The quality of damage identification is independent of the mode shape utilized. However, the damage coefficients were less accuracy when the damage identification was made with mode shape 3.

Table 5.11 shows the application of the identification procedure with mass estimation (section 5.2.2). “Real values” are the same already shown in table 5.10, used as reference values. m1/m3 and m2/m3 ratios are the results of the mass estimation. The identification procedure permits good quality adjustments of α_i and $m_{i.,}$ allowing mass ratios identification, damage values assessment and damage localization.

5.5 CONCLUSIONS

Two identification procedures are proposed. They may be applied to framed buildings with shear behavior to evaluate the structural damage in terms of stiffness reduction values, as well as to determine the location of these stiffness variations. Thought, the methodologies presented has an application limited to framed structures, the procedures here described have the advantage of using only a coordinate for floor and a limited number of modals (1 or 2 according to the case). This represents an advantage beside other methods, in which even if they are of more extensive application, they require a complex and expensive experimental test, with major number coordinates of

measurement, being some of them difficult to obtain the rotational coordinates and refined FE models.

The numerical simulation demonstrated a reasonable agreement between the damage estimated and damage assumed. The numerical results demonstrated that the method is independent of the order mode shape utilized. Also, demonstrated that the quality of the damage identification is very more sensitive to the perturbation of the mode shapes than that of frequencies. However, the frequency is more stable that the mode shape in real dynamic test. Important level errors in measured mode shapes would affect the damage identification, for this reason special attention would have in the signal processing. It is found that the damage identification is affect by damage severity of the structure. For the large damage in any level, the quality of damage identification dependent of the mode shape utilized. When de damage severity is large the low modes shapes identifies with best precision that the high modes shapes.

Both methods are applied to an experimental model of a three level framed building. The undamaged structure is evaluated and three cases representing various damage conditions are studied. Both identification methods proved adequate to identify the stiffness reduction and damage location.

6. DAMAGE IDENTIFICATION OF SIMPLY-SUPPORTED BEAMS

6.1 INTRODUCTION

A method for identification and quantification of damage based in the known modal shapes and vibration frequencies of the simply-supported beams is presented in this chapter. Damage is defined in terms of changes in sections stiffness. To apply this methodology, it is necessary to previously determine the two modal frequencies of the system with their respective modal shapes and the system mass matrix. A numeric simulation of a real bridge is performed to study the effectiveness of the methodology in identifying damage and the influence of measurement errors and noise in the modal data is also present. A dynamic-test experiment is run on one simply-supported wide-flanged steel beam which suffers a progressive damage in three sections.

Bridges are indispensable to modern society; the deterioration or partial collapse of a single structure can have a drastic impact on the economic and social activity of a region or city [111]. For this reason, the analysis of serviceable conditions and their vulnerabilities are commonly spoken of in the scientific literature [112]. Throughout its lifetime, a bridge suffers damage due to the strain caused by continuous traffic, the weight of vehicles, impacts, corrosion, and moderate earthquakes. It is necessary to remark that some structures built a few decades ago now appear vulnerable in the light of new standards [113, 114].

The focus of this study is on those bridges relying on simply supported beams, which are commonly used for pedestrians, cars, and trains. National Bridge Inventory statistics show that one-third of all steel bridges are simply supported [115]. This paper suggests a method to estimate the stiffness of simply supported beams, which can later be applied to the study of bridges.

6.2 ESTIMATION OF FLEXURE DAMAGE IDENTIFICATION IN SIMPLY-SUPPORTED BEAMS

An algorithm for identification of flexure in simply-supported beams it is described. The application of this method requires a previous experimental analysis, in which at least two modal frequencies, modal shapes and system mass matrix must be known. It is shown briefly the method description and the expressions derived from its formulation.

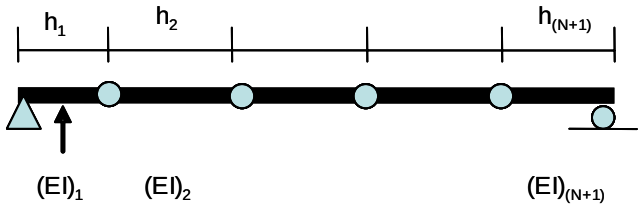

Figure 6.1 Simply-supported beam

The dynamic parameters of the structure in figure 6.1 can be obtained from [98]:

$$(\lambda_i^{-1} - F.M)\phi_i = 0 \qquad (6.1)$$

with:

F= flexibility matrix

M= mass matrix

$\lambda_i=\omega_i^2$, ω_i = ith modal frequency

ϕi= ith eigenvector .

Introducing in the equation (6.1) F and M matrixes, and developing each equation for the modal frequencies ω_a y ω_b and the modal shapes ϕ_a y ϕ_b, we obtain the present system:

$$
\begin{aligned}
&(f_{11}m_{11}+\ldots+f_{1N}m_{N1})\varphi_a^1+\ldots\ldots\ldots+(f_{11}m_{1N}+\ldots+f_{1N}m_{NN})\varphi_a^N=\varphi_a^1/\omega_a^2\\
&(f_{11}m_{11}+\ldots+f_{1N}m_{N1})\varphi_b^1+\ldots\ldots\ldots+(f_{11}m_{1N}+\ldots+f_{1N}m_{NN})\varphi_b^N=\varphi_b^1/\omega_b^2\\
&\qquad\qquad\qquad\vdots\\
&(f_{N1}m_{11}+\ldots+f_{NN}m_{N1})\varphi_a^1+\ldots\ldots\ldots+(f_{N1}m_{1N}+\ldots+f_{NN}m_{NN})\varphi_a^N=\varphi_a^N/\omega_a^2\\
&(f_{N1}m_{11}+\ldots+f_{NN}m_{N1})\varphi_b^1+\ldots\ldots\ldots+(f_{N1}m_{1N}+\ldots+f_{NN}m_{NN})\varphi_b^N=\varphi_b^N/\omega_b^2
\end{aligned}
\qquad (6.2)
$$

For the beam showed in figure 6.1, each flexibility value can be evaluated as follows:

$$F(i,j)=a(j)\tau_{ab}(i)-\tau_{bc}(i,j)$$

$$a(j)=\sum_{l=j+1}^{N+1}h_l\Big/\sum_{l=1}^{N+1}h_l \qquad j=1,\ldots,N \qquad (6.3)$$

$$
\begin{aligned}
\tau_{ab}(i)=&\left[\sum_{l=1}^{i}\frac{h_l^2}{2(EI)_l}\frac{\sum_{k=i+1}^{N+1}h_k}{\sum_{k=1}^{N+1}h_k}\left(\frac{2h_l}{3}+\sum_{k=1}^{l-1}h_k\right)\right]+\left[\sum_{l=2}^{i}\frac{h_l}{(EI)_l}\frac{\sum_{k=i+1}^{N+1}h_k}{\sum_{k=1}^{N+1}h_k}\left(\sum_{k=1}^{l-1}h_k\right)\left(\frac{h_l}{2}+\sum_{k=1}^{l-1}h_k\right)\right]+\\
&\left[\sum_{l=i+1}^{N+1}\frac{h_l^2}{2(EI)_l}\frac{\sum_{k=1}^{i}h_k}{\sum_{k=1}^{N+1}h_k}\left(\frac{h_l}{3}+\sum_{k=1}^{l-1}h_k\right)\right]+\left[\sum_{l=i+1}^{n}\frac{h_l}{(EI)_l}\frac{\sum_{k=1}^{i}h_k}{\sum_{k=1}^{N+1}h_k}\left(\frac{h_l}{2}+\sum_{k=1}^{l-1}h_k\right)\left(\sum_{k=l+1}^{N+1}h_k\right)\right] \qquad i=1,\ldots,N
\end{aligned}
$$

$$
\tau_{bc}(i,j)=\left[\sum_{l=j+1}^{n+1}\frac{h_l^2}{2(EI)_l}\frac{\sum_{k=1}^{i}h_k}{\sum_{k=1}^{N+1}h_k}\left(\sum_{k=j+1}^{l-1}h_k+\frac{h_k}{3}\right)\right]+\left[\sum_{l=j+1}^{N}\frac{h_l}{(EI)_l}\frac{\sum_{k=1}^{i}h_k}{\sum_{k=1}^{N+1}h_k}\left(\left(\sum_{k=j+1}^{l-1}h_k+\frac{h_l}{2}\right)\left(\sum_{k=l+1}^{N+1}h_k\right)\right)\right] \qquad \begin{matrix}i=1,\ldots,N\\ j=1,\ldots,N\end{matrix}
$$

With:

h_i= length section “i”

E_i=elasticity modulus of the section “I”

$I_{i=}$ Inertia modulus of the section “I”

N: number of coordinates of measure in the beam.

The goal of this procedure is the evaluation of the stiffness coefficients $(EI)_i$, for each section “i”, with i = 1 to N+1. Considering equations (6.2) and (6.3) we come to:

$$A=\begin{bmatrix} a^a_{1,1} & a^a_{1,2} & \cdots & \cdots & a^a_{1,N+1} \\ \vdots & \vdots & \cdots & \cdots & \vdots \\ \vdots & & & & \vdots \\ a^a_{N,1} & a^a_{N,2} & & & a^a_{N,N+1} \\ a^b_{N+1,1} & a^b_{N+1,2} & & & a^b_{N+1,N+1} \end{bmatrix} \begin{bmatrix} \dfrac{1}{(EI)_1} \\ \\ \\ \dfrac{1}{(EI)_N} \\ \dfrac{1}{(EI)_{N+1}} \end{bmatrix} = \begin{bmatrix} \dfrac{1}{\omega_a^2}\phi_a^1 \\ \\ \\ \dfrac{1}{\omega_a^2}\phi_a^N \\ \dfrac{1}{\omega_b^2}\phi_b^1 \end{bmatrix} \tag{6.4}$$

Equation (6.4) defines a system of *N+1* equations with *N+1* unknowns, where the unknown are coefficients (EI) of each section. This fact imposes the requirement of two modal shapes and their corresponding frequencies in order to produce *N+1* equations. The corresponding two modal shapes are:

$$\phi_{\mathrm{a}} = \left\{ \phi_a^1 \quad ... \quad \phi_a^i \quad ... \quad \phi_a^N \right\}^{\mathrm{t}} \quad \mathrm{y} \quad \phi_{\mathrm{b}} = \left\{ \phi_b^1 \quad ... \quad \phi_b^i \quad ... \quad \phi_b^N \right\}^{t} \tag{6.5}$$

The two modal shapes define the following coefficients:

$$A_1(i,j) = \frac{h_j}{L_t}\left(\sum_{l=i+1}^{N+1} h_l\right)\left\{\left[\left(\sum_{k=1}^{j-1} h_k\right)\left(\left(\frac{h_j}{2}+\sum_{k=1}^{j-1} h_k\right)\gamma\right)-\left(\sum_{k=1}^{j-1}\left(\frac{h_j}{2}+\sum_{k=l+1}^{j-1} h_k\right)\alpha\right)\right]-\left(\sum_{k=1}^{j-1}\left(\frac{2h_j}{3}+\sum_{k=l+1}^{j-1} h_k\right)\alpha\right)\right\}$$

$$i = 2..,N \qquad j = 2..,i$$

$$A_2(i,j) = \frac{h_j}{L_t}\left(\sum_{l=1}^{i} h_l\right)\left(\sum_{l=j+1}^{N+1} h_l\right)\left\{\left(\left(\frac{h_j}{2}+\sum_{k=1}^{j-1} h_k\right)\gamma\right)-\left(\sum_{k=1}^{j-1}\left(\frac{h_j}{2}+\sum_{k=l+1}^{j-1} h_k\right)\alpha\right)\right\}$$

$$i = 1..,N-1 \qquad j = i+1..,N$$

$$A_3(i,j) = \frac{{h_j}^2}{2L_t}\left(\sum_{l=1}^{i} h_l\right)\left[\left(\frac{h_j}{3}+\sum_{k=1}^{j-1} h_k\right)\gamma-\sum_{l=1}^{j-1}\left(\frac{h_j}{3}+\sum_{k=l+1}^{j-1} h_k\right)\alpha\right] \tag{6.6}$$

$$i = 1..,N \qquad j = i+1..,N+1$$

$$A_4(i,j) = \left(\frac{{h_j}^2}{2L_t}\left(\sum_{l=i+1}^{N+1} h_l\right)\right)\left(\frac{2h_j}{3}+\sum_{k=1}^{j-1} h_k\right)\gamma$$

$$i = 1..,N \qquad j = 1..,i$$

$$\alpha = \sum_{k=1}^{N} m_{lk}\phi_a^k \qquad \gamma = \sum_{l=1}^{N}\sum_{k=1}^{N}\left(\sum_{u=k+1}^{N+1} h_u \Big/ L_t\right) m_{lk}\phi_a^k \quad L_t = \sum_{l=1}^{N+1} h_l$$

Thus,

$$A(i,j) = A_1(i,j) + A_2(i,j) + A_3(i,j) + A_4(i,j)$$

With:

h_i= length section “i”

m_{lk} the lk mass coefficient

ϕ_a^k modal coordinate k of modal shape “a”

ω_a modal frequency of mode “a”

The system (6.4) can be rewritten as:

$$[A](x) = (c) \tag{6.7}$$

Where *(x)* is the unknown vector, that includes the stiffness coefficients EI_i of each section of the beam.

6.3 NUMERICAL STUDY

To demonstrate the effectiveness of our damage identification method in simply supported beams, we begin by conducting a numerical study using a finite element model of a real bridge. The dynamic parameters of the undamaged model are compared to a scenario where various sections of the deck have been damaged. The effect of noise on the measurement of modal shapes and natural frequencies is also studied.

6.3.1 NUMERICAL MODEL

Figure 6.2 shows the geometric characteristics of a bridge model from Nelson et al. [115], which is also used in this study. The bridge is composed of three simply supported spans. The lateral spans are 12.2 m long, and the central span is 24.4 m. long. The deck is supported on eight steel girders spaced 1.83 m apart; the deck is thus 15 m wide (Figure

6.2).

The natural frequencies and mode shapes of the bridge were calculated by performing a finite element analysis with SAP2000 [108]. Following Nelson et al. [115], the deck sections are composed of a material equivalent to homogeneous steel, with an elastic modulus of 200 GPa [115]. Table 6.1 shows the elastic proprieties of the middle span and the two end spans [115].

This study is limited to measurements of the middle span. In the simulation the middle span is divided into eight sections, defining seven coordinates of measurement for the modal shapes (figure 6.3).

Span	**A ($m^{2)}$**	**$I_z(m^4)$**	**$I_y(m^4)$**	**Weight (kN/m)**
End	0.51	0.03	9.78	39.00
Center	0.68	0.11	13.00	52.00

Table 6.1 Elastic properties of deck sections [115]

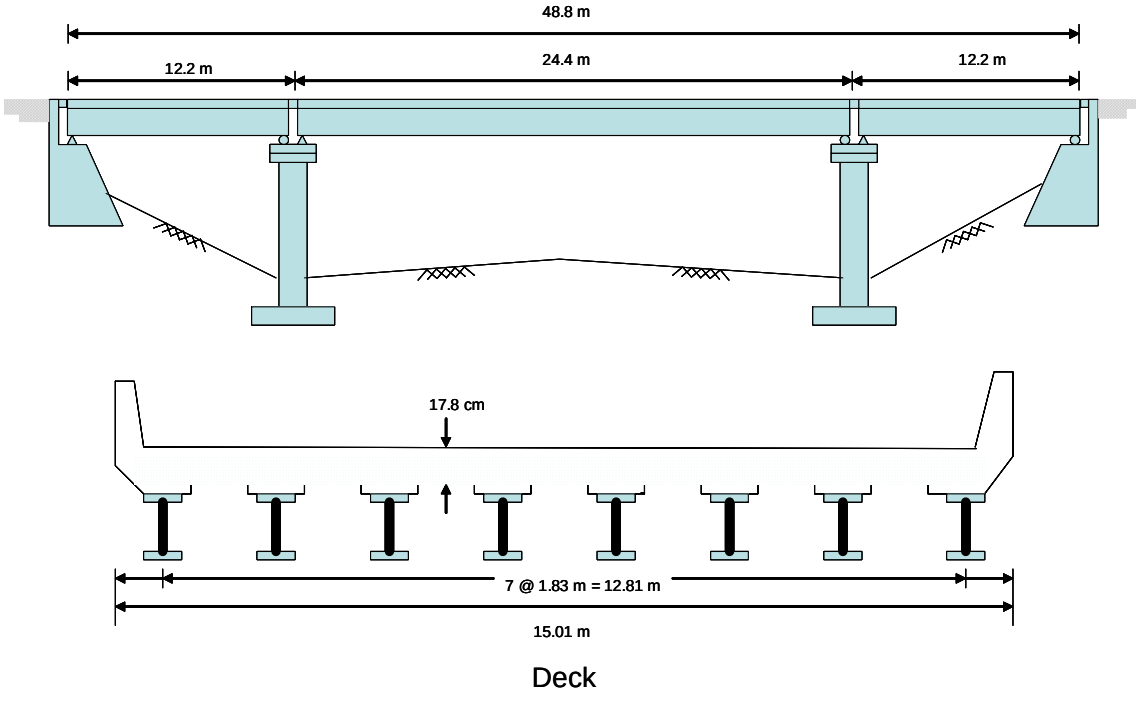

Figure 6.2 Geometrical characteristics of the bridge [115]

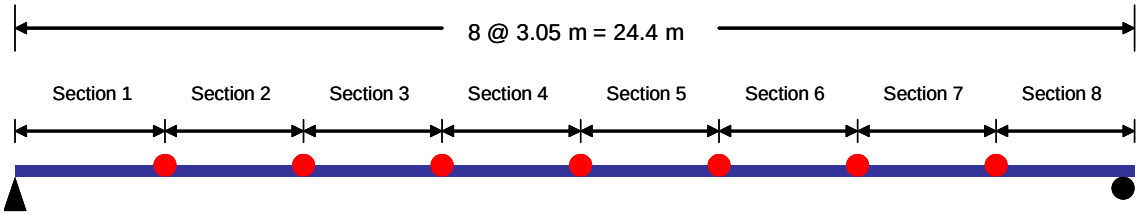

Figure 6.3 Numerical model of the middle span

6.3.2 STUDY CASES

Two cases were examined: a) the initial (undamaged) structure, b) damage in four sections (see Table 6.2). The natural frequencies and shapes of the middle section's vertical vibration modes are obtained (Figure 6.4).

Section	**1**	**2**	**3**	**4**	**5**	**6**	**7**	**8**
$\mathbf{EI_0/EI_f}$	0.90	1.0	0.70	0.70	0.80	1.0	1.0	1.0

Table 6.2 Stiffness for case b

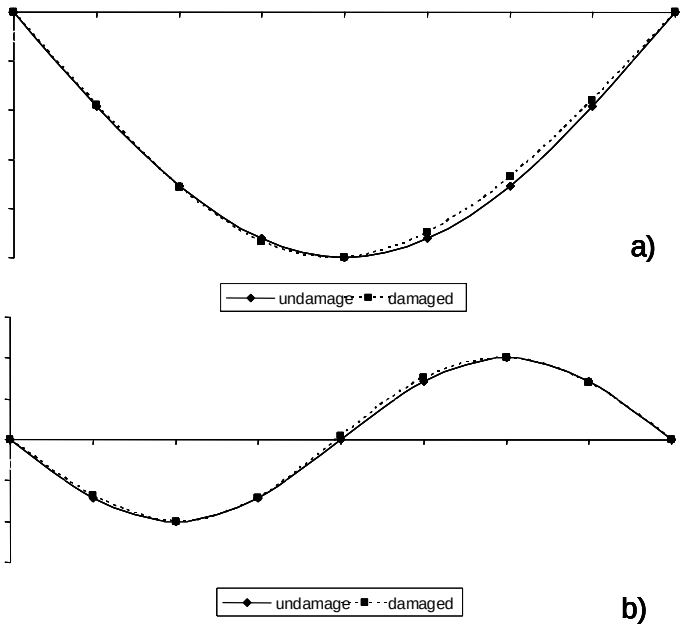

	undamage	damaged
T_1 (s)	0.200	0.220
T_2 (s)	0.049	0.052

c)

Figure 6.4 a) first mode shapes, b) second mode shape, c) period

6.3.3 EFFECTS OF ERRORS IN DYNAMIC MEASUREMENTS

In order to study the effect of noise on the measurement of modal shapes and frequencies on the damage estimation method, the modal shapes obtained from the numerical simulation were corrupted using the Sohn and Law algorithm [109]:

$$\phi_c(n) = \phi\left(1 + \frac{p}{100} R\right) \tag{6.8}$$

Where $\phi_c(n)$ is the corrupted modal shape, ϕ is the uncorrupted modal shape obtained from numerical simulations, p is a specified percentage of noise level, and R is a random number between 0 and 1. A set of ten vibration tests was carried out. It was used the normally distributed random number from Matlab [110].

Three cases were used to study the effect of measurement noise on damage identification:

a: The frequency is corrupted and the mode shape is uncorrupted

b: The frequency is uncorrupted and the mode shape is corrupted

c: Both frequency and mode shape are corrupted at the same signal-to-noise level.

Six values noise level were considered: 0.1%, 0.5%, 1%, 2%, 5% and 10%.

6.3.3.1 Results

Tables 6.3, 6.4 and 6.5 show the results of our damage estimation procedure. The location of the damage is identified with precision, as are the changes in stiffness. The damage identification is affected by noise in the measurement, but is usually quite good. The quality of damage identification does not depend on whether measurement errors reside in the frequencies or modal shapes.

	Noise Level					
Section	**0.1%**	**0.5%**	**1%**	**2%**	**5%**	**10%**
1	-0.04	0.04	-0.03	0.39	1.12	1.01
2	0.02	0.02	0.00	-0.29	-0.50	-0.66
3	-0.01	0.00	0.01	0.29	0.15	0.70
4	0.01	0.02	-0.05	-0.34	-0.09	-0.97
5	-0.01	-0.04	0.05	0.34	0.00	0.87
6	0.01	0.06	-0.04	-0.32	0.15	-0.60
7	0.01	-0.06	0.05	0.28	-0.16	0.45
8	-0.01	0.08	-0.07	0.15	0.38	-0.62

Table 6.3 Relative Errors Case a

	Noise Level					
Section	**0.1%**	**0.5%**	**1%**	**2%**	**5%**	**10%**
1	-0.01	-0.23	0.54	0.79	-1.39	1.99
2	0.10	-0.05	0.21	1.02	0.29	0.03
3	0.03	-0.14	0.40	0.89	-0.59	1.08
4	0.07	-0.10	0.25	0.99	-0.13	0.56
5	0.04	-0.15	0.40	0.89	-0.65	1.15
6	0.09	0.06	0.23	1.00	0.15	0.20
7	0.01	-0.20	0.44	0.86	-1.01	1.58
8	0.14	0.02	0.10	1.09	0.89	-0.74

Table 6.4 Relative Errors Case b

	Noise Level					
Section	**0.1%**	**0.5%**	**1%**	**2%**	**5%**	**10%**
1	-0.09	0.18	1.36	1.96	-3.73	1.03
2	0.02	-0.14	0.41	-1.37	0.10	-0.56
3	-0.02	-0.07	0.52	0.98	-1.55	-1.78
4	0.00	-0.06	0.56	-0.71	-1.21	0.58
5	-0.03	-0.17	0.45	0.81	-1.51	-0.41
6	0.00	0.12	0.88	-0.84	-0.61	-3.15
7	-0.04	-0.29	0.00	0.73	-2.16	3.48
8	0.06	0.27	1.36	-1.48	0.31	-8.63

Table 6.5 Relative Errors Case c

6.3.4 SEVERE DAMAGE

To study the effect of damage severity on the stiffness identification, we examined multiple scenarios with a 2% random measurement error in the frequencies and modal shapes. The structure was subjected to several different types of simulated damage. Table 6.6 defines the individual cases. In each case damage is simulated simply by reducing the stiffness of one or more sections in the finite element model.

CASE	Damage Location	Damage severity (%)
a	Section 1	10
	Section 3, 4	30
	Section 5	20
b	Section 1	10
	Section 3	90
	Section 4	80
	Section 5	20
c	Section 1	10
	Section 3,	90
	Section 4, 5	80
d	Section 1	10
	Section 3, 6	90
	Section 4, 5	80
e	Section 1	10
	Section 3, 6	90
	Section 4, 5, 7	80

Table 6.6 Simulated damage cases

6.3.4.1 Results

The effects of multiple damage and severe stiffness reductions on the damage identification are presented in Table 6.7, which reports the relative error in our stiffness estimation relative to the actual damage defined in Table 6.6. Taken together, these results show that the method works just as well when the damage is severe or there are multiple damaged sections. In all cases the methodology identifies the location of damage and quantifies the stiffness variations with precision.

	Case				
Section	**a**	**b**	**c**	**d**	**e**
1	0.36	-1.93	-2.47	2.06	-1.92
2	-0.95	1.54	-1.65	0.97	-0.26
3	-0.33	0.09	-1.86	1.45	-0.23
4	-0.47	0.14	-1.86	1.43	-1.07
5	-0.64	0.63	-1.89	1.48	0.30
6	-0.35	-0.71	-1.56	1.41	-0.73
7	-0.50	1.44	-2.40	2.08	0.05
8	-0.57	-2.22	-1.05	-0.42	-2.52

Table 6.7 Relative errors. Severe Damage

6.4. EXPERIMENTAL ASSESSMENT

To verify the effectiveness of this damage estimation method, we also tested the dynamic modes of a physical model. The dynamical parameters of the model are determined from the experimental data (section 3.3).

6.4.1 STUDY CASES AND ESTIMATION RESULTS

After measuring the natural vibration modes, damage was introduced into the beam in several stages. To reduce the stiffness of a beam segment, cracks were made in the flanges (figure 6.5). These cracks were in the center of the affected section. Four cases were established:

Case a: Initial undamaged beam
Case b: Beam with damage in the 2nd section
Case c: Beam with damage in the 2nd and 3rd sections
Case d: Beam with damage in the 2nd, 3rd and 4th sections

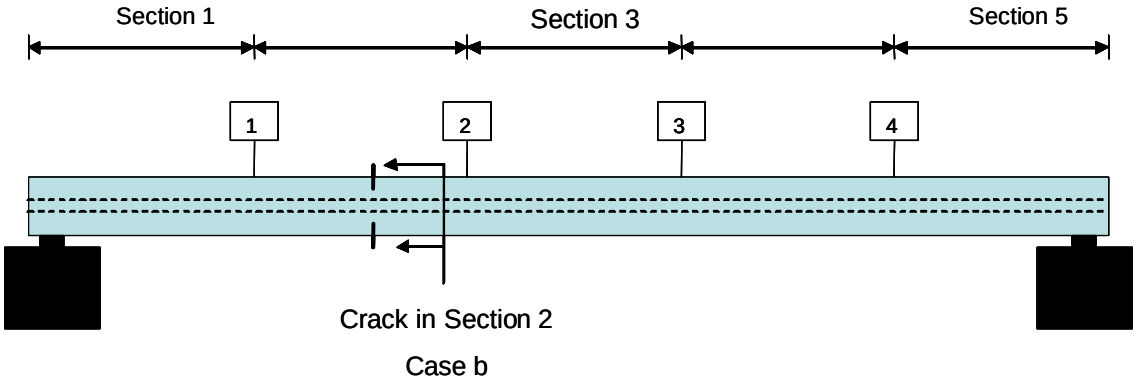

Figure 6.5 Studied Case with damage in 2nd section (case b)

A variety of free vibration tests were performed for each of the cases described above. In this manner we were able to compare several records, and to choose those which provided the most information on the structure. The modal frequencies and mode shapes determined for each case are reported in Table 6.8 and Figures 6.7, 6.8 and 6.9 respectively. Given the beam mass and this experimental information, a linear system is

formed (6.4) from the expressions described in (6.6). Solving system (6.4), we obtain the stiffness changes for every case relative to the initial structure (case a).

Table 6.9 shows the final damage estimations for cases b, c, and d. In each case, the damaged and undamaged sections are identified correctly. In the undamaged sections, the maximum error in the stiffness estimation is 2%. The methodology precisely estimated the degree of damage in other sections as well, in terms of a change in stiffness relative to case (a).

	ω_1 (rad/s)	ω_2 (rad/s)	ω_3 (rad/s)
Undamaged	25.50	97.60	---
Case b	25.12	95.87	---
Case c	24.93	95.68	219.55
Case d	23.01	87.63	196.93

Table 6.8 Natural frequency from the free vibration test

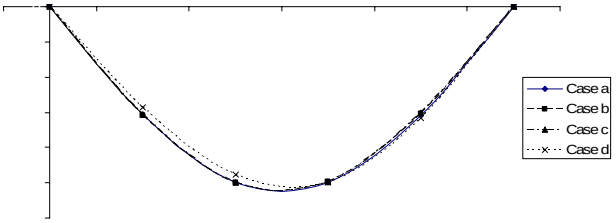

Figure 6.6 First mode shape from free vibration test

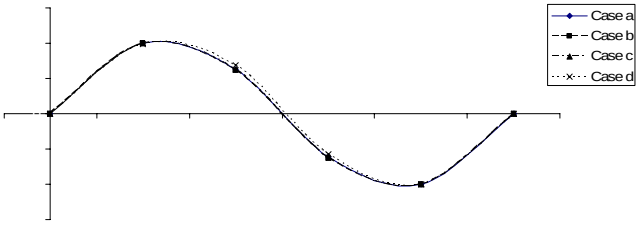

Figure 6.7 Second mode shape from free vibration test

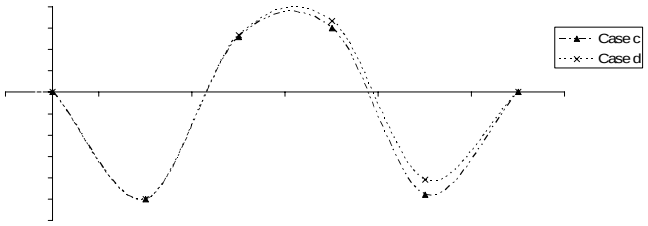

Figure 6.8 Third mode shape from free vibration test

	Case b Damage in the 2nd section	Case c Damage in the 2nd and 3rd section	Case d Damage in the 2nd, 3rd and 4th section
Section	**EI_f/ EI_o**	**EI_f/ EI_o**	**EI_f/ EI_o**
1	0.99	1.01	1.02
2	0.92	0.93	0.93
3	0.99	0.89	0.90
4	0.99	0.99	0.63
5	0.99	0.99	1.00

Table 6.9 Stiffness changes estimation

6.5 CONCLUSION

The damage identification procedure for a simply supported beam was proposed The methodology requires that the mass matrix and two of the beam's natural vertical vibration modes (shape and frequency) are known beforehand

The damage identification procedure was illustrated with a numerical example: a finite element model of a real bridge. Damage to the model was successfully estimated with low relative error. It has been shown that the method also behaves satisfactorily under noisy conditions. The quality of damage identification does not depend on whether measurement errors reside in the frequencies or modal shapes.

The accuracy of our damage identification method is also unaffected by the severity of damage. Whether the stiffness of a section is greatly reduced or multiple sections are

affected, the method accurately estimates the location and magnitude of stiffness changes.

A real steel beam was progressively damaged and subjected to the same method. In all three cases, the estimation method performed just as well as in the numerical models.

This approach can be applied not only to simply supported beams but also to simply supported girder bridges. It has two important advantages: only a small number of natural vibration modes need to be known beforehand, and stiffness changes can be accurately estimated using a small number of dynamical tests. Furthermore, this method requires only measurements along a single axis; rotational coordinates and refined FE models are unnecessary.

7. IDENTIFICATION METHOD FOR FLEXURE AND SHEAR BEHAVIOR OF CANTILEVER STRUCTURES

7.1 INTRODUCTION

The shear wall buildings, masonry wall buildings, Industrial Chimneys, Towers, tanks, balconies and cantilever projections could be modeled as a cantilever fixed at the foundation. Flexural and Shear deformation are present in those structures; depending on the geometric parameters a structure will be able to have bending deformation behavior or shear.

This chapter presents an identification method for the assessment of flexure and shears stiffness of cantilever structures or shear wall buildings. The method estimates stiffness whenever flexural (EI) or shear (GA) values are relevant or are irrelevant. An initial formula includes both shear and flexural components.

Three numeric simulations and one experimental application are performed to study the effectiveness of the methodology. A numerical simulation of a real chimney is performed to study the effectiveness of the method to identify damage. After, a shear wall building is simulated to study the influence of the initial mass model on the stiffness identification of shear wall buildings. Finally the method is applied on the stiffness identification of a confined masonry structure and the influence of the geometry and openings are also studied.

The last part of this chapter presents an experimental application of an Identification methodology of one steel cantilever which suffers damage in two sections.

7.2. SHEAR AND FLEXURAL STIFFNESS EVALUATION FOR CANTILEVER STRUCTURES AND SHEAR WALL BUILDINGS

7.2.1GENERAL METHODOLOGY FOR FLEXURAL AND SHEAR STIFFNESS EVALUATION

Figure 7.1 shows the structural model considering flexural and shear behavior, rigid slabs, non vertical deformations and consistent masses. The structure is idealized with N dynamic degrees of freedom (dof), with an unknown flexibility matrix F (or its corresponding stiffness matrix K) and a known mass matrix M. accepted that the dynamic analysis allows the research of m modal frequencies and their corresponding mode shapes with m<N.

Consider the equation of motion for an undamped N degrees-of-freedom (DOF) structure, given by:

$$M\ddot{u} + Ku = f(t) \tag{7.1}$$

Where

M=mass matrix

K=Stiffness Matrix

$\ddot{u}$=acceleration vector

u=displacement vector

$f(t)$=excitation vector force

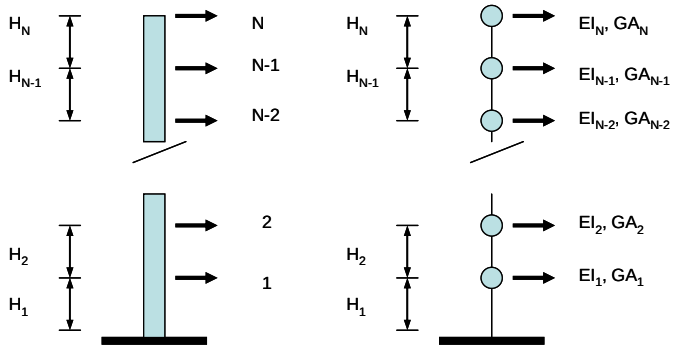

Figure 7.1 *N* dof Structural Model

Consider the corresponding characteristics equation:

$$(K - \lambda_i M)\phi_i = 0 \tag{7.2}$$

Equation (7.2) can be rewritten as:

$$(\lambda_i^{-1} - F.M)\phi_i = 0 \tag{7.3}$$

With

F= Flexibility matrix,

$\lambda_i = \omega_i^2$, ω_i= ith modal frequency, i= 1 to N

ϕ_i = ith eigenvector.

Equation (7.3) corresponds to:

$$\left\{\begin{bmatrix} 1/\lambda_a & \cdots & 0 \\ \vdots & 1/\lambda_a & \vdots \\ 0 & \cdots & 1/\lambda_a \end{bmatrix} - \begin{bmatrix} f_{11} & \cdots & f_{1N} \\ \vdots & f_{ij} & \vdots \\ f_{N1} & \cdots & f_{NN} \end{bmatrix} \begin{bmatrix} m_{11} & \cdots & m_{1N} \\ \vdots & m_{ij} & \vdots \\ m_{N1} & \cdots & m_{NN} \end{bmatrix}\right\} \begin{pmatrix} \phi_a^1 \\ \vdots \\ \phi_a^N \end{pmatrix} = \begin{pmatrix} 0 \\ \vdots \\ 0 \end{pmatrix} \qquad (7.4)$$

with :

m_{ij}= *ij* coefficient of the matrix *M*

f_{ij}= *ij* coefficient of the matrix *F*

ϕ_a^i = coordinate of the ith level of mode shape a

$1/\lambda_a = 1/\omega_a^2$ and ω_a modal frequency of mode "a".

Considering two eigenvalues related to modal frequencies ω_a and ω_b, and the mode shapes ϕ_a and ϕ_b, equation (7.2) becomes:

$$\begin{array}{l} (f_{11}m_{11}+\ldots+f_{1N}m_{N1})\varphi_a^1+\ldots\ldots\ldots+(f_{11}m_{1N}+\ldots+f_{1N}m_{NN})\varphi_a^N=\varphi_a^1/\omega_a^2 \\ (f_{11}m_{11}+\ldots+f_{1N}m_{N1})\varphi_b^1+\ldots\ldots\ldots+(f_{11}m_{1N}+\ldots+f_{1N}m_{NN})\varphi_b^N=\varphi_b^1/\omega_b^2 \\ \vdots \\ (f_{N1}m_{11}+\ldots+f_{NN}m_{N1})\varphi_a^1+\ldots\ldots\ldots+(f_{N1}m_{1N}+\ldots+f_{NN}m_{NN})\varphi_a^N=\varphi_a^N/\omega_a^2 \\ (f_{N1}m_{11}+\ldots+f_{NN}m_{N1})\varphi_b^1+\ldots\ldots\ldots+(f_{N1}m_{1N}+\ldots+f_{NN}m_{NN})\varphi_b^N=\varphi_b^N/\omega_b^2 \end{array} \qquad (7.5)$$

Each flexibility value can be derived as follows:

$$f_{ij}=\sum_{k=1}^{N}\frac{1}{(EI)_k}\alpha_{ijk}\cdot 1_{k\le Min(i,j)}+\sum_{k=1}^{N}\frac{1}{(\frac{GA}{\gamma})_k}\beta_k\cdot 1_{k\le Min(i,j)} \qquad \forall \quad i,j \qquad (7.6)$$

$$with: 1_{k\le Min(i,j)}\begin{cases} 1: if\ k\le Min(i,j) \\ 0: otherwise \end{cases}$$

$$\alpha_{ijk}=H_k\left[\left(\sum_{l=k+1}^{i}H_l\right)\left(\sum_{l=k+1}^{j}H_l\right)+\frac{H_k}{2}\left(\sum_{l=k+1}^{i}H_l+\sum_{l=k+1}^{j}H_l\right)+\frac{H_k^2}{3}\right] \qquad \beta_k=H_k \qquad (7.7)$$

Where:

H_k= story height of level "k"

E_k= elasticity modulus of the material of level "k"

I_k= Inertia modulus of level "k"

G_k= shear modulus the material of level "k"

(A_k/γ)= shear transversal surface of level "k".

The goal of this procedure is the evaluation of the stiffness coefficients $(EI)_k$ and $(GA/\gamma)_k$, for each level "k", with k = 1 to N. Combined equations (7.5), (7.6) and (7.7) it yields:

$$\begin{bmatrix} a_{11}^a & b_{11}^a & 0 & \cdots & 0 \\ a_{11}^b & b_{11}^b & 0 & \cdots & 0 \\ \vdots & \vdots & & \ddots & \vdots \\ a_{N,1}^a & b_{N,1}^a & \cdots & a_{NN}^a & b_{NN}^a \\ a_{N,1}^b & b_{N,1}^b & \cdots & a_{NN}^b & b_{NN}^b \end{bmatrix} \begin{Bmatrix} 1/(EI)_1 \\ 1/(GA/\gamma)_1 \\ \\ 1/(EI)_N \\ 1/(GA/\gamma)_N \end{Bmatrix} = \begin{pmatrix} \phi_a^1/\omega_a^2 \\ \phi_b^1/\omega_b^2 \\ \\ \phi_a^N/\omega_a^2 \\ \phi_b^N/\omega_b^2 \end{pmatrix} \qquad (7.8)$$

Involving the following coefficients definitions:

$$\begin{aligned} a_{ik}^a &= \sum_{l=k}^{N}\sum_{u=1}^{N} m_{lu}.\phi_a^u.\alpha_{ijk}.1_{k\le Min(i,j)} \qquad & b_{ik}^a &= \beta_k.\sum_{l=k}^{N}\sum_{u=1}^{N} m_{lu}.\phi_a^u 1_{k\le Min(i,j)} \\ a_{ik}^b &= \sum_{l=k}^{N}\sum_{u=1}^{N} m_{lu}.\phi_b^u.\alpha_{ijk}.1_{k\le Min(i,j)} \qquad & b_{ik}^b &= \beta_k.\sum_{l=k}^{N}\sum_{u=1}^{N} m_{lu}.\phi_b^u 1_{k\le Min(i,j)} \end{aligned} \quad \text{for k = 1 to } N \qquad (7.9)$$

Equation (7.8) defines a system of 2N equations with $2N$ unknowns, as two unknown coefficients (EI) and (GA/γ) are considered for each level. This fact requires the knowledge of two mode shapes and their corresponding frequencies so as the problem to be well posed.

7.2.2 ONE STORY STRUCTURE AND SOME SINGULARITIES

A one store system leads to a singularity. Given matrix $[A]$, equations (7.5) to (7.7):

$$\begin{bmatrix} a_{11}^{a} & b_{11}^{a} \\ a_{11}^{b} & b_{11}^{b} \end{bmatrix} \begin{Bmatrix} 1/(EI)_1 \\ 1/(GA/\gamma)_1 \end{Bmatrix} = \begin{pmatrix} \phi_a^1 / \omega_a^2 \\ \phi_b^1 / \omega_b^2 \end{pmatrix} \tag{7.10}$$

As there is only 1 dof $\omega_a=\omega_b=\omega$. The determinant is equal to:

$$\begin{bmatrix} a_{11}^{a} & b_{11}^{a} \\ a_{11}^{b} & b_{11}^{b} \end{bmatrix} = m_1^2 \frac{H_1^4}{3} \left(\phi_a^1 \phi_b^1 - \phi_b^1 \phi_1^1 \right) = 0 \tag{7.11}$$

7.2.3 GENERAL CASE AND SINGULARITY IN THE HIGHEST LEVEL «N»

A singularity is found at the highest level "*N*", so the last two equations of eq. (7.8) shall have a particular treatment. The solution for the first *N-1* levels is (i = 1, *N-1*):

$$\begin{bmatrix} a_{11}^{a} & b_{11}^{a} & 0 & \cdots & 0 \\ a_{11}^{b} & b_{11}^{b} & 0 & \cdots & 0 \\ \vdots & & & & \vdots \\ a_{N-1,1}^{a} & b_{N-1,1}^{a} & & a_{N-1,N-1}^{a} & b_{N-1,N-1}^{a} \\ a_{N-1,1}^{b} & b_{N-1,1}^{b} & & a_{N-1,N-1}^{b} & b_{N-1,N-1}^{b} \end{bmatrix} \begin{Bmatrix} 1/(EI)_1 \\ 1/(GA/\gamma)_1 \\ \vdots \\ 1/(EI)_{N-1} \\ 1/(GA/\gamma)_{N-1} \end{Bmatrix} = \begin{pmatrix} \phi_a^1 / \omega_a^2 \\ \phi_b^1 / \omega_b^2 \\ \vdots \\ \phi_a^{N-1} / \omega_a^2 \\ \phi_b^{N-1} / \omega_b^2 \end{pmatrix} \tag{7.12}$$

7.2.4 DAMAGE AND RESIDUAL PROPERTIES

It is assumed that the damage affecting the k-*th* storey stiffness might be expressed through the following damage indicators:

$$\begin{cases} (EI)_i = (1 - \mathrm{D_i^f}).(EI)_i^0 \\ (GA/\gamma)_i = (1 - \mathrm{D_i^v}).(GA/\gamma)_i^0 \end{cases} \tag{7.13}$$

Where:

D_i^f = damage indicator that affects the "flexural coefficient" for storey "i"

D_i^v = damage indicator that affects the "shear coefficient"

$(EI)_i^0$ = its initial "flexural coefficient"

$(GA/\gamma)_i^0$ = its initial "shear coefficient"

Due to the singularity of the sub-matrix involving the N-*th* storey, it is assumed that the same level of damage affects both the flexural and shear coefficient:

$$D_N^f = D_N^v = 1 - \frac{a_{NN}^b \cdot \frac{1}{(EI)_N^0} + b_{NN}^b \cdot \frac{1}{(GA/\gamma)_N^0}}{\frac{\phi_b^N}{\omega_b^2} - \sum_{k=1}^{N-1}\left(a_{Nk}^b \cdot \frac{1}{(EI)_k} + b_{Nk}^b \cdot \frac{1}{(GA/\gamma)_k} \right)} \tag{7.14}$$

Once the residual factor values (*EI* and *GA*) for each storey are known, the stiffness matrix is completely known.

7.2.5 FLEXURE STIFFNESS EVALUATION

Structures with predominant flexural behavior (so shear terms can be neglected), only (*EI*) terms are significant. In this case a pair of eigenvalues is solely required so the flexure stiffness values can be obtained from the simplified system of equations obtained from eq. (7.8):

$$\begin{bmatrix} a_{11}^a & 0 & \cdots & \cdots & 0 \\ \vdots & \ddots & \ddots & \cdots & \vdots \\ a_{i1}^a & \vdots & a_{ii}^a & \ddots & \vdots \\ \vdots & & \cdots & \ddots & 0 \\ a_{N,1}^a & \cdots & a_{Ni}^a & \cdots & a_{NN}^a \end{bmatrix} \begin{Bmatrix} 1/(EI)_1 \\ \vdots \\ 1/(EI)_i \\ \vdots \\ 1/(EI)_N \end{Bmatrix} = \begin{pmatrix} \phi_a^1 / \omega_a^2 \\ \vdots \\ \phi_a^i / \omega_a^2 \\ \vdots \\ \phi_a^N / \omega_a^2 \end{pmatrix} \tag{7.15}$$

7.2.6 SHEAR STIFFNESS EVALUATION

In the case of significant values of shear stiffness compared to the flexure stiffness, this latter one can be neglected and only *(GA/γ)* terms are significant. Only one eigenpair is required and shear stiffness coefficients are given by:

$$\begin{bmatrix} b_{11}^a & 0 & \cdots & \cdots & 0 \\ \vdots & \ddots & \ddots & \cdots & \vdots \\ b_{i1}^a & \vdots & b_{ii}^a & \ddots & \vdots \\ \vdots & & \cdots & \ddots & 0 \\ b_{N,1}^a & \cdots & b_{Ni}^a & \cdots & b_{NN}^a \end{bmatrix} \begin{Bmatrix} 1/(GA/\gamma)_1 \\ \vdots \\ 1/(GA/\gamma)_i \\ \vdots \\ 1/(GA/\gamma)_N \end{Bmatrix} = \begin{pmatrix} \phi_a^1 / \omega_a^2 \\ \vdots \\ \phi_a^i / \omega_a^2 \\ \vdots \\ \phi_a^N / \omega_a^2 \end{pmatrix} \tag{7.16}$$

7.3 NUMERICAL STUDY

To demonstrate the effectiveness of the identification procedures developed in the section 7.2, a numerical study using a finite element model of the steel chimney conducted. Simulated real steel chimney without damage and with assumed damage sections are considered. Figure 7.2 shows the geometric values of the steel chimney employed for the numerical study, from Ambrosini et al. [116]. The chimney is a cylindrical steel structure of 28 m high with 0.914 m diameter, cross section is 12 mm at the base and 3 mm at the top (figure 7.2). The simulated steel chimney is divided into 10 two-dimensional sections (Figure 7.2). Three sections (No. 2, 5 and 8) are assumed to be subjected to 10%, 30% and 10% stiffness reduction. The modal data (mode shapes and frequencies) before and after damage (Fig. 3) have been calculated by using the finite element program SAP2000 [108].

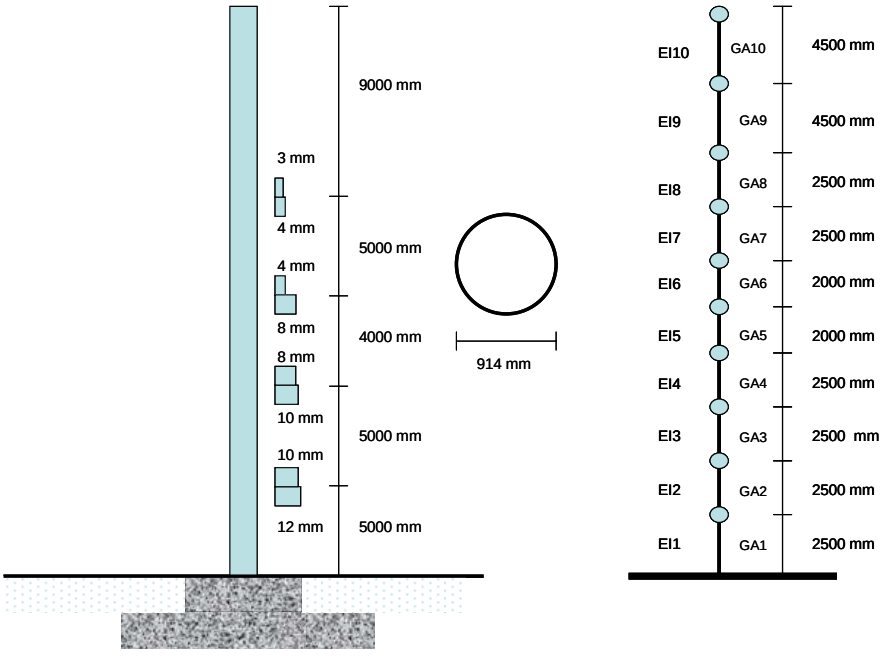

Figure 7.2 A simulated steel chimney [116]

7.3.1 EFFECTS OF ERRORS IN DYNAMICS MEASUREMENTS

In order to study the effect of noise on the measurement of mode shapes and frequencies for the stiffness identification method, the mode shapes obtained from the numerical simulation were corrupted using the Sohn and Law algorithm [109]:

$$\phi_c(n) = \phi\left(1 + \frac{p}{100} R\right) \tag{7.17}$$

Where ϕ_c(n) is the corrupted mode shape, ϕ is the uncorrupted mode shape obtained from numerical simulations, p is a specified percentage of noise level, and R is a random number between 0 and 1. A set of ten vibration tests was carried out. Normally distributed random number from Matlab [110] was used.

Three study cases were proposed to study the effect of measurement noise on the damage identification:

Case a: frequency is corrupted and modal shape uncorrupted

Case b: frequency is uncorrupted and modal shape corrupted

Case c: frequency is corrupted and modal shape corrupted with same noise level.

Six values noise level were considered: 0.1%, 0.5, 1, 2%, 5% and 10%.

7.3.3.1 Results

The stiffness identification is carried out using Eqs. (7.12) and (7.14) with noisy mode shapes and mass matrix, the coefficients *EI* and *GA* were obtained for undamaged and damaged states.

The damage identification with different level of noise in frequency or mode shapes was performed to verify the efficiency and accuracy of the proposed method. Tables 7.1 to 7.6 show the relative errors in the damage identification for the defined cases in 7.3. The following observations can be made:

1. The quality of the damage identification is more sensitive to the perturbation of the mode shapes than that of frequencies.

2. The estimation of coefficients GA is made with less precision than coefficients EI. As expected a better adjustment of the flexural coefficient was obtained than the shear coefficient, for the chimney is mainly characterized by a flexural behavior

3. The damage identification with level noise in the modal parameters give a reasonable agreement between the damage estimated and damage assumed. For the EI coefficients, in all cases the methodology identifies with precision the location of the stiffness changes as well as the variation of stiffness. For the study noise level the relative error of the estimation remain smaller that 9%.

4. The Shear coefficients (GA) are identified with acceptable precision. Only the large error was present and was not corrected, for example in section 8 case c with noise level 5%, the obtained error is closed to 20%.

	Noise Level					
Section	**0.1%**	**0.5%**	**1%**	**2%**	**5%**	**10%**
1	0.00	0.00	0.00	0.00	0.00	-0.01
2	0.00	0.00	0.00	0.00	0.00	-0.01
3	0.00	0.00	0.00	0.00	0.00	0.00
4	0.00	0.00	0.00	0.00	0.01	-0.04
5	0.00	-0.01	0.00	-0.01	-0.01	0.13
6	0.00	0.00	0.00	0.00	0.00	0.03
7	0.00	0.00	0.00	0.00	0.01	-0.06
8	0.00	0.00	0.00	0.00	-0.01	0.04
9	0.00	0.00	0.00	0.00	0.00	0.01
10	0.00	0.00	0.00	0.00	0.00	0.03

Table 7.1 Relative error Coefficients EI case a

	Noise Level					
Section	**0.1%**	**0.5%**	**1%**	**2%**	**5%**	**10%**
1	0.00	0.00	0.00	0.00	0.01	0.00
2	0.00	-0.01	0.01	0.10	0.12	0.06
3	0.00	-0.02	-0.01	0.12	0.17	-0.15
4	0.00	-0.01	0.00	-0.31	-0.50	0.08
5	0.04	-0.40	-0.56	-2.47	-3.43	-4.13
6	0.01	-0.07	-0.26	-0.64	-0.79	-4.05
7	-0.01	0.07	0.12	0.13	0.32	0.85
8	-0.04	0.00	0.03	-0.29	0.96	1.44
9	-0.10	-0.01	0.37	0.06	-0.38	3.15
10	0.35	-0.79	-1.78	-1.36	3.01	8.41

Table 7.2 Relative error Coefficients GA case a

	Noise Level					
Section	**0.1%**	**0.5%**	**1%**	**2%**	**5%**	**10%**
1	0.00	0.00	0.00	0.00	0.01	0.00
2	0.00	-0.01	0.01	0.10	0.12	0.06
3	0.00	-0.02	-0.01	0.12	0.17	-0.15
4	0.00	-0.01	0.00	-0.31	-0.50	0.08
5	0.04	-0.40	-0.56	-2.47	-3.43	-4.13
6	0.01	-0.07	-0.26	-0.64	-0.79	-4.05
7	-0.01	0.07	0.12	0.13	0.32	0.85
8	-0.04	0.00	0.03	-0.29	0.96	1.44
9	-0.10	-0.01	0.37	0.06	-0.38	3.15
10	0.35	-0.79	-1.78	-1.36	3.01	8.41

Table 7.3 Relative error Coefficients EI case b

	Noise Level					
Section	**0.1%**	**0.5%**	**1%**	**2%**	**5%**	**10%**
1	0.00	0.01	-0.05	-0.12	-0.28	0.01
2	-0.02	0.48	-0.02	-0.66	-1.90	7.73
3	0.00	-0.20	0.17	-0.38	-1.44	-0.80
4	-0.03	-0.09	-0.11	-0.72	0.77	-0.16
5	-0.93	-3.01	4.20	5.10	3.03	1.72
6	-0.18	-2.42	-0.08	-5.43	3.57	3.98
7	0.39	-0.75	1.48	3.52	-0.79	3.99
8	0.59	-1.29	-2.17	-1.32	0.77	-3.13
9	1.23	-4.60	5.49	3.13	3.73	6.52
10	0.35	-0.79	-1.78	-1.36	3.01	8.41

Table 7.4 Relative error Coefficients GA case b

	Noise Level					
Section	**0.1%**	**0.5%**	**1%**	**2%**	**5%**	**10%**
1	0.00	0.00	0.00	0.00	0.00	0.01
2	0.00	0.02	0.01	-0.06	-0.27	-0.02
3	0.00	0.02	0.04	-0.03	-0.09	0.28
4	0.00	0.02	-0.11	0.17	-0.19	-0.80
5	0.01	-0.60	-1.19	2.01	-3.69	-8.11
6	0.02	-0.08	-0.38	0.25	-2.12	-2.34
7	-0.01	0.06	0.12	-0.06	0.17	1.31
8	-0.02	-0.01	0.09	-0.07	-0.28	1.22
9	0.01	-0.01	-0.03	-2.96	0.49	8.00
10	-0.09	-0.10	0.76	4.31	0.76	5.75

Table 7.5 Relative error Coefficients EI case c

	Noise Level					
Section	**0.1%**	**0.5%**	**1%**	**2%**	**5%**	**10%**
1	0.00	-0.13	0.07	-0.01	0.08	-0.29
2	-0.02	1.11	-0.93	0.16	-1.74	-3.03
3	0.05	-1.47	0.48	-0.26	0.52	-1.80
4	-0.05	-3.19	1.11	-2.73	1.84	1.49
5	0.01	1.61	-6.13	0.64	-8.79	-8.43
6	-0.37	-3.17	-0.82	0.85	5.79	3.96
7	0.35	-0.60	2.12	-3.06	4.25	3.93
8	-0.40	5.78	0.21	-0.32	-1.87	-7.14
9	-0.78	0.62	1.46	5.60	18.90	5.93
10	-0.09	-0.10	0.76	4.31	0.76	5.75

Table 7.6 Relative error Coefficients GA case c

7.3.2 INFLUENCE OF DAMAGE SEVERITY

To study the effect of damage severity on the stiffness identification, multiple damage scenarios in frequency and modes were performed with 2% noise. The chimney was subjected to different simulated damage cases shown in table 7.7. The damage was simulated by reducing the stiffness section.

CASE	Damage Location	Damage severity (%)
a	Section 2	70
	Section 5	30
	Section 8	10
b	Section 2, 5	70
	Section 8	10
c	Section 2, 5, 8	70
d	Section 2, 3, 5, 8	70
e	Section 2, 3, 4, 5, 8	70
e	Section 2,3,4, 5,6, 8	70
f	Section 2,3,4,5,6,7,8	70

Table 7.7 Simulated damage cases

7.3.2.1 RESULTS

The effect of multiple and severe stiffness reductions on the damage identification was carried out. Tables 7.8 and 7.9, show the relative error in stiffness estimation defined in Table 3.3. The following observations were generated through review of the obtained results:

1. The Flexure stiffness coefficients (*EI*) which had acceptable precision were corrected. The Shear coefficients (*GA)* had unacceptable precision and major errors, and were not corrected, for example in section 8 case g, the obtained errors reached up to 100%. Such as in section 7.3, it was expected a better adjustment of the flexural coefficient than the shear coefficient, because of the chimney mainly flexural

behavior.

2. In spite of the important damage in cases e, f and g, the methodology managed to identify with acceptable precision the damage zones for the estimation of EI coefficients.

	Case						
Section	**a**	**b**	**c**	**d**	**e**	**f**	**g**
1	0.06	0.00	-0.03	0.00	-0.01	-0.06	-0.02
2	0.13	0.63	-0.63	0.17	0.17	-0.10	0.27
3	0.85	1.12	0.03	-0.50	-0.70	-0.27	-0.90
4	-1.59	-0.98	-1.83	1.51	2.67	1.63	1.13
5	-0.07	1.77	0.10	2.63	-3.27	-1.43	0.03
6	-2.25	2.85	3.69	9.60	-14.20	2.07	-1.50
7	-0.43	-2.07	-4.75	-7.66	0.71	3.36	1.43
8	1.71	-0.13	-1.60	-3.30	-1.50	10.53	-2.80
9	2.57	-0.73	-1.18	-10.57	-14.88	10.10	-1.00
10	-1.26	14.78	-3.62	22.39	28.56	20.99	-16.40

Table 7.8 Relatives Errors *EI* coefficients

	Case						
Section	**a**	**b**	**c**	**d**	**e**	**f**	**g**
1	-2.36	-0.04	1.07	0.05	0.59	2.45	1.11
2	-24.67	-2.50	-25.33	-3.13	-23.23	-28.87	-5.97
3	10.38	8.86	24.42	-3.20	-20.97	-18.53	-2.60
4	7.12	-13.53	26.62	7.40	-23.37	-21.20	5.37
5	-6.77	3.37	-37.10	19.17	-33.33	-34.20	-0.23
6	16.88	31.30	-1.82	-1.24	36.46	-42.67	-23.37
7	23.40	1.62	25.97	24.44	41.77	80.82	66.09
8	5.49	22.71	-40.84	-16.03	15.87	-33.40	-125.17
9	66.23	24.25	16.68	39.24	27.61	52.07	81.45
10	-1.26	14.78	-3.62	22.39	28.56	20.99	-16.40

Table 7.9 Relatives Errors *GA* coefficients

7.4 INFLUENCE OF MASS MODELS AND NONPARAMETRIC MASS NORMALIZATION ON STRUCTURAL STIFFNESS IDENTIFICATION: CASE OF BUILDING SHEAR WALLS

Generally, stiffness identification methods for buildings are based on simplified mass models [52, 117]. Often, lumped masses at each store are supposed, leading to diagonal mass matrices. In the analysis of the shear wall buildings the Consistent mass models are less often employed. In this section, the influence of the initial mass model on the stiffness identification of shear wall buildings is discussed. As the initial lumped mass model leads to poor identification results, the influence of consistent mass models is evaluated. A nonparametric mass matrix normalizing procedure based on experimental data is introduced, leading to more accurate results for the stiffness identification of the analyzed shear wall buildings.

7.4.1 NONPARAMETRIC MASS MATRIX ADJUSTMENT

A direct nonparametric adjustment procedure for the initial structural mass matrix has been presented in earlier work [118, 119]. Let us consider a structural system with an unknown mass matrix *M* and an initial theoretical mass matrix $\tilde{M}$.

Let us denote by M the adjusted mass matrix to be evaluated, which has dimensions (*NxN*), where *N* is the number of degrees of freedom and Φ is the eigenvector matrix. The real structure has *N* eigenvectors. This matrix has *N* rows and *m* columns, where *m* is the number of mode shapes obtained experimentally (*m*<*N*).

7.4.2 MASS MATRIX ADJUSTMENT

To obtain M, a function *f(M)* is defined; it represents the "distance" between M and $\tilde{M}$:

$$f(M) = \left\| \tilde{M}^{-1/2} \cdot (M - \tilde{M}) \cdot \tilde{M}^{-1/2} \right\| \tag{7.18}$$

M must satisfy the orthogonality condition:

$$\Phi^{t}.\mathrm{M}.\Phi = \mathrm{I} \tag{7.19}$$

A minimization problem under equality constraint may be solved by means of Lagrange's theorem, with the following objective function:

$$h(M,\Lambda) = f(M) + \Lambda g(M) \tag{7.20}$$

where Λ = Lagrange's operators matrix.

Minimizing the function $h(M,\Lambda)$ requires the following conditions:

$$\left.\frac{\partial h(M)}{\partial M}\right)_{ij} = 0 \tag{7.21}$$

and

$$\left.\frac{\partial h(M)}{\partial \Lambda}\right)_{ij} = 0 \tag{7.22}$$

Finally, this leads to:

$$2 \cdot \tilde{M}^{-1} \cdot \left(M - \tilde{M}\right) \cdot \tilde{M}^{-1} + \Phi \cdot \Lambda \cdot \Phi^{t} = 0 \tag{7.23}$$

$$\Phi^{t} \cdot \left(M - \tilde{M}\right) \cdot \Phi + M_{a} - I = 0 \tag{7.24}$$

where: $M_{a} = \Phi^{t} \cdot \tilde{M} \cdot \Phi$.

As M and Λ are unknowns, the solution can be written as, [118, 119]:

$$M = \tilde{M} + \tilde{M} \cdot \Phi \cdot M_{a}^{-1} \cdot \left(I - M_{a}\right) \cdot M_{a}^{-1} \cdot \Phi^{t} \cdot \tilde{M} \tag{7.25}$$

7.4.3 NUMERICAL STUDY

A dynamic analysis was performed with the SAP2000 software [108], using the finite-element method (FEM) and various mass models for each shear-wall structure.

The corresponding dynamic parameters (ω, ϕ) are numerically obtained. Afterwards, the stiffness identification is carried out using Eqs. (7.12) and (17.14) with dynamic parameters and the previously adjusted mass matrix (by applying Eq. 7.25); the coefficients EI and GA were estimated for each floor.

The stiffness coefficients used in the FEM are reference values to be compared with the estimated coefficients. The relative difference between these results, or the error matrix, is evaluated using the following expressions:

$$\text{Error: } \Delta(EI_i) = \left(\frac{EI_i^{MEF} - EI_i^*}{EI_i^{MEF}} \right) * 100 \qquad (7.26)$$

and

$$\text{Error: } \Delta(GA_i) = \left(\frac{GA_i^{MEF} - GA_i^*}{GA_i^{MEF}} \right) * 100 \qquad (7.27)$$

where:

EI_i^{MEF} = flexure stiffness for storey "i" (FEM values)

EI_i^* = the estimated flexure stiffness for storey "i"

GA_i^{MEF} = shear stiffness for storey "i" (FEM values)

GA_i^* = the estimated shear stiffness for storey "i"

7.4.3.1 FEM modeling

Plane shell elements are used for the wall model [108]. They simulate membrane or plate behavior (Figure 7.3). Compatible lateral displacements are considered for each floor because this condition leads to better results than free lateral displacements. Actually, this condition has been previously evaluated; it might lead to less than 2% relative error [120].Wall masses are uniformly distributed for each FE node, and the

slab mass is lumped to the nodes belonging to each floor. The building is clamped at ground level.

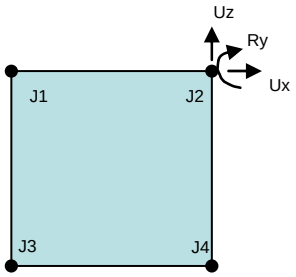

Figure 7.1 Shell Element

7.4.3.2 Mass Models

Four mass matrix configurations are analyzed:

a) Diagonal Mass matrix (MD): it is the simplest and the most used procedure; it considers the structural masses as lumped at each level.

b) Consistent mass matrix (MC): The structure is modeled as a cantilever involving plane beams with 3 DOF per node, and a consistent mass model is assigned to each beam **(**Figure 7.4**)**. The system degrees of freedom are *2N*, and Guyan reduction is used to condense rotational DOF [121] (vertical displacements are neglected).

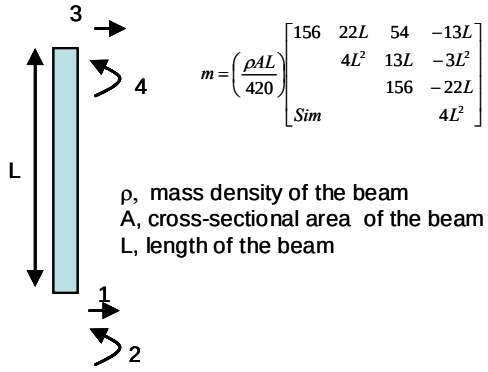

Figure 7.2 Beam element and consistent mass matrix

c) Adjusted diagonal mass matrix (MDA): This matrix is obtained from the original diagonal (MD) matrix by applying the nonparametric normalization. This normalization requires two eigenpairs.

d) Adjusted consistent mass matrix (MCA): This matrix is obtained from the adjustment of the consistent mass matrix by applying the nonparametric normalization.

7.4.3.3 Results

Four mass models have been considered. For each model, the flexural and shear stiffness are calculated for each floor. For illustrative purposes, a five-story building with 1, 2, or 3 bays is considered **(**Figure 7.5**)**. To evaluate the numerical accuracy of the estimation procedure, a ten-story structure is considered as an additional example.

7.4.3.3.1 Structures with five stories

The following set of values is adopted for the models:

L_v= 3 m (bay length)

H_p= 3 m (story height)

e_w = 0.2 m (wall thickness)

E= 25 10^3 MPa (elasticity modulus)

G= 10.4 10^3 MPa (shear modulus)

The lumped masses at each storey level are 500, 1000, 1500 kg for the cases of 1, 2 and 3 bays respectively.

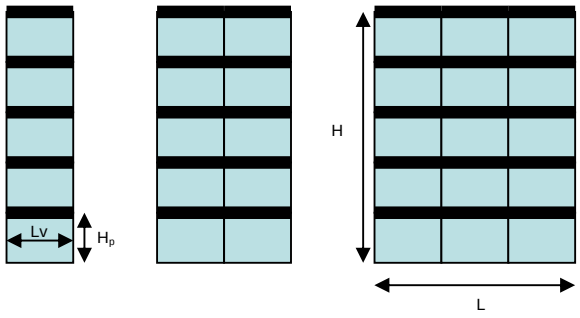

Figure 7.3 Buildings with 5 stories and different numbers of bays

A summary of the results is given in Tables 7.10-7.12. The accuracy of the stiffness prediction depends on the mass model:

1. Mass models MDA and MCA provide the best results, with relative errors of flexural stiffness (EI) and shear stiffness (GA/γ) less than 10%. The largest relative error (~15%) corresponds to the top (fifth) story. The MCA mass model provides better stiffness identification.

2. Mass models MD and MC provide acceptable results for the first two stories, but the relative error becomes very large for upper stories.

	|Error| (%)			
	MC	**MD**	**MCA**	**MDA**
$(EI)_1$	3.7	2.7	1.9	0.5
$(EI)_2$	0.6	14	7.3	1.7
$(EI)_3$	17	56	0.60	0.6
$(EI)_4$	72	134	5	3.4
$(EI)_5$	154	80	6.2	5.1

	|Error| (%)			
	MC	**MD**	**MCA**	**MDA**
$(GA)_1$	12	7	9	7
$(GA)_2$	13	2	4	3
$(GA)_3$	30	18	2	3
$(GA)_4$	1080	60	2	4
$(GA)_5$	154	80	6	5

Table 7.10 Relative errors for the flexural and shear stiffness: 5 storey building with 3 bays

	|Error| (%)			
	MC	**MD**	**MCA**	**MDA**
$(EI)_1$	1.6	5	0.4	1.2
$(EI)_2$	0.9	11	1.8	1.2
$(EI)_3$	12	61	0.9	1.8
$(EI)_4$	63	134	1.5	4.1
$(EI)_5$	138	88	1.2	11

	|Error| (%)			
	MC	**MD**	**MCA**	**MDA**
$(GA)_1$	11	0.9	6	5
$(GA)_2$	17	14	3	0.4
$(GA)_3$	50	38	3	1
$(GA)_4$	258	78	3	4
$(GA)_5$	138	88	1	11

Table 7.11 Relative errors of the flexural and shear stiffness: 5 storey building with 2 bays

	|Error| (%)					|Error| (%)		
	MC	**MD**	**MCA**	**MDA**		**MC**	**MD**	**MCA**	**MDA**
$(EI)_1$	0.9	18	0.4	1.3	$(GA)_1$	12	43	5	0.1
$(EI)_2$	1.1	26	0.7	0.8	$(GA)_2$	30	70	4	0.8
$(EI)_3$	7	580	0.4	0.1	$(GA)_3$	139	87	3	5
$(EI)_4$	43	114	0.6	1.4	$(GA)_4$	153	97	4	7
$(EI)_5$	1.39	97	1.3	15	$(GA)_5$	138	97	1	15

Table 7.12 Relative errors of the flexural and shear stiffness: 5 storey building with 1 bay

7.4.3.3.2 Structure with 10 stories

To investigate the effect of the number of stories on the accuracy of the stiffness prediction, an additional ten-story structure is considered with the following properties:

L= 9 m (total bays length)

H_p= 3 m (storey height)

e_w = 0.3 m (wall thickness)

E= 25 10^3 MPa (modulus of elasticity)

G= 10.4 10^3 MPa (shear modulus)

M= 1500 kg (lumped mass by story)

	|Error| (%)					|Error| (%)		
	MC	**MD**	**MCA**	**MDA**		**MC**	**MD**	**MCA**	**MDA**
$(EI)_1$	1.5	12	0.8	0.8	$(GA)_1$	10	20	7	7
$(EI)_2$	1.1	14	2.6	2.6	$(GA)_2$	10	31	2.4	2.4
$(EI)_3$	2.3	9	1	1	$(GA)_3$	15	38	2.2	2.1
$(EI)_4$	3	7	1.6	1.6	$(GA)_4$	25	46	1.6	1.6
$(EI)_5$	8	22	2	2.2	$(GA)_5$	52	58	1.8	1.8
$(EI)_6$	22	377	1.2	1.3	$(GA)_6$	190	71	2.2	2
$(EI)_7$	53	137	2.2	2.4	$(GA)_7$	287	85	1.7	1.4
$(EI)_8$	87	105	1.9	3	$(GA)_8$	124	95	0.3	0.5
$(EI)_9$	99	100	9.6	3.3	$(GA)_9$	103	99	2.2	3
$(EI)_{10}$	101	100	6.7	8	$(GA)_{10}$	101	100	6.7	8.3

Table 7.13 Relative errors of the flexural and shear stiffness: 10 storey building with 3 bays

A summary of the results in this case is given in Table 7.13. Results obtained for this case were similar to those reported in the previous section. The accuracy of stiffness prediction depends on the mass model:

1. Mass models MDA and MCA provide the best results, with relative errors of flexural stiffness (EI) and shear stiffness (GA/γ) less than 10%. The MCA mass model provides better stiffness identification.

2. Mass models MD and MC provide acceptable results for the first five stories, but the relative error becomes very large for the upper stories.

7.5 LATERAL STIFFNESS IDENTIFICATION OF CONFINED MASONRY STRUCTURES

Now and for many years, many countries suffer from a lack of housing, especially for low-income people. The traditional way of tackling this problem is by construction of mass housing. This housing is generally built with the same repetitive characteristics throughout the whole country. In many countries in Latin America and Europe, shear walls and confined masonry are extensively used, with the latter preferred by those building their own homes. This chapter considers a large number of existing structures which need to be evaluated for the purpose of estimating their future performance in possible situations such as an earthquake and their likely condition after its occurrence.

The method developed in section 7.2 was applied on stiffness identification of confined masonry structures. The influence of the geometry and openings was studied.

7.5.1 NUMERICAL STUDY

Figure 7.6 shows the assessment procedure used in the numeric simulation. The dynamic analysis was performed with SAP2000 [108] using the finite element method (FEM) and various mass models for each structure. Dynamic parameters are determined to apply the mass matrix adjustments and the stiffness identification procedure presented in sections 7.2 and 7.4. *EI* and *GA* values are then estimated for each story. Once the residual rigidity values (*EI* and *GA*) for each story are known, the flexibility matrix has been completely estimated.

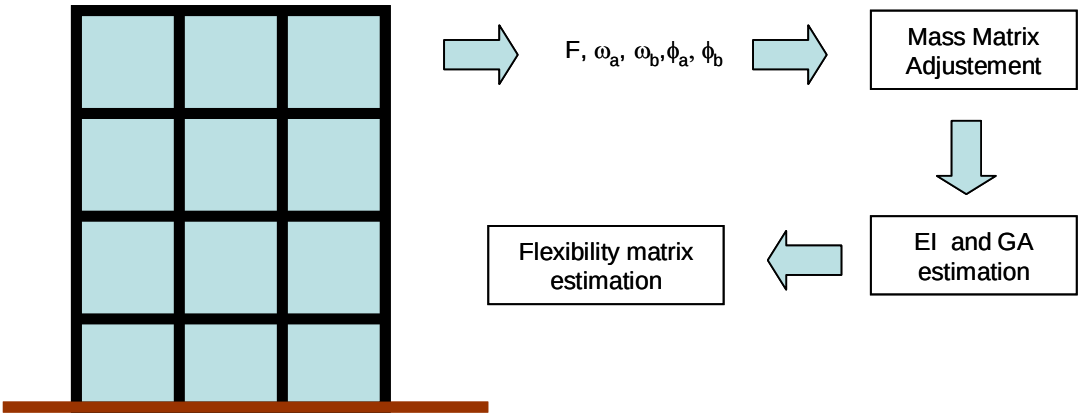

Figure 7.4 Evaluation process of the estimation method

The numerical values obtained with the FEM are considered as "exact" or reference values to determine the quality of the identification results.

$$ErrorF_{ii} = \left(\frac{F_{ii}^{MEF} - F_{ii}^{*}}{F_{ii}^{MEF}} \right) * 100 \qquad (7.28)$$

With:

F_{ii}^{MEF} = ii flexibility coefficient of the flexibility matrix (FEM values)

F_{ii}^{*} = Estimated ii flexibility coefficient of the flexibility matrix.

7.5.2 DESCRIPTION OF THE FINITE-ELEMENT SIMULATION

Figure 7.7a shows a confined masonry structure, with the masonry wall confined by reinforced-concrete (RC) vertical and horizontal elements; a planar finite element model of the structure was constructed using the SAP2000 software [108]. The vertical and horizontal confined elements were modeled by quadrilateral planar "shell" elements. The shell elements have bending and membrane stiffness with three degrees of freedom at each node (Figure 7.7b) [108]. The masonry wall was modeled using a quadrilateral planar "plane" element. The plane element has two degrees of freedom at each node (Figure 7.7b). The shell and plane elements have the same dimension (w x t = 0.15 m x 0.15).

Compatible lateral displacements are considered for each floor because this condition leads to better results than free lateral displacements. Actually, the impact of this condition was previously evaluated; it might lead to less than 2% relative error for a wall without openings and 5% for a wall with openings [120]. Wall masses are uniformly distributed for each FE node and the slab mass is lumped to the nodes belonging to each floor. The building is fixed at ground level, and the analysis is linear.

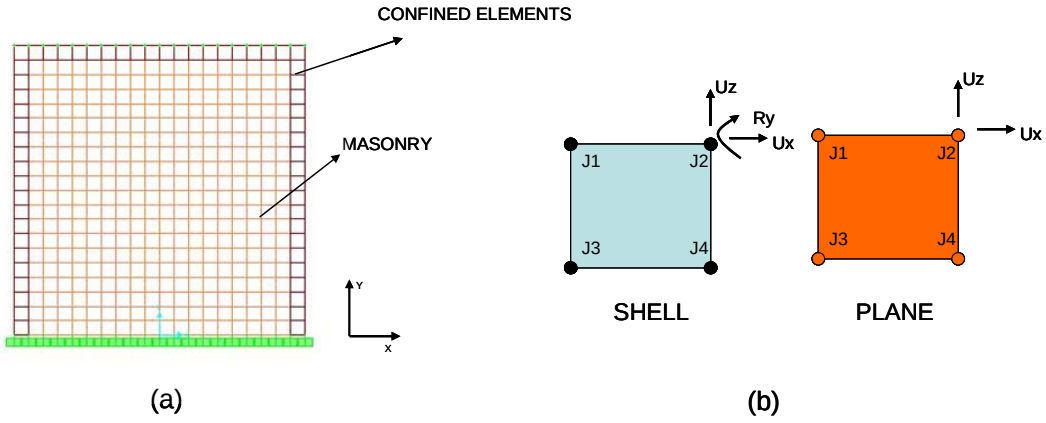

Figure 7.5 Confined masonry model simulated in SAP2000

7.5.3 PROPERTIES OF THE STRUCTURE TO BE ANALYZED

Figure 7.8 shows the geometrical and mechanical characteristics of the confined masonry structure. Dimensions and material properties are the same in all analyses. The models vary only in the number of stories and bays. Figure 7.8 shows the property values for materials in common use in Venezuela.

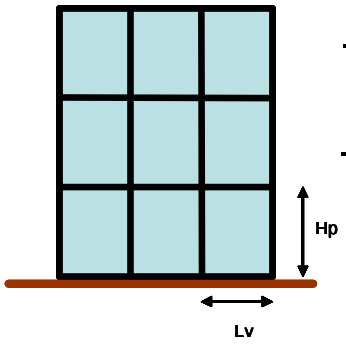

	Masonry	Concrete
Elasticity Modulus (Mpa)	7000	25400
Shear Modulus (Mpa)	2800	14200
Mass (kg/m^3)	1000	2500

Lv= 3 m (bay length)

Hp= 3 m (story height)

Wall thinckness = 0.15 m

The lumped masses at each storey level is 42 kg for bay

Figure 7.6 General characteristics of the confined masonry structure employed

7.5.4 LATERAL STIFFNESS ESTIMATION UNDER DIFFERENT GEOMETRY CONDITIONS

A study of confined masonry structures with different numbers of floors (3, 4, or 5) and numbers of bays (1, 2, or 3) has been performed to verify the efficiency and accuracy of the proposed identification method. Table 7.14 gives the relative error values for estimation of the lateral flexibility coefficients (F_{ii}) for the nine cases. In this study, small errors were observed throughout. The results for all the cases are well-specified, with relative error values less than 1.65%.

	Error F_{ii} (%)				
	F_{11}	**F_{22}**	**F_{33}**	**F_{44}**	**F_{55}**
			5 storey building		
1 bay	1.65	0.21	-0.01	0.05	-0.14
2 bays	1.65	0.27	-0.05	0.07	0.32
3 bays	1.42	0.27	-0.16	0.04	-0.62
			4 storey building		
1 bay	1.09	0.04	0.07	-0.10	
2 bays	1.11	0.04	0.08	-0.25	
3 bays	1.34	0.06	0.07	-0.54	
			3 storey bulding		
1 bay	0.53	0.08	-0.07		
2 bays	0.82	0.14	-0.18		
3 bays	1.11	0.17	-0.24		

Table 7.14 Stiffness estimation results for two different geometries

7.5.5 LATERAL STIFFNESS ESTIMATION WITH OPENINGS IN THE WALL SECTION

The five-story, one-bay model is used to calibrate the stiffness identification method for a shear wall with openings. The study is performed for shear-wall buildings with window and door openings. The geometrical and mechanical properties of the model under study are the same as in section 7.5.3.

7.5.5.1 Shear wall with window openings

The analysis was performed for the cases of a/b ratio equal to 0.2, 0.3, 0.4, and 0.5, as shown in Figure 7.9. The relative errors were similar in all cases because the effect of openings was not found to be significant. Nevertheless, the errors were greater for larger a/b ratios.

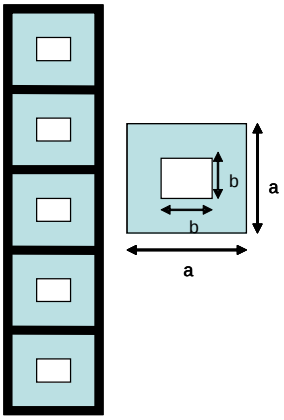

(a)

		Error F_{ii} (%)				
b (m)	**a/b**	**F_{11}**	**F_{22}**	**F_{33}**	**F_{44}**	**F_{55}**
0.6	0.2	0.44	0.05	-0.03	0.01	-0.6
0.9	0.3	-0.03	-0.03	-0.04	0.01	-0.06
1.2	0.4	-0.89	-0.21	-0.13	-0.03	-0.10
1.5	0.5	-2.05	-0.52	-0.28	-0.10	-0.15

(b)

Figure 7.7 Walls with windows openings

7.5.5.2 Shear wall with door openings

In this section, the lateral stiffness estimation of a five-floor, one-bay confined masonry building with variations in door height and width is discussed; results are shown in Figures 7.10 and 7.11.

7.5.5.2.1 Door height variation

For the chosen structure, various ratios of door and story height (H/Hv) from 0.5 to

0.8 were investigated (Figure 7.10a). Figure 7.10b illustrates that as the H/Hv ratio increases, the quality of the results decreases, but is usually quite good.

Because of this, an additional structural behavior study was performed by increasing the number of bays while maintaining an H/Hv ratio of 0.8 (Figure 7.10c). A slight increase in the error with increasing number of bays is observed. A large increase in door height increases wall flexibility, especially in the area near the slab. This invalidates the assumption of a cantilever structure (used in section 7.2) in this simulation, especially given the behavior of the zone adjacent to the slab floor.

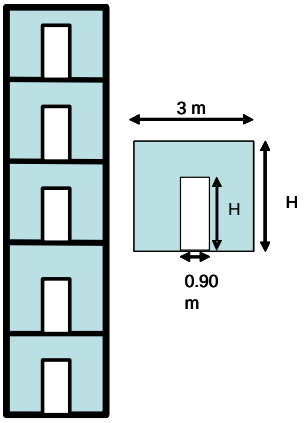

(a)

		Error F_{ii} (%)				
H (m)	**H/Hv**	**F_{11}**	**F_{22}**	**F_{33}**	**F_{44}**	**F_{55}**
1.5	0.5	-0.94	-0.17	-0.13	-0.05	-0.10
1.8	0.6	-2.09	-0.41	-0.22	-0.09	-0.13
2.1	0.7	-4.36	-0.91	-0.44	-0.22	-0.17
2.4	0.8	-8.97	-1.95	-0.93	-0.55	-0.27

(b)

	Error F_{ii} (%)				
Bays	**F_{11}**	**F_{22}**	**F_{33}**	**F_{44}**	**F_{55}**
1	-8.97	-1.95	-0.93	-0.55	-0.27
2	-9.08	-2.42	-1.38	-0.98	-0.50
3	-9.76	-2.82	-1.80	-1.50	-0.63
4	-9.96	-3.01	-2.06	-1.82	-0.83

(c)

Figure 7.8 Walls with door openings. Case: Height variation.

7.5.5.2.2 Width door variation

The estimation errors for the lateral flexibility of the confined masonry structure are shown in Figure 7.11a. The increased L/Lv ratio does not affect the quality of the stiffness estimation (Figure 7.11b).

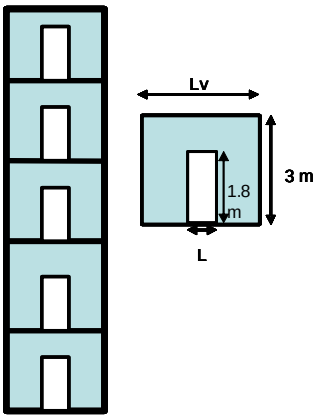

(a)

		Error F_{ii} (%)				
L (m)	**L/Lv**	**F_{11}**	**F_{22}**	**F_{33}**	**F_{44}**	**F_{55}**
0.9	0.3	-2.09	-0.41	-0.22	-0.09	-0.13
1.2	0.4	-2.41	-0.50	-0.28	-0.14	-0.16
1.5	0.5	-2.23	-0.51	-0.31	-0.14	-0.20
1.8	0.6	-1.53	-0.38	-0.27	-0.12	-0.24
2.1	0.78	-0.41	-0.14	-0.18	-0.04	-0.38

(b)

Figure 7.9 Walls with door openings. Case: width variation

7.6 EXPERIMENTAL ASSESSMENT

To verify the experimental effectiveness of the stiffness estimation method presented, we tested the dynamic modes of one cantilever beam. The physical parameter of the model, experimental test developed and its results are describes in section 4.4.

7.6.1 STUDY CASES AND ESTIMATION RESULTS

Consecutive damage was made to the beam, in order to evaluate the proposed methodology. Cracks were made in the beam flanges. Cracks were localized in the half of the section. Three study cases were established:

Case a: Initial undamaged beam (reference for evaluation of stiffness change)
Case b: Beam with damage in the 2nd section
Case c: Beam with damage in the 2nd and 4th sections.

For each of the cases described above, free vibration tests were performed with excitation in different coordinates, in order to obtain records and to choose those with more quality and information. Dynamic properties were obtained for every case: The mode shapes and frequencies for each study case are show in figures 7.12 to 7.14 and table 7.15. Once the beam mass is estimated and the experimental data analyzed, a linear system is formed (7.12). Solving the system, we obtain changes of stiffness for every case in relation to the initial structure (case a).

Table 7.16 shows the results of damage estimation in case b, and c. In each of the two studied cases, damage and undamaged sections are identified with accuracy; in the case of undamaged sections, the maximum error estimation is 3 %. In relation to reference values (case a), the methodology, in the two studied cases, identifies with precision the location of damaged sections as well as the variation of stiffness.

	ω_1 (rad/s)	ω_2 (rad/s)	ω_3 (rad/s)
Undamaged	12.46	78.96	218.78
Case b	11.89	78.39	207.47
Case c	11.87	77.24	202.49

Table 7.15 Natural frequency from the free vibration test

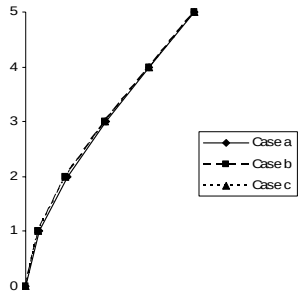

Figure 7.10 First mode shape from free vibration test

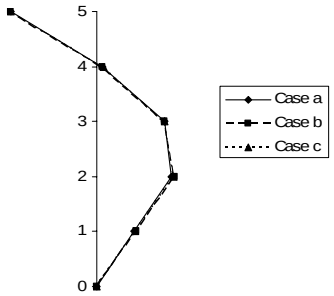

Figure 7.11 Second mode shape from free vibration test

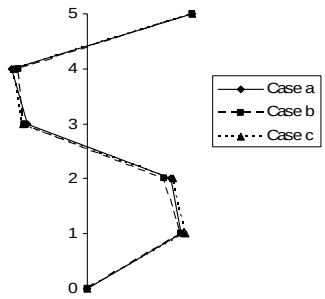

Figure 7.12 Third mode shape from free vibration test

	Case b	Case c
Section	EI_f/EI_0	EI_f/EI_0
1	1.00	1.00
2	0.72	0.72
3	1.01	1.01
4	0.97	0.88
5	1.02	1.00

Table 7.16 Stiffness estimation changes of cantilever

7.7 CONCLUSION

The damage identification procedure for a cantilever structures was proposed. This methodology requires a known mass matrix and two natural frequencies with their corresponding mode shapes.

The stiffness identification procedure was illustrated with a numerical example of a real chimney, achieving good precision for stiffness changes in each section under different noise signal conditions. Also, the methodology of stiffness estimation was applied in an experimental study of a steel cantilever beam. Damage was performed in two sections of the beam. The method identified with precision the change of stiffness as well as the damage location.

This approach can be applied in cantilever structures (chimneys, control towers, grandstands roofs, etc.).The presented algorithm has the advantage that it only requires the knowledge of two mode shapes with their respective frequencies (without doing the measurement of rotational coordinates, which generally are difficult to obtain). This implies that the proposed methodology is a powerful tool for the prompt

decision about the future of this type of structure. This methodology has very wide usage with little amount of experimental measurement which drastically reduces the excessive costs and number of tests. Therefore, it is convenient to apply this approach in order to identify structural cantilever typologies.

The results show that the quality of the damage identification is very more sensitive to the perturbation of the mode shapes than that of frequencies. Multiple and severe stiffness reductions affect the quality of the damage identification, for the Flexure stiffness coefficients (EI) the results give a reasonable agreement between the damage identified and damage assumed. But, the Shear coefficients (GA) had unacceptable precision and major errors, and were not corrected. As expected a better adjustment of the flexural coefficient than the shear coefficient, because of the chimney mainly flexural behavior.

Influence of mass models and nonparametric mass normalization on structural stiffness identification

The influence of the choice of initial mass model on the stiffness identification of shear-wall buildings is discussed.

Four mass models with lumped masses at each floor level were investigated: (a) diagonal mass matrix (MD), which assumes that the structural masses are lumped at each floor level, (b) consistent mass matrix (MC) which models the structure as a cantilever of which the components are plane beams with 3 DOF per node and a consistent mass model imposed on each beam, (c) adjusted diagonal mass matrix (MDA) derived by nonparametric normalization of the original diagonal matrix, and (d) adjusted consistent mass matrix (MCA) obtained by adjustment of the consistent mass matrix by applying the nonparametric normalization.

Two buildings are considered as illustrations: a five-story building with one up to three bays, and a ten-story building with one bay. The results obtained show that:

- Mass models MDA and MCA provide the best results, with relative errors of flexural stiffness (EI) and shear stiffness (GA/γ) less than 15%. The MCA mass model provides better stiffness identification.
- Mass models MD and MC provide acceptable results for the lower stories, but the relative error becomes excessive for upper stories.

Nonparametric mass normalization based on dynamic data leads to a better stiffness coefficient assessment for each floor. The absence of nonparametric mass normalization leads to high error values for the estimation of stiffness coefficients.

In addition, it has been shown that the behavior of the proposed method with noise in the modal signal is satisfactory.

Lateral stiffness identification of confined masonry structures

The stiffness identification method for shear wall buildings was applied to masonry wall structures of three to five stories, obtaining results of good precision by means of a simple and efficient process.

The principal conclusions that can be derived from the various applications of this method reported in this paper can be summarized as follows:

1. As the same as the shear wall building case, special attention must be paid to the mass model which provides the initial data for structural stiffness identification. The theoretical models are not necessarily orthogonal to the experimental modal values. In this work, a methodology is proposed for the preliminary adjustment of the initial mass matrix.
2. The method proposed for identification of lateral stiffness is adequate for the structures analyzed: masonry wall structures of three to five stories and one to three bays. The results obtained were very close to values which can be considered exact.
3. Wall openings for doors and windows (with geometries in common use) do not affect the lateral stiffness identification.

8. CONCLUSIONS AND FUTHER RESEARCH

8.1 CONCLUSIONS

The goal of this study was to develop and validate in a numeric and experimental manner methods of identification of damage in structures considering dynamic data. A bibliographical study carried out showed that there is a lack of methods that use a reduced level of experimental information and provide information of location of the damage of the structure. In general, the methods that use reduced experimental information or few sensors produce results or overall calculations of the damage in the structure. Other types of methods required the measurement of various coordinates and the support of detailed simulations in finite elements.

On the basis of knowledge of the forms of the matrixes of stiffness or flexibility, identification methods for three specific types of structures were developed:

- Framed buildings**.**
- Structures composed of simply supported beams**,** specially designed bridges.
- Structures that can be simulated as a cantilever, with flexural and shear behavior.

These methodologies are unique because of the limited dynamic information required (one or two modal forms with its corresponding frequency), obtaining as a result, the value of the change of local stiffness of the structure (story or section).

The following is a summary of the conclusions for each method:

8.1.1 FRAMED BUILDINGS

Two identification procedures are proposed. They may be applied to framed buildings with shear behavior to evaluate the structural damage in terms of stiffness reduction values, as well as to determine the location of these stiffness variations. The methodologies presented has an application limited to framed structures, and the procedures described here have the advantage of using only a coordinate for floor and a limited number of modes (1 or 2 according to the case).

The numerical simulation demonstrated a reasonable agreement between the damage estimated and damage assumed. The numerical results demonstrated that the method is independent of the order of mode shape utilized. Also, it has been demonstrated that the quality of the damage identification is very more sensitive to the perturbation of the mode shapes than that of frequencies. However, the frequency is more stable that the mode shape in real dynamic test. Important level errors in measured mode shapes would affect the damage identification, so special attention would have to be paid to signal processing. It is found that the damage identification is affected by damage severity of the structure. For the large damage in any level, the quality of damage identification is dependent on the mode shape utilized. When the severity of damage is high, the low mode shapes can be used to identify the damage with best precision compared with high mode shapes.

Both methods are applied to an experimental model of a three-level framed building. The undamaged structure is evaluated and three cases representing various damage conditions are studied. Both identification methods proved adequate to identify the stiffness reduction and damage location.

8.1.2 SIMPLY SUPPORTED BEAM

The damage identification procedure for a simply supported beam was proposed. This methodology required a known mass matrix and two natural frequencies and their corresponding mode shapes.

The damage identification procedure was illustrated with a numerical example of the real bridge. The ratio EI_f/ EI_o was estimated with low relative errors. It has been shown that the behavior of the proposed method with noise is satisfactory. The accuracy of the damage identification depends on the noise level, which is generally quite good. The quality of damage identification is independent of whether noise is localized in the frequencies or mode shapes

The results show that the damage identification method is not affected by damage

severity or multiple damage sections of the structure. In all cases, the methodology identifies with precision the location of the changes in stiffness as well as the variation of stiffness.

The methodology of stiffness estimation was applied in an experimental study to a wide-flanged I-beam. A progressive damage was made in three sections of the beam, which corresponds to the three damage cases studied. In these three cases, the estimation method identified with precision the change of stiffness as well as its location.

This approach can be applied not only to the simply supported beams but also to the simply supported girder bridges. An important advantage of this approach is that it needs only a small number of mode shapes and simple dynamic tests. This method required only unidirectional coordinates; it does not require rotational coordinates and refined FE models. Therefore, it is very convenient to apply this approach to identify damage in simply supported girder bridges or beams.

8.1.3 CANTILEVER STRUCTURES

The damage identification procedure for a cantilever structure was proposed. This methodology requires a known mass matrix and two natural frequencies with their corresponding mode shapes.

The stiffness identification procedure was illustrated with a numerical example of a real chimney, achieving good precision for changes in stiffness in each section under different noise signal conditions. Also, the methodology of stiffness estimation was applied in an experimental study of a steel cantilever beam. Damage was made in two sections of the beam. The method identified with precision the change in stiffness as well as the damage location.

The results show that the quality of the damage identification is very sensitive to the perturbation of the mode shapes than that of frequencies. Multiple and severe stiffness

reductions affect the quality of the damage identification; with respect to the Flexure stiffness coefficients (EI), the results give a reasonable agreement between the damage identified and damage assumed. But, the shear coefficients (GA) showed unacceptable precision and major errors and were not corrected. As expected, a better adjustment was made using the flexural coefficient than that using the shear coefficient, which is mainly attributed mainly to the flexural behavior of the chimney.

This approach can be applied to cantilever structures (chimneys, control towers, grandstands roofs, etc.). An important advantage of this approach is the need of only two mode shapes and simple dynamic tests. This method requires only unidirectional coordinates; it does not require rotational coordinates and refined FE models. Therefore, it is convenient to apply this approach in order to identify structural cantilever typologies.

8.1.3.1 Influence of the mass model on stiffness determination

The influence of choice of mass model on the stiffness identification was investigated.

Four mass models with lumped masses at each floor level are investigated: (a) Diagonal Mass matrix (MD), which assumes that the structural masses are lumped at each floor level; (b) Consistent Mass matrix (MC), which models the structure as a cantilever whose components are plane beams with 3 DOF per node and a consistent mass model is imposed to each beam; (c) Adjusted Diagonal Mass Matrix (MDA) derived by nonparametric normalization from the original diagonal matrix; and (d) Adjusted Consistent Mass Matrix (MCA) obtained from the adjustment of the Consistent Mass Matrix after the nonparametric normalization is applied.

Two buildings are considered as illustration: a 5-storey building with 1–3 bays and a 10-storey building with 1 bay. The results show that:

- Mass models MDA and MCA provide the best results as the relative errors on the flexural stiffness (EI) or the shear stiffness (GA/γ) remain lesser than 15%. The MCA mass model provides better stiffness identification.

- Mass models MD and MC provide acceptable results for the first lower stories; however, the relative error is high for upper stories.

Mass nonparametric normalization based on dynamic data leads to better stiffness coefficients assessment for each floor. The absence of mass nonparametric normalization leads to high error values for the estimation of stiffness coefficients.

Also, it has been showed that the behavior of the proposed method with noise in the modal signal is satisfactory.

8.1.3.2 Stiffness identification of confined masonry

The stiffness identification method was applied to masonry wall structures of 3–5 storey, obtaining results of a good precision and indicating a simple and efficient process.

The principal observations derived from the different applications of this method performed in this study are summarized:

- As the same as the shear wall building case, we propose the previous adjustment of the initial mass matrix.
- The method proposed to identify the lateral stiffness is adequate for the structures analyzed: masonry wall structures of 3–5 storeys and of 1–3 bays. The results obtained were very close to those considered as exact.
- The wall opening of doors or windows (with common use geometry) does not affect the lateral stiffness identification.

8.2 FUTHER RESEARCH

The methods of estimation of the stiffness developed have shown that the noise in the measurements represents a variable that can impact, in a great manner, the quality of the results. This makes us review and enhance the process of gathering and treatment of the signal in order to reduce its maximum experimental and numeric error input.

The methods of identification suggested in this study were validated through numerical and experimental applications, obtaining results that, satisfactorily, relate the changes in

stiffness proposed to the ones forecasted. The next challenge is to apply them to real structures, particularly, to carry out processes of structural identification in the following structures:

- Real framed building;
- A bridge with simply supported beams;
- An industrial chimney or a control tower of an airport;
- Confined masonry structure or building of reinforced concrete walls;

Each test must undergo an evaluation to determine the influence of the iteration soil-structure and rotational displacement.

REFERENCES

1. Chase, S.B., Laman, J.A., *Dynamics and field testing of bridges, Transportation in the New Millennium.* http://www.nationalacademies.org/trb/publications/millennium/00029.pdf, 2000.
2. Risk Management Solutions, I., *The Northridge, California Earthquake.* RMS 10-year Retrospective, 2004. **http://www.rms.com/publications/northridgeeq_retro.pdf**.
3. León, R., *Vulnerabilidad y riesgo sísmico de edificios. Aplicación a entornos urbanos en zonas de amenaza alta y moderada.* Tesis Doctoral. Universidad politécnica de Cataluña, 2003: p. 465 pp.
4. Park, Y.J., Ang, A.H.S., Wen, Y.K, *Damage limiting aseismic design of buildings.* Earthquake Spectra, 1987. **3 (1)**: p. 1-26.
5. Anagnostopoulos, S.A., Petrovski, J., Bouwkamp, J. G, *Emergency earthquake damage and usability assessment of buildings.* Earthquake Spectra, 1989. **5(3)**: p. 461-476.
6. Bracci, J.M., Reinhorn, A. M., Mande, J. B.,Kunnath, S. K., *Deterministic model for seismic damage evaluation of RC structures.* Technical Report NCEER-89-0033, State University of New York at Buffalo, 1989.
7. Earthquake Engineering Research Institute, *Expected seismic performance of building, technical report, publication number SP-.* EERI, Oakland CA., 1994.
8. Cawley, P., Adams, R. D., *The Locations Of Defects In Structures From Measurements Of Natural Frequencies.* Journal of Strain Analysis, 1979. **14(2)**: p. 49-57.
9. Rytter, A., *Vibration Based Inspection of Civil Engineering Structures.* PhD Thesis, Aalborg University, Denmark., 1993.
10. Richardson, M.H., *Detection of Damage in Structures from Changes in their Dynamic (Modal) Properties- A survey.* U.S. Nuclear Regulatory Commission, Washington, D.C., NUREG/CR-1431, 1980.
11. Hemez, F.M., *Theoretical and Experimental Correlation Between Finite Element Models and Modal Tests in the Context of Large Flexible Space Structures,.* Ph. D. Dissertation, Dept. of Aerospace Engineering Sciences, University of Colorado, Boulder, CO., 1993.
12. Kaouk, M., *Finite Element Model Adjustment and Damage Detection Using Measured Test Data.* Ph. D. Dissertation, Dept. of Aerospace Engineering Mechanics and Engineering Science, Univ. of Florida, Gainesville, FL., 1993.
13. Doebling, S.W., *Measurement of Structural Flexibility Matrices for Experiments with Incomplete Reciprocity.* Ph. D. Dissertation, University of Colorado, Boulder, CO,Department of Aerospace Engineering Sciences, CU-CAS-95-10, 1995.
14. Mottershead, J.E., Friswell, M. I, *Model Updating in Structural Dynamics: A Survey.* Journal of Sound and Vibration, 1993. **167**(2): p. 347–375.
15. Bishop, C.M., *Neural Networks and Their Applications.* Review of Scientific Instrumentation, 1994. **65**(6): p. 1803-1832.
16. Doebling, S.W., Farrar, C. R., Goodman, R. S.,, *Effects of Measurement Statistics on the Detection of Damage in the Alamosa Canyon Bridge.* Proceedings 15th International Modal Analysis Conference, Orlando, FL., 1997: p. 919-929.

17. Stubbs, N., Osegueda, R, *Global Non-Destructive Damage Evaluation In Solids.* Modal Analysis: The International Journal of Analytical and Experimental Modal Analysis, 1990. **5 (2)**: p. 67-79.
18. Stubbs, N., Osegueda R., *Global Damage Detection In Solids-Experimental Verification.* Modal Analysis: The International Journal of Analytical and Experimental Modal Analysis, 1990. **5 (2)**: p. 81-97.
19. Sanders, D., Kim, Y. I., Stubbs, R. N., *Nondestructive Evaluation Of Damage In Composite Structures Using Modal Parameters.* Experimental Mechanics, 1992. **32**: p. 240-251.
20. Hearn, G., Testa, R. B., *Modal Analysis for Damage Detection in Structures.* Journal of Structural Engineering, 1991. **117**: p. 3042-3062.
21. Chen, H.L., Spyrakos, C.C., Venkatesh, G., *Evaluating structural deterioration by dynamic response.* Journal of Structural Engineering, 1995. **121(8)**: p. 1197-1204.
22. Messina, A., Williams, E.J., Contursi, T, *Structural damage detection by sensitivity and statistical-based method.* Journal of sound and vibration, 1998. **216(5)**: p. 791-808.
23. De Roeck, G., Peeters, B. , Maeck, J., *Dynamic monitoring of civil engineering structures. In:.* Computational Methods for Shell and Spatial Structures, IASS-IACM 2000, Chania, Crete, Greece., 2000.
24. Boltezar, M., Strancar, B., Kuhelj, A., *Identification of Transverse Crack Location in Flexural Vibrations of Free-Free Beams.* Journal of Sound and Vibration, 1998. **211**: p. 729-734.
25. Sampaio, R.P.C., Maia, N. M. M., Silva, J. M. M,, *The Frequency Domain Assurance Criterion as a Tool for Damage Identification.* Proceedings of the 5th International Conference on Damage Assessment of Structures (DAMAS 2003), Southampton, England, UK., 2003: p. 69-76.
26. Zang, C., Friswell, M. I. ,Imregun, M., *Structural Health Monitoring and Damage Assessment using Measured FRFs from Multiple Sensors, Part I: The Indicator of Correlation Criteria.* Proceedings of the 5th International Conference on Damage Assessment of Structures (DAMAS 2003), Southampton, England, UK, 2003: p. 131-140.
27. Yuen, M.M.F., *A Numerical Study of the Eigenparameters of a Damaged Cantilever.* Journal of Sound and Vibration, 1985. **103**: p. 301-310.
28. Allemang, R.J., Brown, D. L., *A Correlation Coefficient for Modal Vector Analysis.* Proceedings of the 1st International Modal Analysis Conference (IMAC I), Orlando, Florida, USA., 1982: p. 110-116.
29. Lieven, N.A., Ewins, D. J., *Spatial Correlation of Mode Shapes: The Coordinate Modal Assurance Criterion (COMAC).* Proceedings of the 6th International Modal Analysis Conference (IMAX VI), Kissimmee, Florida, USA., 1988: p. 690-695.
30. Ewins, D. J., *Modal testing: theory and practice.* Research Studies Press Ltd., London, 1984.
31. Fox, C.H.J., *The location of defects in structures: a comparison of the natural frequency and mode shape correlation.* Proc 10th IMAC, San Diego, California, USA, 1992. **I**: p. 522-528.

32. Mayes, R.L., *Error localization using mode shapes-an application to a two link robot arm.* Proc. 10th International Modal Analysis Conference, 1992: p. 886-891.
33. Pandey, A.K., Biswas M., Samman, M. M., *Damage detection from changes in curvature mode shapes.* Journal of Sound and Vibration, 1991. **145(2)**: p. 321-332.
34. Salawu, O.S., Williams, C., *Damage Location Using Vibration Mode Shapes.* Proc. of 12th International Modal Analysis Conference, 1994: p. 933-939.
35. Wahab, M., De Roeck, G., *Damage detection in bridges using modal curvatures: applications to a real damage scenario.* Journal of Sound and Vibration, 1999. **226(2)**: p. 217-235.
36. Ho, Y.K., Ewins, D. J., *On the Structural Damage Identification with Mode Shapes.* Proceedings of the European COST F3 Conference on System Identification and Structural Health Monitoring Madrid, Spain, 2000: p. 677-686.
37. Ren, W.-X., De Roeck, G., *Structural damage identification using modal data. II: Test verification.* Journal of Structural Engineering, 2002. **128(1)**: p. 96-104.
38. Kim, J.-T., Stubbs, N., *Model-uncertainty impact and damage-detection accuracy in plate girder.* Journal of Structural Engineering, 1995. **121(10)**: p. 1409-1417.
39. Kim, J.-T., Stubbs, N., *Improved damage identification method based on modal information.* Journal of Sound and Vibration, 2002. **252(2)**: p. 223-238.
40. Stubbs, N., Kim, J.-T., *Damage localization in structures without baseline modal parameters.* AIAA Journal, 1996. **34(8)**: p. 1644-1649.
41. Farrar, C.R., Doebling, S.W., *Damage detection II: field applications to large structures.* In: Silva, J.M.M. and Maia, N.M.M. (eds.), Modal Analysis and Testing, Nato Science Series. Dordrecht, Netherlands: Kluwer Academic Publishers., 1999.
42. Choi, S., Stubbs, N,, *Damage Identification in Structures using the Time-Domain Response.* Journal of Sound and Vibration, 2004. **275,**: p. 577-590.
43. Patil, D.P., Maiti, S. K., *Experimental Verification of a Method of Detection of Multiple Cracks in Beams based on Frequency Measurements.* Journal of Sound and Vibration, 2005. **281**: p. 439-451.
44. Pandey, A.K., Biswas, M., *Damage Detection In Structures Using Changes In Flexibility.* Journal of Sound and Vibration, 1994. **169(1)**: p. 3-17.
45. Pandey, A., Biswas, M., *Experimental verification of flexibility difference method for locating damage in structures.* Journal of Sound and Vibration, 1995. **184**(2): p. 311-328.
46. Doebling, S.W., Paterson L. D., *Computing statically complete flexibility from dynamically measured flexibility.* Journal of Sound and Vibration, 1997. **205(5)**: p. 631-645.
47. Lim, T.W., *A submatrix approach to stiffness using modal test data.* AIAA Journal, 1990. **28(6)**: p. 1123-1130.
48. Lim, T.W., *Structural damage detection using modal test data.* AIAA Journal, 1991. **29(12)**: p. 2271-2274.
49. Park, Y.S., Park, H. S., Lee, S. S., *Weighted-error-matrix application to detect stiffness damage-characteristic measurement.* Modal Analysis: The International Journal of Analytical and Experimental Modal Analysis, 1988. **3(3)**: p. 101-107.

50. Yan, A., Golinval, J-C., *Structural Damage localization by cobining flexibility and stiffness methods.* Engineering Structures, 2005. **27**: p. 1752-1761.
51. Garcés, F., Genatios C., Mebarki, A., Lafuente, M, *Reajuste de Matrices De Rigidez y Flexibilidad Para Sistemas Aporticados.* BOLETÍN TÉCNICO IMME, 2002. **40(3)**.
52. Yuan, P., Wu, Z. ,Ma, X., *Estimated mass and stiffness matrices of shear building from modal test.* Earthquake Engineering and Structural Dynamics, 1998. **27**: p. 415-421.
53. Garcés, F., Genatios, C., Lafuente, M., Mebarki, A, *Identification des rigidités résiduelles de systémes á murs porteurs chaînes.* Revue française de Génie Civil, 2004. **8**: p. 889-904.
54. Garcés, F., García P., Genatios C., Mébarki A., Lafuente M, *Damage Identification of Simply-Supported Beams Using Dynamic Analysis: Experimental and Theoretical Aspects.Proceedings of the Eight international conference on computational Structures Technology.Tooping BHV., Montero G., Montenegro R., editors. Civil-Comp Press, 2006, ISBN 1-905088-X, ISBN 1-905088-8, ISBN 1-905088-6. Strinlngshire, Scotland.* 2006.
55. Sheinman, I., *Damage detection and updating of stiffness and mass matrices using mode data.* Computers and Structures, 1996. **59(1)**: p. 149-156.
56. Kosmatka, J.B., Ricles, J.M., *Damage detection in structures by modal vibration characterization.* Journal of Structural Engineering, 1999. **125(12)**: p. 1384-1392.
57. Farhat, C., Hemez, F.M., *Updating finite element dynamic models using an element-by-element sensitivity methodology.* AIAA Journal, 1993. **31(9)**: p. 1702-1711.
58. Brown, G.W., Farhat, C. ,Hemez, F.M., *Extending sensitivity-based updating to lightly damped structures.* AIAA Journal, 1997. **35(8)**: p. 1369-1377.
59. Castello, D.A., Stutz, L.T. ,Rochinha, F.A., *A structural defect identification approach based on a continuum damage model.* Computers and Structures, 2002. **80**: p. 417-437.
60. Ge, M., Lui, E., *Structural damage identification using system dynamics properties.* Computers and Structures, 2005. **83**: p. 2185-2196.
61. Baruch, M., *Optimization procedure to correct stiffness and flexibility matrices using vibration test.* AIAA journal, 1978. **16**: p. 1208-1210.
62. Berman, A., *Mass matrix correction using and incomplete set of measured modes.* AIAA journal, 1979. **17**: p. 1147-1148.
63. Berman, A., Nagy, E., *Improvement of a large Analytical Model test data.* AIAA journal, 1983. **21**: p. 1168-1173.
64. Kabe, A., *Stiffness Matrix adjustment using mode data.* AIAA journal, 1985. **23(9)**: p. 1431-1436.
65. Chen, J.-C., Garba, J. A., *On-Orbit Damage Assessment for Large Space Structures.* AIAA Journal, 1988. **26(9)**: p. 1119-1126.
66. Kim, H.M., Bartkowicz, T. J., *Damage Detection and Health Monitoring of Large Space Structures.* Sound and Vibration, 1993. **27(6)**: p. 12-17.
67. Zimmerman, D.C., Kaouk, M., *Structural Damage Detection Using a Minimum Rank Update Theory.* Journal of Vibration and Acoustics, 1994. **116**: p. 222-230.

68. Kaouk, M., Zimmerman, D. C., *Structural Damage Detection Using Measured Modal Data and No Original Analytical Model.* Proc. of the 12th International Modal Analysis Co, 1994: p. 731-737.
69. Zimmerman, D.C., Kaouk, M., Simmermacher, T, *Structural Damage Detection Using Frequency Response Functions.* Proc. of the 13th International Modal Analysis Conf, 1995: p. 179-184.
70. Zimmerman, D.C., Kaouk M., *Eigenstructure Assignment Approach for Structural Damage Detection.* AIAA Journal, 1992. **30(7)**: p. 1848-1855.
71. Li, C., Smith, S. W., *A Hybrid Approach for Damage Detection in Flexible Structures," in Proc. of 35th AIAA/ASME/ASCE/AHS/ASC Structures.* Structural Dynamics, and Materials Conference, 1994: p. 285-295.
72. Li, C., Smith, S. W, *Hybrid Approach for Damage Detection in Flexible Structures.* Journal of Guidance, Control, and Dynamics, 1995. **18(3)**: p. 419-425.
73. Cobb, R., Liebst, B., *Structural damage identification using assigned partial eigenstructure.* AIAA journal, 1997. **35(1)**: p. 52-158.
74. Teughels, A., Maeck, J. De Roeck, G., *Damage assessment by FE model updating using damage functions.* Computers and Structures, 2002. **80**: p. 1869-1879.
75. Jaishi, B., Ren, W., *Damage detection by finite element model updating using modal flexibility residual.* Journal of sound and vibration, 2006. **290**: p. 369-687.
76. Titurus, B., Friswell, M.,Starek, L., *Damage detection using generic elements: Part II. Damage detection.* Computers and Structures, 2003. **81**: p. 2287-2299.
77. Titurus, B., Friswell, M. , Starek, L., *Damage detection using generic elements: Part I. Model updating.* Computers and Structures, 2003. **81**: p. 2273-2286.
78. Modena, C., Sonda, D., Zonta, D., *Damage Localization in Reinforced Concrete Structures by Using Damping Measurements, Damage Assessment of Structures.* Proceedings of the International Conference on Damage Assessment of Structures (DAMAS 99), Dublin, Ireland, 1999: p. 132-141.
79. Zonta, D., Modena, C., Bursi, O.S., *Analysis of Dispersive Phenomena in Damaged Structures.* European COST F3 Conference on System Identification and Structural Health Monitoring, Madrid, Spain, 2000: p. 801-810.
80. Keye, S., Rose, M., Sachau, D., *Localizing Delamination Damages in Aircraft Panels from Modal Damping Parameters.* Proceedings of the 19th International Modal Analysis Conference (IMAC XIX), Kissimmee, Florida, USA., 2001: p. 412-417.
81. Feng, M.Q., Bahng, E.Y., *Damage assessment of jacketed RC columns using vibration tests.* Journal of Structural Engineering, 1999. **125(3)**: p. 265-27.
82. Mangal, L., Idichandy, V.G., Ganapathy, C., *ART-based multiple neural networks for monitoring offshore platforms.* Applied Ocean Research, 1996. **18**: p. 137-143.
83. Waszczyszyn, Z., Ziemianski, L., *Neural networks in mechanics of structures and materials - new results and prospects of applications.* Computers and Structures, 2001. **79**: p. 2261-2276.
84. Zubaybi, A., Haddara, M.R. ,Swamidas, A.S.J., *Damage identification in a ship's structure using neural networks.* Ocean Engineering, 2002. **29**: p. 1187-1200.

85. Ramu, S.A., Johnson, V.T., *Damage assessment of composite structures - a fuzzy logic integrated neural network approach.* Computers and Structures, 1995. **57(3)**: p. 491-502.
86. Pandey, P.C., Barai, S.V., *Multilayer perceptron in damage detection of bridge structures.* Computers and Structures, 1995. **54(4)**: p. 597-608.
87. Marwala, T., *Damage identification using committee of neural networks.* Journal of Engineering Mechanics, 2000. **126(1)**: p. 43-50.
88. Michalewicz, Z., Fogel, D.B., *How to Solve It: Modern Heuristics. Berlin, Heidelberg, Germany: Springer-Verlag.* 2000.
89. Chiang, D.-Y., Lai, W.-Y., *Structural damage detection using the simulated evolution method.* AIAA Journal, 1999. **37(10)**: p. 1331-1333.
90. Moslem, K., Nafaspour, R., *Structural damage detection by genetic algorithms.* AIAA Journal, 2002. **40(7)**: p. 1395-1401.
91. Ostachowicz, W., Krawczuk, M., Cartmell, M., *The location of a concentrated mass on rectangular plates from measurements of natural vibrations.* Computers and Structures, 2002. **80**: p. 1419-1428.
92. Van Den Abeele, K., De Visscher, J., *Damage assessment in reinforced concrete using spectral and temporal nonlinear vibration techniques.* Cement and Concrete Research, 2000. **30**: p. 1453-1464.
93. Neild, S.A., Williams, M.S., McFadden, P.D., *Non-linear behaviour of reinforced concrete beams under low-amplitude cyclic and vibration loads.* Engineering Structures, 2002. **24**: p. 707-718.
94. Vanlanduit, S., Parloo, E., Guillaume, P., De Vos, W, *Validation of on-line linear and nonlinear fatigue crack detection techniques.* Proceedings of 1st European Workshop on Structural Health Monitoring. Paris, France., 2002: p. 219-226.
95. Genatios, C., *Contribution A L'evaluation des procedes experimentaux pour la determination des proprietes dynamiques des structures.* Tesis Doctoral Institut National des Sciences Appliquées, 1991.
96. Genatios, C., *Evaluación de procedimientos para la determinación experimental de propiedades dinámicas de estructuras.* Trabajo de Ascenso para Profesor Asistente, IMME/UCV, 1985.
97. Chopra, A., *Dynamics of structures: theory and applications to earthquake engineering.* Prentice Hall, 2001.
98. Clough, R., Penzien, J, *Dynamics of structures.* McGraw-Hill, Inc., 1995.
99. Proakis, J., Manolakis, D., *Tratamiento de señales: principios, algoritmos y aplicaciones.* Prentice Hall, 2000.
100. Cooley, J.W., Tukey, J.W, *An Algorithm for Machine Calculation of Complex Fourier Series.* Math.Computation, 1965. **19**.
101. Genatios, C., Lafuente, M., Garcés, F., Morales, S., Bellan, P., Lorrain M, *On the evaluation of structural dynamic properties and model adjustment: practical and numerical considerations.* 11th European Conference on Earthquake Engineering, 1998.
102. López, O., Genatios, C., Cascante G, *Determinación experimental de las propiedades dinámicas de un edificio aporticado de cinco pisos.* Boletín Técnico IMME, 1994. **32 (2)**: p. 17-41.

103. García, P., *Simulación, identificación y problema inverso en dinámica experimental de estructuras con aplicación a cuatro modelos a escala 1/6.* Tesis de maestría, Universidad Central de Venezuela, 2006.
104. Kinemetrics, www.kinemetrics.com.
105. Peeters, B., *System Identification and damage detection in civil engineering.* PhD Thesis, Civil engineering departament, Ctaholic University of Leuven, Belgium., 2000.
106. García, P., Genatios, C., Garcés, F., Lafuente, M, *SADEX: Sistema Computacional para la Simulación e Identificación de Estructuras.* Boletín Técnico del IMME, 2006. **44 (2)**.
107. Craig, R., *Structural Dynamics.* John Wiley & Sons, 1981.
108. SAP 2000, *Analysis Reference Manual.* Computers and Structures, Inc. Berkeley, California, USA. Version 8.0, 2002.
109. Sohn, H., Law, K, *Application of load-dependent Ritz vectors to Bayesian probabilistic damage detection.* Probabilistic engineering mechanics, 2000. **15 (2)**: p. 139-153.
110. MATLAB, *The Language of Technical Computing.* The Math Works, Inc, 2000.
111. Roberts, J., *Performance of concrete bridges in recent earthquakes.* Proceedings of the Institution of Civil Engineering -Structural Concretes, 2001. **2 (2)**: p. 73-91.
112. Kwan, N., *Reducing damage to concrete stitches in bridge decks.* Proceedings of the Institution of Civil Engineering -Bridge Engineering, 2006. **159 (2)**: p. 53-62.
113. Cavell , D., Waldron, P, *Parametric study of the residual strength of deteriorating simply-supported post-tensioned concrete.* Proceedings of the Institution of Civil Engineering -Structures and Building, 2001. **146 (4)**: p. 341-352.
114. Pavic, A., Armitage, T., Reynolds, P., Wright, J., *Methodology for modal testing of the Millennium Bridge, London.* Proceedings of the Institution of Civil Engineering -Structures & Buildings, 2003. **152 (2)**: p. 111-121.
115. Nielson, B., Desroches, R., *Influence of model assumptions o the seismic response of multi-span simply supported steel girder bridges in moderate seismic zones.* Engineering Structures, 2006. **28 (8)**: p. 1083-1092.
116. Ambrosini, R., Riera, J., Danesi, R., *Analysis of structures subjected to random wind loading by simulation in the frequency domain.* Probabilistic Engineering Mechanics, 2002. **17**: p. 233-239.
117. Li, G., Hao, K., Lu, Y. ,Chen, S. A., *Flexibility approach for damage identification of cantilever-type structures with bending and shear deformation.* Computers and Structures, 1999. **73(6)**: p. 565-572.
118. Genatios, C., Garcés, F., Bellan, P. , Lafuente, M., *Direct Matrix Adjustement in Experimental Dynamics.* 11 European Conference on Earthquake Engineering, 1998.
119. Rouanet, C., *Contribution à l'identification structurale: adéquation d'un modèle mathématique à des résultats d'essais.* Thèse Doctorat. Ecole Nationale Supérieure de l'Aéronautique et de l'Espace, Toulouse, France, 1987: p. 206.
120. Garcés, F., *Identificación de la rigidez lateral de edificios de muros.* Trabajo de Ascenso a la categoría de profesor Agregado. IMME Universidad Central de Venezuela, Caracas, 2004.

121. Guyan, R.J., *Reduction of stiffness and mass matrices.* AIAA Journal, 1965. **3(2)**: p. 380.